

ENHANCEMENT OF FLAME RETARDANCY OF POLYETHYLENE AND
POLYPROPYLENE BLENDS BY CYCLIC PHOSPHAZENE ADDITIVES

A THESIS SUBMITTED TO
THE GRADUATE SCHOOL OF NATURAL AND APPLIED SCIENCES
OF
MIDDLE EAST TECHNICAL UNIVERSITY

BY

MUZAFFER KAAAN KARAÖZ

IN PARTIAL FULFILLMENT OF THE REQUIREMENTS
FOR
THE DEGREE OF DOCTOR OF PHILOSOPHY
IN
POLYMER SCIENCE AND TECHNOLOGY

JUNE 2018

Approval of the Thesis:

**ENHANCEMENT OF FLAME RETARDANCY OF POLYETHYLENE AND
POLYPROPYLENE BLENDS BY CYCLIC PHOSPHAZENE ADDITIVES**

submitted by **MUZAFFER KAAN KARAÖZ** in partial fulfillment of the requirements for the degree of **Doctor of Philosophy in Polymer Science and Technology Department, Middle East Technical University** by,

Prof. Dr. Halil Kalıpçılar
Dean, Graduate School of **Natural and Applied Sciences**

Prof. Dr. Necati Özkan
Head of Department, **Polymer Science and Technology**

Prof. Dr. İsmail Teoman Tinçer
Supervisor, **Polymer Science and Technology Dept., METU**

Prof. Dr. Yunus Karataş
Co-Supervisor, **Chemistry Dept., Kırşehir Ahi Evran University**

Examining Committee Members:

Prof. Dr. Halil İbrahim Ünal
Chemistry Dept., Gazi University

Prof. Dr. İsmail Teoman Tinçer
Polymer Science and Technology Dept., METU

Prof. Dr. Ülkü Yılmazer
Chemical Engineering Dept., METU

Prof. Dr. Ahmet Muhtar Önal
Polymer Science and Technology Dept., METU

Prof. Dr. Murat Şen
Chemistry Dept., Hacettepe University

Date: 20.06.2018

I hereby declare that all information in this document has been obtained and presented in accordance with academic rules and ethical conduct. I also declare that, as required by these rules and conduct, I have fully cited and referenced all material and results that are not original to this work.

Name, Last name: Muzaffer Kaan Karaöz

Signature:

ABSTRACT

ENHANCEMENT OF FLAME RETARDANCY OF POLYETHYLENE AND POLYPROPYLENE BLENDS BY CYCLIC PHOSPHAZENE ADDITIVES

Karaöz, Muzaffer Kaan

Ph. D., Department of Polymer Science and Technology

Supervisor: Prof. Dr. İsmail Teoman Tinçer

Co-Supervisor: Prof. Dr. Yunus Karataş

June 2018, 132 pages

The objective of this study is the analysis of mechanical, physical, thermal and flame retardant properties of polyolefin blends of polyethylene (PE) and polypropylene (PP) containing non-halogenated cyclic phosphazenes. The thermal and flame retardant characteristics of blends were tested by methods Differential Scanning Calorimetry, Thermal Gravimetric Analysis, Underwriters Laboratory Test (UL-94), Limiting Oxygen Index, and Cone Calorimeter tests. Finally, the samples were characterized by mechanical tests and Scanning Electron Microscopy.

Non-halogenated cyclic phosphazenes were synthesized by using hexachlorocyclotriphosphazenes (HCTP) via nucleophilic substitution reactions. Cyclic phosphazenes of hexaphenoxycyclotriphosphazene (HPCTP) and hexakis(propylamino)cyclotriphosphazene (HPACTP) were produced following the reactions of HCTP with phenol and propyl amine, respectively.

In the progress of the thesis, the blends of PE and PP with HPCTP and HPACTP were prepared by adding cyclic phosphazenes at 10%, 20% and 30% by weight. Blends were characterized accordingly.

Aromatic structure of HPCTP is responsible for having high values of limiting oxygen index and good performances of UL-94 and cone calorimeter tests for both PE-HPCTP and PP-HPCTP blends in comparison to blends prepared with HPACTP which has an aliphatic structure. PP-HPCTP blend with 20% of HPCTP by weight is the best choice in terms of mechanical properties in all the flame retardant blends.

Keywords: Flame Retardancy, Mechanical Properties, Polyethylene, Polypropylene, Cyclic Phosphazenes, Polymer Blends

ÖZ

HALKALI FOSFAZEN KATKILARI İLE POLİETİLEN VE POLİPROPİLEN KARIŞIMLARININ ALEV GECİKTİRİCİLİĞİNİN GELİŞTİRİLMESİ

Karaöz, Muzaffer Kaan

Doktora, Polimer Bilim ve Teknolojisi Bölümü

Tez Yöneticisi: Prof. Dr. İsmail Teoman Tinçer

Ortak Tez Yöneticisi: Prof. Dr. Yunus Karataş

Haziran 2018, 132 sayfa

Bu çalışmanın amacı, halojensiz halkalı fosfazenler içeren polietilen (PE) ve polipropilen (PP) ile hazırlanmış poliolefin karışımlarının mekanik, fiziksel, termal ve alev geciktirici özelliklerini incelemektir. Polimer karışımlarının termal ve alev geciktirici özellikleri Diferansiyel Taramalı Kalorimetre, Termal Gravimetrik Analiz, Underwriters Laboratuvar Testi (UL-94), Sınırlayıcı Oksijen İndeksi ve Konik Kalorimetre testlerinin uygulanması sonucu incelenmiştir. Numuneler, mekanik testler ve Taramalı Elektron Mikroskobu ile karakterize edilmiştir.

Halojensiz halkalı fosfazenler, heksaklorosiklotrifosfazenden (HCTP) nükleofilik yer değiştirme reaksiyonları ile sentezlenmiştir. HCTP'nin fenol ve propil amin ile reaksiyonları neticesinde heksafenoksisiklotrifosfazen (HPCTP) ve heksakis(propilamino)siklotrifosfazen (HPACTP) sentezlenmiştir.

Tezin ilerleyişinde, HPCTP ve HPACTP katkılarının ağırlıkça %10, %20 ve %30 derişimlerde eklenmesi ile PE ve PP karışımları hazırlanmıştır. Karışımlar karakterize edilmiştir.

Alifatik yapıya sahip HPACTP ile hazırlanan karışımlar ile karşılaştırıldığında, PE-HPCTP ve PP-HPCTP karışım gruplarının her ikisinin de daha yüksek sınırlayıcı oksijen indeksi değerlerine sahip olmaları ve UL-94 ile konik kalorimetre testlerinde iyi performans göstermeleri HPCTP'nin aromatik yapısının bir sonucudur. Tüm alev geciktirici karışımlar arasında en iyi mekanik özelliklere sahip olan karışım, ağırlıkça %20 HPCTP ile hazırlanmış PP karışımıdır.

Anahtar Kelimeler: Alev Geciktiricilik, Mekanik Özellikler, Polietilen, Polipropilen, Halkalı Fosfazenler, Polimer Karışımları.

To Melodi

ACKNOWLEDGMENTS

I would first like to thank my thesis supervisor Prof. Dr. İsmail Teoman Tinçer for his guidance, support, encouragement and understanding. His critics and advices widened my vision and gave me a good chance for advancement in my thesis. I always feel lucky to be his student.

I wish to express my thanks to my co-supervisor Prof. Dr. Yunus Karataş for his great effort and trust. His kind supports gave me the chance of acceleration and new perspectives in my study.

I would like to acknowledge my thesis supervising committee members Prof. Dr. Ülkü Yılmaz, Prof. Dr. Ahmet Muhtar Önal and Prof. Dr. Erdal Bayramlı and my thesis jury members Prof. Dr. Halil İbrahim Ünal and Prof. Dr. Murat Şen for their constructive criticism and important contributions.

For their friendship and invaluable assistances, I wish to express my sincere thanks to Dr. Ümit Tayfun, Burak Gündüz, Sümeyye Köybaşı, Dr. Tuğba Kaya Deniz, Burcu Koç Haskılıç, Dr. Dursun Can Özcan, Nedim Altan Yılmaz, Dr. Yurdaer Babuçuoğlu and Dr. Aydın Mert Akgün. In addition, I would also like gratefully thank to all my colleagues from METU, TÜBİTAK and Kırşehir Ahi Evran University for their companionship.

I would like to express my heartfelt thanks to all my family members for their support and kindness all through my life.

And with my sincerest feelings, I would like to thank ma belle femme Melodi Pak Karaöz for her inspiring ideas, limitless patience, tenderness and precious heart. All the things of life become possible, smooth and beautiful by her love.

TABLE OF CONTENTS

ABSTRACT.....	v
ÖZ	vii
ACKNOWLEDGMENTS	x
TABLE OF CONTENTS.....	xi
LIST OF TABLES	xv
LIST OF FIGURES	xvi
LIST OF EQUATIONS	xviii
LIST OF ABBREVIATIONS	xix
CHAPTERS	
1. INTRODUCTION.....	1
2. BACKGROUND INFORMATION.....	5
2.1 Polyolefins	5
2.1.1 Polyethylene.....	5
2.1.2 Polypropylene	7
2.2 Property of flame retardancy	8
2.3 General Approaches to Obtain Flame Retardancy	9
2.3.1 Additive Approach.....	10
2.4. Flame Retardant Additives	10
2.4.1 General Mechanism of Flame Retardant Additives.....	10
2.4.2 Types of Flame Retardants	13
2.4.2.1 Halogenated flame retardants.....	15
2.4.2.2. Phosphorus-based flame retardants	15
2.4.2.3. Mineral filler flame retardants.....	16

2.4.2.4 Intumescent flame retardants	17
2.4.2.5 Polymer nanocomposites	19
2.4.2.6 Inorganic flame retardants	20
2.5. Phosphazenes	21
2.5.1. Polyphosphazenes	22
2.5.2. Cyclic phosphazenes	23
2.6. Fundamentals of Polymer Blends	25
2.6.1 Immiscible Polymer Blends	27
2.6.2 Miscible Polymer Blends	28
2.6.3 Compatible Polymer Blends.....	29
2.7 Characterization Methods	30
2.7.1 Nuclear Magnetic Resonance (NMR)	30
2.7.2 Underwriters Laboratory Test, UL-94	31
2.7.3 Limiting Oxygen Index (LOI).....	33
2.7.4 Thermal Gravimetric Analysis (TGA)	35
2.7.5 Differential Scanning Calorimetry (DSC).....	35
2.7.6 Cone Calorimeter	36
2.7.7 Tensile Tests.....	39
2.7.8 Scanning Electron Microscopy (SEM)	41
2.8 Production Methods of Polymer Blends	42
2.8.1 Extrusion	42
2.8.2 Injection Molding	43
2.8.3 Compression Molding	43
3. EXPERIMENTAL.....	45
3.1 Materials	45
3.2 Synthesis of Hexaphenoxycyclotriphosphazene (HPCTP).....	47

3.3 Synthesis of Hexakis(propyl amino) cyclotriphosphazene (HPACTP).....	48
3.4 Characterization Methods	50
3.4.1 NMR.....	50
3.4.2 Differential Scanning Calorimetry (DSC)	50
3.4.3 Thermal Gravimetric Analysis (TGA).....	50
3.4.4 Underwriters Laboratory UL-94 Test	50
3.4.5 Limiting Oxygen Index (LOI).....	51
3.4.6 Thermal Gravimetric Analysis (TGA).....	51
3.4.7 Differential Scanning Calorimetry (DSC)	51
3.4.8 Cone Calorimeter	51
3.4.9 Tensile Tests.....	51
3.4.10 Scanning Electron Microscopy	52
3.5 Preparation of PE and PP Blends with Phosphazene Derivatives and Their Characteristics.....	53
3.5.1 Sample Preparation for the Characterization of the Blends.....	53
4. RESULTS AND DISCUSSION	57
4.1 The Thermal Properties of Cyclic Phosphazenes	58
4.1.1 Hexaphenoxycyclotriphosphazene (HPCTP).....	58
4.1.1.1 Thermogravimetric Analysis (TGA) for HPCTP	59
4.1.1.2 Differential Scanning Calorimetry (DSC) for HPCTP.....	60
4.1.2 Hexakispropylaminocyclotriphosphazene (HPACTP)	62
4.1.2.1 Thermogravimetric Analysis (TGA) for HPACTP	62
4.1.2.2 Differential Scanning Calorimetry (DSC) for HPACTP.....	64
4.2 The Mechanical Properties of Polyolefins and Cyclic Phosphazenes Blends	66
4.2.1 Tensile Properties of PE-HPCTP and PE-HPACTP Blends.....	66
4.2.2 Tensile Properties of PP-HPCTP and PP-HPACTP Blends	68

4.2.3 SEM Analysis of PE-HPCTP and PE-HPACTP Blends.....	70
4.2.4 SEM Analysis of PP-HPCTP and PP-HPACTP Blends	73
4.3 Thermal Properties of Polyolefins and Cyclic Phosphazenes Blends	75
4.3.1 PE-HPCTP and PE-HPACTP Blends	75
4.3.1.1 Thermogravimetric Analysis (TGA) for PE-HPCTP and PE-HPACTP Blends.....	76
4.3.1.2 Differential Scanning Calorimetry (DSC) for PE-HPCTP and PE-HPACTP Blends.....	79
4.3.2 PP-HPCTP and PP-HPACTP Blends.....	83
4.3.2.1 Thermogravimetric Analysis (TGA) for PP-HPCTP and PP-HPACTP Blends.....	84
4.3.2.2 Differential Scanning Calorimetry (DSC) for PP-HPCTP and PP-HPACTP Blends.....	86
4.4 Flame Retardancy of Polyolefins and Cyclic Phosphazenes Blends	91
4.4.1 PE-HPCTP and PE-HPACTP Blends	91
4.4.1.1 Limiting Oxygen Index (LOI) for PE-HPCTP and PE-HPACTP Blends	91
4.4.1.2 UL-94 for PE-HPCTP and PE-HPACTP Blends	94
4.4.1.3 Cone Calorimetry for PE-HPCTP Blends	95
4.4.2 PP-HPCTP and PP-HPACTP Blends.....	98
4.4.2.1 Limiting Oxygen Index (LOI) for PP-HPCTP and PP-HPACTP Blends	98
4.4.2.2 UL-94 for PP-HPCTP and PP-HPACTP Blends.....	100
4.4.2.3 Cone Calorimetry of PP-HPCTP Blends.....	101
5. CONCLUSIONS	105
REFERENCES.....	111
APPENDIX.....	127
NMR SPECTRA OF HPCTP AND HPACTP	127
CURRICULUM VITAE	131

LIST OF TABLES

TABLES

Table 2.1 Main differences between the types of polymer blends [152].	26
Table 2.2 Criteria for UL-94 classifications (time in seconds) [162].....	33
Table 3.1 The properties of materials.....	46
Table 4.1 $T_{5\%}$, $T_{50\%}$ and T_{\max} values of Hexaphenoxycyclotriphosphazene (HPCTP) under the conditions of N_2 atmosphere	60
Table 4.2 T_m and ΔH_m values of hexaphenoxycyclotriphosphazene (HPCTP) under the conditions of N_2 atmosphere	62
Table 4.3 TGA of Hexakispropylaminocyclotriphosphazene (HPACTP) under the conditions of N_2 atmosphere	64
Table 4.4 DSC Data of Hexakispropylaminocyclotriphosphazene (HPACTP) under the conditions of N_2 atmosphere	65
Table 4.5 Tensile Test Results of PE-HPCTP and PE-HPACTP Blends	67
Table 4.6 Tensile Test Results of PP-HPCTP and PP-HPACTP Blends.....	70

LIST OF FIGURES

FIGURES

Figure 2.1 Molecular formula of polyethylene.	5
Figure 2.2 Branching structures of polyethylene [6].....	6
Figure 2.3 Molecular formula of polypropylene	7
Figure 2.4 General structures of polypropylene: (a) isotactic, (b) syndiotactic and (c) atactic [1], [13].	8
Figure 2.5 General schematic of polymer decomposition and burning [17].....	9
Figure 2.6 General mechanisms of flame retardant additives [24].	12
Figure 2.7 Representative structures of phosphazenes [52].	22
Figure 2.8 General structure of polyphosphazenes. R can be organic or organometallic or a combination of different functional groups [61].	23
Figure 2.9 General reaction scheme for the preparation of hexa-substituted cyclo (organophosphazene)s. [113].	24
Figure 2.10 Variation of polymer blend property as a function of composition [153].	28
Figure 2.11 The schematic view of the UL-94 test [162].	32
Figure 2.12 The schematic view of the LOI test [162].	34
Figure 2.13 Schematic representation of cone calorimeter [162].	37
Figure 2.14 Characteristic HRR curves for different typical burning behaviours [167].	39
Figure 2.15 Stress-strain curve for a typical crystalline polymeric material [169]..	40
Figure 3.1 Synthesis route of hexaphenoxycyclotriphosphazene (HPCTP).	47
Figure 3. 2 Synthesis route of hexakis(propyl amino) cyclotriphosphazene (HPACTP).....	49
Figure 3.3 The photograph of tensile test machine used in this study.	52
Figure 3.4 The twin screw extruder used in this study for the production of blends.	54
Figure 3.5 The laboratory scale injection-molding machine.....	55

Figure 4.1 TG and DTG Curve of Hexaphenoxycyclotriphosphazene (HPCTP) under the conditions of N ₂ atmosphere.	59
Figure 4.2 DSC Curve of hexaphenoxycyclotriphosphazene (HPCTP) under the conditions of N ₂ atmosphere	61
Figure 4.3 TG and DTG Curve of Hexakispropylaminocyclotriphosphazene (HPACTP) under the conditions of N ₂ atmosphere	63
Figure 4.4 DSC Curve of Hexakispropylaminocyclotriphosphazene (HPACTP) under the conditions of N ₂ atmosphere	65
Figure 4.5 Stress-strain Curve of PE-HPCTP and PE-HPACTP Blends.....	68
Figure 4.6 Stress-strain Curve of PP-HPCTP and PP-HPACTP Blends.	69
Figure 4.7 SEM micrographs of fractured surfaces of PE-HPCTP and PE-HPACTP blends.	72
Figure 4.8 SEM micrographs of fractured surfaces of PP-HPCTP and PP-HPACTP blends.	74
Figure 4.9 TG Curve of PE-HPCTP and PE-HPACTP Blends under the conditions of N ₂ atmosphere.....	76
Figure 4.10 DTG Curves of PE-HPCTP and PE-HPACTP Blends.....	77
Figure A.1 ¹ H NMR spectrum synthesized hexaphenoxycyclotriphosphazene (HPCTP).....	127
Figure A.2 ¹³ C NMR spectrum synthesized hexaphenoxycyclotriphosphazene (HPCTP).....	128
Figure A.3 ³¹ P NMR spectrum synthesized hexaphenoxycyclotriphosphazene (HPCTP).....	128
Figure A.4 ¹ H NMR spectrum synthesized Hexakispropylaminocyclotriphosphazene (HPACTP).....	129
Figure A.5 ¹³ C NMR spectrum synthesized Hexakispropylaminocyclotriphosphazene (HPACTP).	129
Figure A.6 ³¹ P NMR spectrum synthesized Hexakispropylaminocyclotriphosphazene (HPACTP).....	130

LIST OF EQUATIONS

EQUATIONS

Equation 2.1 Limiting oxygen index calculation	33
Equation 2.2 Engineering stress.....	40
Equation 2.3 Engineering strain.....	40
Equation 2.4 Modulus of elasticity	41
Equation 4.1 Percent Crystallinity Calculation.....	79

LIST OF ABBREVIATIONS

ABS	Acrylonitrile butadiene styrene
DSC	Differential Scanning Calorimetry
DTG	Differential Thermal Gravimetric
EPDM	Ethylene propylene diene monomer
HCTP	Hexachlorocyclotriphosphazene
HDPE	High density polyethylene
HPACTP	Hexakis(propylamino)cyclotriphosphazene
HPCTP	Hexaphenoxycyclotriphosphazene
LDPE	Low density polyethylene
LLDPE	Linear low density polyethylene
LOI	Limiting Oxygen Index
NMR	Nuclear Magnetic Resonance
PA	Polyamide
PA6	Polyamide 6
PA6,6	Polyamide 6,6
PE	Polyethylene
PE-HPCTP	Polyethylene blends prepared with hexaphenoxycyclotriphosphazene
PE-HPACTP	Polyethylene blends prepared with hexakis(propylamino)cyclotriphosphazene
PHRR	Peak heat release rate
PP	Polypropylene
PP-HPCTP	Polypropylene blends prepared with hexaphenoxycyclotriphosphazene
PP-HPACTP	Polypropylene blends prepared with hexakis(propylamino)cyclotriphosphazene
PPO	Polyphenylene oxide

SEM	Scanning Electron Microscopy
T _{5%}	5% decomposition temperature
T _{50%}	50% decomposition temperature
T _{max}	Maximum decomposition temperature
TG	Thermal Gravimetric
TGA	Thermal Gravimetric Analysis
THE	Total heat evolved
THE/TML	Total-heat-evolved / total-mass-loss ratio
TML	Total mass loss
TTI	Time to ignition
T _m	Melting point temperature
ΔH _m	Enthalpy of melting
ΔH ^o _m	Enthalpy of melting value for 100 % crystalline polymer
χ%	Percent crystallinity
Φ	Mass fraction of additives

CHAPTER 1

INTRODUCTION

Polyolefins are a division of heavily produced polymers. Polyethylene (PE) and polypropylene (PP) are two important members of this class. Typical uses of them can be classified in such diverse applications including films, plastic and fibre. PE and PP have always a major role in polymer applications with respect to their versatile characteristics. They, for example, enable the final products gaining desirable properties in a more economical way in comparison to other alternative materials. Polyolefins give opportunity to researchers and producers to propose new ways of study and particular solutions. The examples of these applications may range from well-designed automobile parts with suitable mechanical properties to inexpensive production of medical components. Furthermore, PE and PP have the potential of gaining new characteristics by preparation of polyolefin blends with proper additives. The weakness of these polymers is their ease of flammability. Flame retardancy with desirable mechanical properties is one of the examples of these characteristics. In this research, it is aimed to provide the property of low flammability to polyolefins by blending them with compatible compounds [1].

Flame retardancy is inhibition or resistance to the ignition and spreading of fire. Flame retardant materials are added for inhibition of the vapour-phase combustion of fuel gases, alteration of thermal degradation pathway of polyolefins creating an insulation coating protecting against thermal energy. A flame retardant polymeric material can be prepared by the help of various approaches [2]. In one of these methods, “reactive method”, a co-monomer with property of flame retardancy is used during polymerization reaction of flame retardant polymer.

In the other method, “the surface approach”, the grafting of the flame retardant materials is applied to obtain surface modified compound. The other most commonly used “additive method” is applied in which flame retardant additives are blended with polymer melt in the course of mixing process. In this study, the last approach is employed.

The general types of flame retardant additives can be divided into subgroups as minerals (such as antimony trioxide, boron compounds, and aluminium hydroxides), halogenated organic compounds and synthetic inorganic materials like phosphazenes which will be explained in detail in Chapter 2. Although the most efficient flame retardant additives are the halogen containing compounds, their use is limited and restricted because firstly the combustion reaction products of halogenated additives exhibit toxicity. Another disadvantage is their harmful characteristics to the ozone layer of the atmosphere. In this study, hexachlorocyclotriphosphazene (HCTP) was used as a starting point for the synthesis of halogen-free phosphazenes derivatives aiming to introduce flame retardant characteristics to polyolefins by blending with them.

HCTP is one of the well-known and most widely studied materials among phosphazenes which comprise a diverse class of compounds which share the common characteristic of a formally saturated phosphorus-nitrogen skeletal bond resulting in unique properties. Different kinds of phosphazene derivatives have been synthesized as a result of substitution reactions of chlorine atoms. The flame retardant cyclic phosphazene derivatives can thus be designed by replacing the chlorine atoms with proper side groups. As a first objective of this study, it is aimed to obtain two derivatives of HCTP as suitable candidates of flame retardant additives. For this purpose, two different phosphazenes with aromatic and with aliphatic side groups were synthesized. Chlorine atoms on HCTP were replaced via nucleophilic substitution reactions with phenoxy groups in order to obtain hexaphenoxycyclotriphosphazene (HPCTP), the first additive. As the second additive, hexakis(propylamino)cyclotriphosphazene (HPACTP) was synthesized via

the reaction of HCTP with propyl amine in the presence of excess triethylamine. The structures of these two compounds were confirmed with ^1H , ^{13}C and ^{31}P NMR spectra. They were in accordance with the values given in the literature [3], [4].

One of the focuses of this research is mixing the targeted non-halogenated phosphazenes with polyolefins to enhance the flame retardant properties. For this purpose, firstly the polymer blends were prepared by using melt mixing of polyolefins with the synthesized phosphazenes. Using melt mixing process, PE and PP were blended with HPCTP and HPACTP additives, respectively. Four different classes of polymer blends with varying additive contents were obtained which were named as PE-HPCTP, PE-HPACTP, PP-HPCTP and PP-HPACTP. Test samples of these blends were prepared with the help of injection molding process. Mechanical tests were applied onto the test samples for their characterizations. Furthermore, Scanning Electron Microscopy (SEM) micrographs were obtained to observe distribution of additives within the PE and PP matrix.

The main objective of this study was the preparation and the analysis of flame retardant properties of polymer blends of polyolefins and non-halogenated phosphazenes. The flame retardancy and thermal properties of the blended polymers were investigated by application of test methods including Underwriters Laboratory (UL-94), Limiting Oxygen Index (LOI), Differential Scanning Calorimetry (DSC), Thermal Gravimetric Analysis (TGA) and Cone Calorimeter tests. The results of these tests were presented together with the outcomes of mechanical tests and SEM in the following sections.

CHAPTER 2

BACKGROUND INFORMATION

2.1 Polyolefins

Polyolefins comprise polymer group with numerous types of polyethylene (PE) and polypropylene (PP). Low-density polyethylene (LDPE) and high-density polyethylene (HDPE) can be presented as two extreme degrees. Polypropylene is another type of plastic under the group of polyolefins with light weight and high melting point [1].

2.1.1 Polyethylene

Ethylene is one of the most important members of petrochemicals. Various techniques of polymerization enable the synthesis of low-molecular weight waxes, polyethylene with a high degree of crystallinity and high molecular weight polyethylene. Imperial Chemical Industries in England manufactured low-density polyethylene (LDPE) in a low crystalline form firstly in 1939 and exploited it for profit. Polyethylene molecular formula is presented in Figure 2.1.

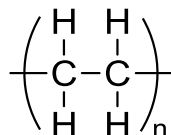


Figure 2.1 Molecular formula of polyethylene.

LDPE has typical density values varying from 0.912 to 0.935 g/cm³. LDPE has stable, flexible and tough characteristics at around 20°C and is resistant to the temperature values till 80°C. Branching structure of LDPE is observed in a clearer way than HDPE. In Figure 2.2, illustrations are given for these different types of polyethylene which are LDPE, HDPE and linear low density polyethylene (LLDPE) [5], [6].

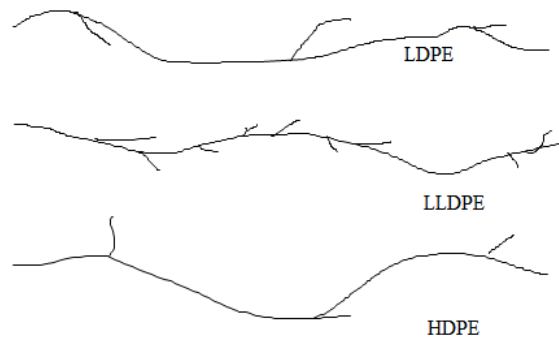


Figure 2.2 Branching structures of polyethylene [6]

Due to side branching, LDPE has low crystallinity and has a low density. Resulting from the branching, LDPE is amorphous around 50% and sheets can allow flowing-through of liquids and gases. Branching and less crystalline structure results in a melting point around 100 °C for LDPE. A melting point around 100 °C is a quite low number regarding the applications needing sterilization by using boiling water. LDPE has a structure with a combination of short and long branches. Ratio of short branch to long branch is one [6], [7].

2.1.2 Polypropylene

Polypropylene (PP) is one of the members of thermoplastic polymers. In comparison to similar polymers, PP has a low cost, and many uses in different sectors like medical, automotive, decoration and furnishing. Density values change between 0.90 and 0.91 g/cm³ [1], [7]. The melting point of PP varies from 145 ° to 195 °C. The changes in melting point occur as a result of different crystalline structures during processing [8], [9]. Since PP is highly flammable polymer, flame retardant property is required and has an important role in industrial applications [10]–[12].

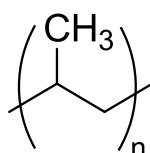


Figure 2.3 Molecular formula of polypropylene

Molecular structure of polypropylene is written above, in Figure 2.3. Depending on the arrangement of pendant methyl groups, three different PP are known. Those are listed as atactic, isotactic and syndiotactic polymers. The structural details of these general classes of polypropylenes are illustrated in Figure 2.4. Isotactic polymers have a higher crystalline structure than syndio- and atactic polypropylenes. The crystallinity values of typical isotactic polypropylenes are observed between 40 and 70%. The melting point of isotactic PP is the highest one (160°C –180°C) as well as density and strength are higher than those of syndiotactic and atactic forms [13].

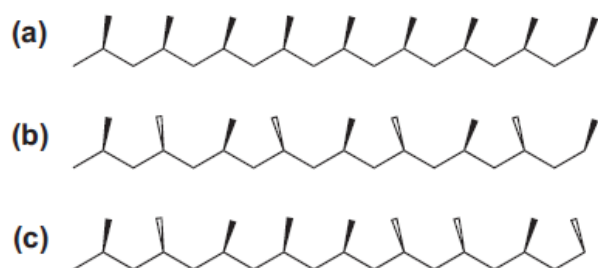


Figure 2.4 General structures of polypropylene: (a) isotactic, (b) syndiotactic and (c) atactic [1], [13].

2.2 Property of flame retardancy

A large number of flame retardants have been evolved for polymers. More than 150 different flame retardant compounds are available in the market [14]. Flame retardants can be broadly divided into two main groups as additives and reactive compounds. Blends of additive compounds with polymers are prepared by processing with no chemical reaction. The polymerization of reactive compounds through a resin is followed by addition into the networks. Effect of two different types of flame retardants are investigated by blending them with polyethylene and polypropylene. As the additive approach is covered in this study, this approach is explained more in detail as below [14].

Flame retardant additives can be divided into two main groups: additives containing halogen, phosphorus, nitrogen, silicon boron and miscellaneous inorganic additives [2], [14]–[16]. Phosphorus and nitrogen based flame retardant compounds are the main focus of this study. Accordingly, the information is presented mainly on these flame retardants in the following sections.

2.3 General Approaches to Obtain Flame Retardancy

Polymer combustion is the result of sequences which are pyrolysis of solid material (polymer) into smaller portions, volatilization, mixing with oxygen, and finally combustion. At the end of this event, a large amount of heat is released during polymer combustion. Therefore the pyrolysis stage on the remaining surface of the polymer exposed to the radiation of heat continues to be driven and combustion does not stop until the level of oxygen, fuel or heat is diminished. After that the fire is extinguished. This explanation is actually simple, on the other hand it covers all the basics of polymer combustion. Thermoplastic polymers have an approach towards dripping and flowing at the conditions of fire. This situation can give rise to further mechanisms in spreading of flames. Opposite to the thermoplastic polymers, thermoset polymers do not drip and flow. Pyrolysis gases are released from the surface of the compound into the condensed phase in a direct manner. A general diagram of these stages is demonstrated in Figure 2.5 [17].

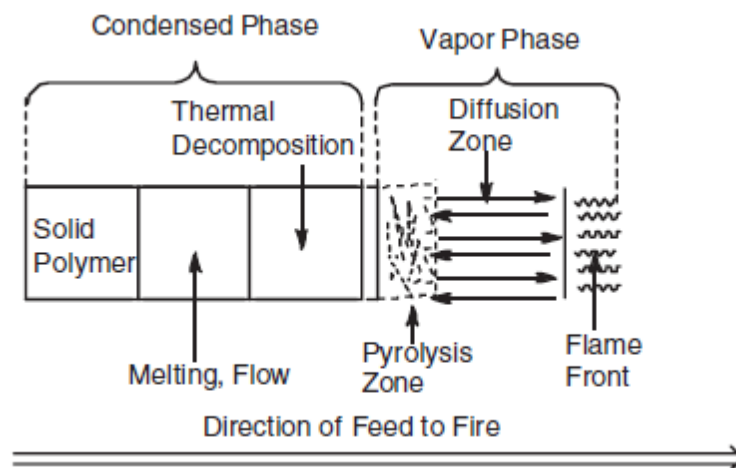


Figure 2.5 General schematic of polymer decomposition and burning [17].

2.3.1 Additive Approach

The synthesis and applications of halogen free cyclic phosphazene based flame retardant additives constitute the main focus of this work. Additive approach finds more place in practical applications, since this option offers a more economical alternative, quite facile incorporation of the additives into a polymer network and there exists a large amount of knowledge on this issue [17].

It should be highlighted that a flame retardant material is a chemical used for a special application just like the other types of chemicals (a pharmaceutical in medical applications or a pigment in textile uses). The uniqueness of a flame retardant additive other than a pigment or a pharmaceutical is its exclusive target which is minimization of flammability [14], [16], [17].

2.4. Flame Retardant Additives

Chemical structures of flame retardant additives and generalized mechanisms of action are the main parameters while dealing with types of flame retardant additives. Chemical and physical actions, individually or together, for all flame retardants are experienced in the condensed phase with or without the gas phase. These actions interfere with minimum one separate step of burning process [16], [18]. It is expected that a flame retardant additive affect more than one of these stages either physically or chemically, in an efficient manner. Flame retardant additive results in a retarded burning process and eliminates the burning mechanism, finally [19].

2.4.1 General Mechanism of Flame Retardant Additives

The materials performing as flame retardants which are active in gas phase take action by removing free radicals. Variations and continuations of chain reactions within fire are carried out by these molecules. Mechanism in the gas phase occurs chemically in this manner. Some types of the flame retardant compounds generate

large amounts of gases that are not combustible. They have an effect of dilution on the combustible gases, endothermic decomposition and reduction of the temperature as a result of heat absorption. This can be explained briefly by the gas phase physical action mechanism [18], [19].

The additives perform in two distinctive styles of action when condensed phase mechanism is considered. At a first glance, flame retardant additives have an effect in acceleration for degrading of polymeric substance and increasing the dripping behaviour of the polymer. As polymer drips at a relatively high rate, fuel source is taken from burning area. Secondly, a char layer of carbon on the surface of polymer can be left by these compounds [19]. This formation of swelling char serves as a barrier acting physically for reduction of both mass and heat transfers, respectively. This occurs between the phases of gas and condensed matter. Hence, the material beneath of charring surface is protected from the effect of flame. The amount of the char is critical for flame retardancy effect in the system of intumescence environment as well as with other properties which are structure of foam, integral nature and stable characteristics. The major advantage of this network comes across as a decreasing trend in amount of heat produced while burning occurs owing to carbon formation apart from the evolution of the gases of CO and CO₂ [20]–[23]. The scheme of common mechanisms concerning flame retardancy by additives is shown in Figure 2.6 [24].

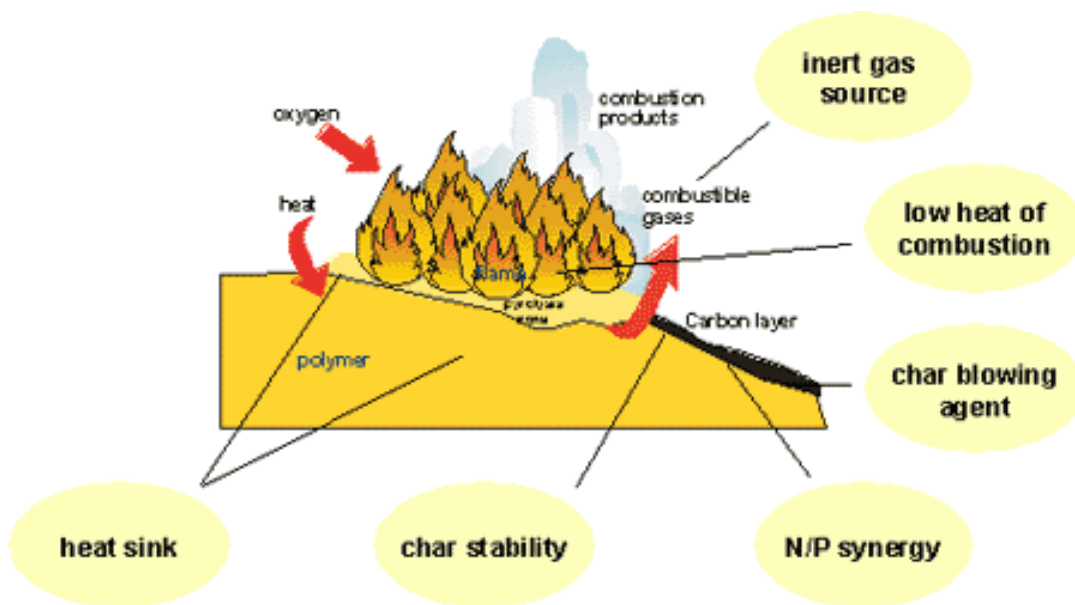


Figure 2.6 General mechanisms of flame retardant additives [24].

As each step of series of burning is taken into consideration, initially, heating step is resulted by a glassy layer forming while an effective flame retardant is present in the fire environment. This layer of coating has low thermal conduction performance as well as with/without high reflection property enabling for repelling heat radiation from the outer source before the substrate is decomposed extensively. A layer of intumescent formation is produced by swelling of additive compounds on heating. These compounds are the examples of additives with flame retardancy which produce a layer on surface at a low level of conduction thermally. [11], [18].

Continuation of degrading and decomposing steps of the combustion course, the destruction of specimen in a thermally oxidative process in which the substrate tends to locate in flammability range is prevented in a chemical way by the additive. It is desired to have less concentration of burnable gases. For reaching this target, charring is promoted by reactions of dehydration and hydrogenation. Therefore, this has an effect in decreasing of amount of burnable hydrocarbon gases [11].

Then, ignition step follows in the sequence of combustion reaction. Effect of potentially flame retardant additive can be resulted from various routes. Mainly, ignition step is prevented during combustion reaction by some mechanisms tending to augment the amount of non-burnable decomposition gases or to diminish the synthesis of half of gases with flammability. This will result in inhibition of combustion reaction while stage of ignition takes place. As well as with these mentioned ways, the flame retardant substance may, additionally, generate, resulting in its own degrading or interacting with the specimen, molecules of scavenging free radicals. Reduction in flame flow is experienced by inhibition effect of these gaseous species. This effect results from interacting with radicals like OH radicals with a very high energy which give a rise to chain propagation., Another additional effect of a gas with a highly density is to offer blanket effect over burnable surface and exclusion of required oxygen which is essential in stage of ignition. [11].

Heat transfer rate at the interface between surroundings and upper boundary of combusting species is another critical point while dealing with the post steps of combusting and propagating in which the sample is already ignited. While heat transfer rate decreases, stages of combusting and propagation can be hindered. For example, a flame retardant additive may produce particles within pre-flaming areas. Particles may create a smoky layer that shields the energy radiating thermally coming from the flaming area. [11].

2.4.2 Types of Flame Retardants

Generally, chemistries of attainable and present flame retardants can be classified into six groups which are halogenated, phosphorous-based, mineral filler, intumescent, polymer nanocomposites and inorganic. While polymerization or melt mixing of thermoplastic compound, normal additives are applied which do not form chemical bonds with the polymer. Ordinary flame retardant materials are applied, and they constitute the portion of the formulated polymers. Whereas, reactively active additives join to the polymer chain during the polymerization. Following the

processing stage, they may also form bond on the polymer back bone. By a post-polymerization stage, they follow a route of copolymerization of a monomer or grafting onto polymer chain. Thus, reactive type additives are less frequent than the common ones [17].

At least one type of flame retardancy mechanism over three mechanisms are observed through flame retardant chemistry. Gas phase flame retardancy effect, endothermically effective flame retardancy, and flame retardancy by char formation are these three mechanisms and a summation is given below:

1. Gas phase flame retardants:

These retardants reduce the heat releases during combustion by removing reactive free radicals generated during combustion. Halogens and phosphorus based materials can be given as examples.

2. Endothermic flame retardants:

These materials are active in the gas phase and condensed phase. Non-flammable gases are released by decomposing flame retardants. Then flammable gas content is diluted. The polymer is cooled due to endothermic decomposition of flame retardants. The pyrolysis rate is slowed down by decreased temperature of substrate. A protection layer is formed over polymer surface. Metal hydroxides and carbonates are some examples of endothermically active flame retardants.

3. Char-formation based flame retardants:

These types of materials serve in the condensed phase and they prevent release of fuel by means of covering fuel in the form of non-pyrolyzing char (carbon). Therefore, the polymer beneath the char is thermally insulated and protected by formation of char layers [17]. For instance, intumescent and nanocomposites fall into char-forming flame retardants.

2.4.2.1 Halogenated flame retardants

Halogenated flame retardants include elements from group VII of the periodic table which are I, Br, Cl and F. They can differentiate largely in their chemical structures. They vary from aliphatic to aromatic carbon substrates in which all the hydrogens are replaced with halogens or inorganic formulations. Through these examples, organohalogen materials reach the most effective level as flame retardant additives for polymers [10]. Organochlorines and organobromines are applied more commonly and the organobromine materials are the most applied ones resulting in the characteristic C-Br bond, proper for fire preventions. The stability of the bond is enough for handling and preparation of the flame retardant blends and the bond is unstable enough to be broken by heat during combustion. Then, the bromine is liberated at the conditions of fire for inhibition of free radical reactions. It should be taken into consideration that flame retardant additives with halogens will be under closer watch and the trade of them should be regulated globally. Through these regulation actions, these materials will be eliminated with time from the list due to the reason that they exhibit toxicity. Therefore, reactive type flame retardants and easy-recyclable derivatives are the focuses of newly applied methods.

2.4.2.2. Phosphorus-based flame retardants

As the name indicates, phosphorus-based flame retardants include incorporated phosphorus into the structure, and many variations of the structure are observable from inorganic to organic types, through oxidation states (0, +3, +5) [25]. It is not economical to synthesize phosphorus-carbon bonds directly and not easy to obtain, then the majority of phosphorus-based flame retardants are converged with the bonds of phosphorus and oxygen bonds with attachments of organic groups to the oxygen, though some flame retardant structures include some phosphorus-carbon bonds. Inorganic forms of phosphorus flame retardants also have a tendency to be phosphates, however, as a unique example, red phosphorus, has its own structure and is the sole phosphorus (0) flame retardant in use. On the contrary, white phosphorus, the other elemental form of phosphorus, ignites spontaneously due to its tetrahedral

structure [26]. It is interesting that even a little change in molecular structure results in a material changing from starting fires to serving as a flame retardant. Phosphorus compounds are peculiar materials that they can have flame retardant effect in vapor phase or in condensed phase. Their chemical structure and the way that they interact with the polymer at the conditions of fire affect the flame retardant characteristics in the gas or condensed phase. It is common for a particular phosphorus flame retardant to be effective mainly in vapour phase in one polymer but in condensed phase in another [27]–[30]. Combinations of phosphorus compounds with other flame retardants result in having synergistic effects, however they only demonstrate vapor phase synergy when they are combined with halogen. The combinations with other materials, are usually for improving char formation or oxidative life span of the chars which are the formations by the phosphorus flame retardant [31].

Although the phosphorus based flame retardant technology dates back to 1940s, there has been a growing interest for nearly 20 years of time as halogenated materials are deselected for the reasons of toxicity and environmental scrutiny described previously. As explained above, they can be effective both in vapor and condensed phases, meaning that they can be useful in low loading levels when combined with polymers that inherently char on their own [32]. Moreover, phosphorus flame retardants tend to do well in high heat flux fire conditions, and through char formation, they can provide superior fire protection in combination with other flame retardants [17].

2.4.2.3. Mineral filler flame retardants

Mineral type flame retardant materials exhibit cooling mechanism endothermically concerning flame retardancy and have a sole activity in vapor and condensed phase. Specially, at the conditions of fire the mineral filler endothermically decomposes while they are exposed to heat. This cools the condensed phase, thus, slowing thermal decomposition of the polymer. Moreover, after decomposing of polymer some filler products appear and they do not have any flammable characteristics.

Thus, the remaining material after breaking down of polymer thermally, which is usually a metal oxide, has a potential of dilution for the whole available polymeric substance, in other words, for attainable fuel being in condensed phase. Non-ignitable gas releasing from the mineral filler assists to thin the available gaseous material ignitable. The fillers used widely for purposes of flame retardancy are metal carbonates and metal hydroxides. Certain filler types are synthesized while some of them are produced by mining activities and being used as additives for aims of extinguishing after a process refinery. None of metal hydroxide and metal carbonate has a property of quenching. The carbonate and hydroxide require to have the ability of releasing their own water. Alternatively, carbon dioxide at increased and sufficient temperatures which suit the conditions for the polymer not undergoes decomposition reaction before activation of mineral filler [17].

Mineral fillers are not pioneers of a contemporary technology. On the contrary, they have roots back to beginning of 1920s. Moreover, there exist certain sources indicating that fillers have been practiced since 17th century. Despite everything, mineral fillers are validated and considered as a eco-friendly technology. Additionally, in a fire scenario, they have tendencies for lowering smoke in large amounts and effect in reduction of harmful gaseous material emitted, inclusively. Since, the mineral filler has the ability of substitution of burnable polymeric substance with non-flammable inorganic content. Also, these substances offer quietly economizing options to the market needs and effortless applications in polymers by their ability of being coated with surface active substances easily. [17].

2.4.2.4 Intumescent flame retardants

Name of intumescent flame retardants comes from their characteristic of flame retardancy at fire conditions. Particularly, foaming of carbon with a shield effect is created by intumescent flame retardants during environment of fire. They swell up while heat flow continues. They are precisely active in condensed phase in both two ways including by supplying their own charring surface and using polymer in

generating carbon char. Intumescent generally constitute three elements with ability of forming carbon char. the first one is an acid catalyst and results in crosslinking of carbon containing material, which is the second element. A formation of carbon with thermal stability is obtained by interaction of first and second elements. Finally, spumific agent, also called gas former, is responsible for foamy carbon formation from a carbon substrate. These three elements perform simultaneously to form intumescent structure. Exposing to heat and flame, they exhibit flame retardant effect yet combining of these materials satisfies armoring needs of polymers.

As an example for a common intumescent flame retardant system can be given as the group of ammonium polyphosphate, pentaerythritol and melamine, to which the roles are distributed as acid source, carbon source and spuming/gas forming agent, respectively. Occasionally, each constituent of an intumescent flame retardant system is a distinctive species, which combines to formulate an intumescence material, and, in other examples, all of these three elements share the same structure to form sole intumescent material. As result, intumescent flame retardancy can be observed both in structure and formulation [21], [33]. To illustrate expanding graphite can be one of the examples of intumescent material, which has its own carbon source and thus does not need any acid catalysts [34], [35]. Otherwise, in fire conditions volume of the graphite enlarges as captured gas is releases through the layers of the graphite, and with the advantage of having larger surfaces, g graphite then exhibits shielding thermally. This results from its portioned/large surface area structure of thermal insulation scales. At the moment, there do not exist any reactive intumescent materials in market. Having mixtures and blends offers effective and commercial intumescent flame retardant alternatives. [36]. Intumescent flame retardants are normally applied to give fire protective ability to for firewall holes, steel, fire barriers and applications needing a meticulous fire safety [17].

2.4.2.5 Polymer nanocomposites

Polymer nanocomposites compose the group of polymers prepared by particles at nanoscale which have a homogeneous dispersion through polymer matrix in a such manner that polymers mostly are all certainly interfacial polymer. There are some differences between conventional polymer composites and interfacial polymer which are generally solely a smaller component whereas fillers and fibers within traditional composite have larger sizes meaning that the polymer is occasionally bulky at the scales of both micro macro. From the side of macroscale, microscale and nanoscale, a polymer nanocomposite exhibits totally interfacial polymer. There exists a huge accessible literature over reviewing books and papers regarding more detailed information which gives structures of polymer nanocomposites particular and distinctive characteristics. [37]–[40]. For flame retardancy, polymer nanocomposites have the characteristics of condensed phase flame retardancy that slow without stopping the mass loss rate of the polymer during fire conditions through formation of a nanoparticle rich fire protection barrier [41]–[43]. This gives rise in a lowered peak heat release rate. Also, melting and dripping of polymer is inhibited during a fire, but the total heat release of the fuel is not lowered. Heat release constitutes a longer time and this let it burn less intensely [44]. In addition, time to ignition of nanocomposites is shorter [45].

Moreover, the polymer nanocomposites have their own retardancy effect for flame growing. However, it does not have a sufficient level for passing tests by themselves in accordance with regulations. Continually, reducing in heat releasing rate and flame growth is remarkable, and also many polymer nanocomposites find their place in market with the help of their other properties such as improved thermal, mechanical and electrical properties. Moreover, nearly in all application areas of polymeric nanocomposites a lowering effect in flame growth of polymer system is noticeable. Since polymer nanocomposites lowering the base flammability of the polymer, they can be combined with other traditional flame retardants to synthesize new flame retardant materials with a better balance of flammability/mechanical properties [19]. More specifically, one can use lower amount of the traditional flame retardant in

combination with the nanocomposite to achieve the same level of fire safety (in some cases better) than that it is obtained from using traditional flame retardant alone. This has been shown in various polymer systems and has worked its way into a few commercial systems as well [19], [46], [47]. In effect, polymer nanocomposite technology, in any case of nanofiller, appears as a class of flame retardant to have synergistic effect, nearly universally. By themselves, flammability is lowered by them, but, they are best when combined with other flame retardants to provide a superior flame retarded and multi-functional material.

The most commonly used nanoparticles for commercial nanocomposite formation are clay nanoparticles (organically treated layered silicates) and carbon nanotubes/nanofibers. Costs for clays is relatively low, but they have limitation due to thermal instability issues associated with the organic treatment on the clay surface [48]–[50]. Carbon nanotubes/nanofibers; on the other hand, do not have this thermal instability problem but have tendency to be much more expensive or do not have a good interface with many polymers resulting in difficulties in constituting the desired nanocomposite structure. Thus, although polymer nanocomposites can greatly improve flame retardancy, while at the same time bringing enhanced material properties, their biggest disadvantage is their newness and unknowns about the technology. Because the technology is not old, it is not fully confirmed in some people's minds for reliable fire safety performance. Furthermore, there is concern about nanoparticle safety and environmental disposition just as there are present both for halogen and phosphorus based retardants.

2.4.2.6 Inorganic flame retardants

This category is a bit of a catch-all category in that it includes a wide range of chemical structures that can perform both in vapor and condensed phases. They either assist other flame retardants to work better, address a particular effect of flame retardancy (such as smoke formation), or have a niche flame retardancy effect in certain polymers. As the name indicates, these flame retardants do not have carbon in

their backbone and cover a large number of elements from the periodic table. Although there are various literature reports on various metal oxides or metal complexes providing flame retardancy in very few systems, these materials are not commercially in use at the moment [51]. Borates, stannates, and silicates are the only members of inorganic flame retardant class used commercially.

The main good point of using these flame retardants is that they address some flaw/weakness of another flame retardant and because of their inorganic structure, are mostly perceived to have minimal environmental impact. On the other hand, they are applied solely sparingly and because of the low use levels, they can be quite expensive. Because of the scrutiny being shown to halogens and phosphorus, this class of flame retardants is at a close inspection, and it may be happened that groups (especially silicon based) commence to become more widely available as flame retardants. Similarly, metal oxides and other inorganics with a capacity of forming additional char layer and unique modes of flame retardant effect may also find more use as they are scaled up and they appeared in the market. There are not any known reactive flame retardants in this class of inorganic additives due to the incompatibility between inorganic and organic chemistry. Stable carbon-inorganic bonds do not form during processing or polymerization [17].

2.5. Phosphazenes

The cyclo- or polyphosphazenes (phosphonitriles) are possibly the best known and most intensively studied phosphorus-nitrogen derivatives. They have different structures with two substituents connected to each phosphorus atom, but there do not exist any substituents on nitrogen, and characterization is done by a valence-unsaturated skeleton for them. As shown in Figure 2.7, representative structures of the phosphazenes can be classified as cyclic trimer (a), the cyclic tetramer (b), and the high polymer (c) [52].

Although, the phosphazenes exhibit unique characteristics in their own right, certain formal similarities to other heteroatom systems can be detected. The phosphorus-nitrogen bonds of phosphazenes are the main reason for having their unique properties.

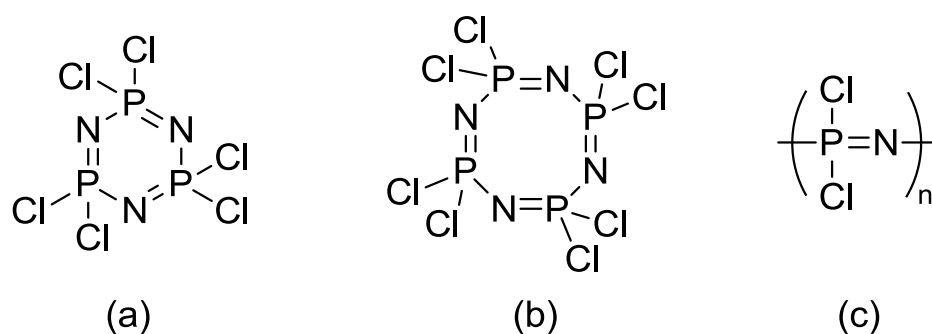


Figure 2.7 Representative structures of phosphazenes [52].

2.5.1. Polyphosphazenes

Polyphosphazenes are inorganic-organic hybrid polymers comprising a particular synthetic polymer class. Nitrogen and phosphorus atoms alternate on the polymer backbone and are linked by alternating single and double bonds. Two side groups, R, (organic or organometallic or a combination of different functional groups) can substitute every phosphorous atom [53]–[55]. The general structure of polyphosphazenes is demonstrated in Figure 2.8 [56]–[58]. The nature and composition of these substituted side groups mainly determine biological, physical and chemical properties of polyphosphazenes [3], [59]. At least 700 polyphosphazene polymers have been reported for different applications which vary from drug delivery to tissue engineering.

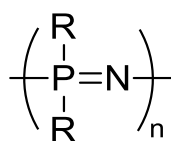


Figure 2.8 General structure of polyphosphazenes. R can be organic or organometallic or a combination of different functional groups [60].

2.5.2. Cyclic phosphazenes

Through the series of cyclic phosphazenes, hexachlorocyclotriphosphazene (HCTP) is the oldest and the most important one, $(\text{NPCl}_2)_3$ represented in Figure 2.7 (a). It is a white, crystalline (m.p. 113-114°C) compound that was produced, firstly by Liebig and Wöhler in 1834 [61] after a reaction of phosphorus pentachloride with gaseous ammonia. Following a time period of one century, the composition and molecular weight of HCTP was identified [62]–[68], its chemical reactivity investigated [69]–[85] and its synthetic procedure established in a more detailed way [77], [86]–[94].

The essential role played by HCTP considering the chemistry of phosphazene materials has been understood more clearly only recently, when this compound was used as a starting material for the synthesis of fully and partially substituted cyclophosphazenes containing organic [95]–[99] and/or organometallic residues [100], [101] and Allcock succeeded thermal polymerization of this compound to polydichlorophosphazene, $(\text{NPCl}_2)_n$, [102]–[104] therefore the way for synthesizing many new poly(organo-phosphazene)s were opened up [105], [106], which was a very new group of organo-inorganic macromolecules.

As drawn in Figure 2.9, cyclo(organo)phosphazenes, actually, are commonly prepared by nucleophilic displacement of the reactive chlorines of HCTP with variable types of aliphatic and aromatic alcohols, [52], [59], [95], [99] aliphatic and aromatic amines [95], [99], [107]–[109] and thio organic derivatives [110], [111].

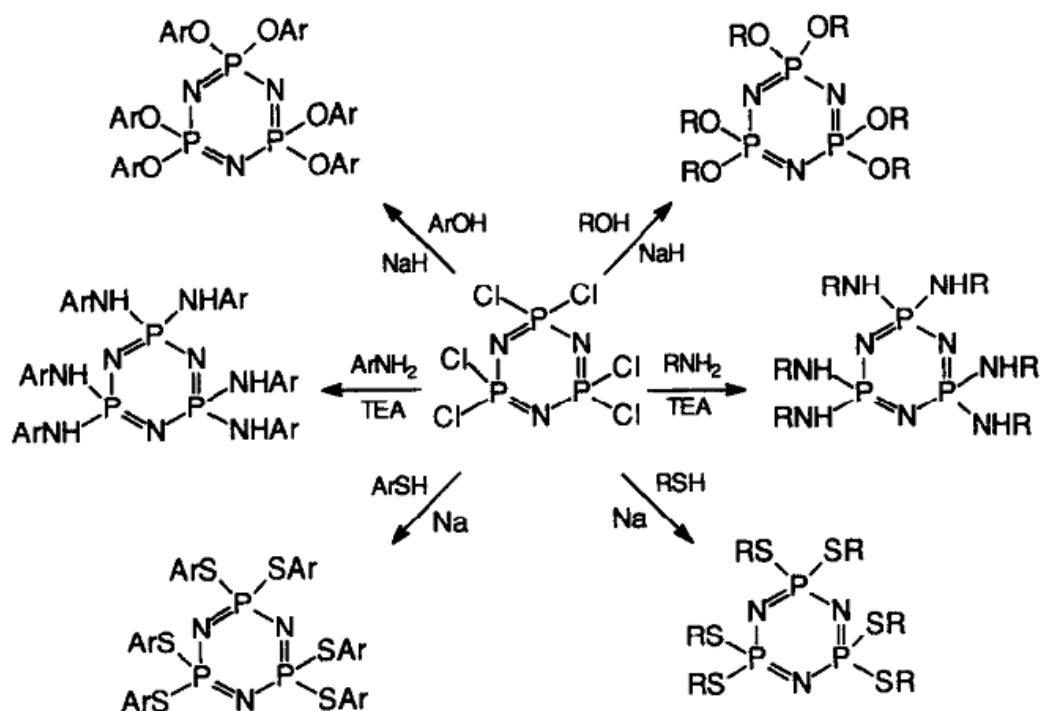


Figure 2.9 General reaction scheme for the preparation of hexa-substituted cyclo(organophosphazene)s. [112].

The characteristics of these processes have been the main target of numerous studies for analysing the stereo- and regioselectivity [113] during substitution, isomer formation, [96], [114], [115] kinetics [96], catalysis [116], [117], etc. During the substitution reaction of HCTP sterically less hindered groups frequently choose patterns of non-geminal substitution [3], [118]–[121]. They also need high temperature [3], high reagent concentration [3], pressure [122], [123]. Substituent groups that remove electrons from the phosphazene ring increase the positive charge on the phosphorus atoms, thus the activity is increased. Therefore this has a driving effect in favouring geminal substitution of the cyclophosphazene chlorines [124]–[128]. The use of catalysts, such as crown ethers [116] or phase-transfer catalysts [117], [129]–[139], augments the basicity of the incoming groups and favours chlorine substitution in the cyclophosphazene [112].

Homosubstituted cyclophosphazenes are generally symmetric and highly crystalline molecules with the melting points usually well above 0°C [52], [59]. On the contrary, cyclophosphazenes including multiple nucleophiles of different chemical structure are deliquescent or oily compounds [129], [132], [133], [140]–[147] due to the destruction of molecular symmetry and the destruction of structural crystallinity [112].

2.6. Fundamentals of Polymer Blends

In earlier times of polymer industry, the major polymers in use were natural rubber, wood, and gutta-percha along with cellulose, protein fibers, and leather which are natural fibers. In the year 1846, the first polymer blend which was natural rubber blended with gutta-percha, was reported in the patents of Hancock and Parkes [148]. A single rotor masticating machine was applied for the blending process. This was followed by the slow development of blending technology. In the first half of the twentieth century, a large group of new polymers were developed by the leading major progress in polymer industry. Later economic ways for developing new monomers were depleted. This gave rise to developments of polymer blending [149]. In the following 100 years, the number of polymer blend patents increased at an exponential rate and the number of papers in literature duplicated after 1993 [150]. Polymer blends are a group of materials in which at least two polymers are combined together giving rise to a new material with different physical properties [151].

The important advantages of polymer blending can be listed as:

- New properties are developed, and existing properties are improved for meeting specific needs.
- Material cost is reduced nearly with no loss of properties.
- Material processing is improved
- The needs of newly emerging industries related with polymers are responded.

Polymer blends can generally be grouped into three main categories:

1. Immiscible polymer blends
2. Miscible polymer blends
3. Compatible polymer blends

The main differences and the important conditions for miscibility are demonstrated in Table 2.1. The success of developing a polymer blend depends on the effectiveness with some essential limitations. These native limitations could be listed below [151].

- The high interfacial tension (Γ_{12} between 1.5×10^{-3} and $1.5 \times 10^{-2} \text{ Jxm}^{-2}$) not letting the dispersion of one polymer in another phase easily
- Low level of interfacial adhesion resulting in narrow interphase width
- Instable nature of immiscible polymer blends

Table 2.1 Main differences between the types of polymer blends [152].

Miscible Blends	Partially Miscible Blends	Immiscible Blends
Homogeneous	Partial phase separation	Complete phase separation
Mechanical properties of components averaged	Mechanical properties of individual polymers mostly retained	Poor interface leading to poor mechanical properties
$\Delta G < 0$	$\Delta G > 0$	$\Delta G > 0$
They show a single glass transition temperature	They show two glass transition intermediate to the component polymers	They show the two glass transition temperatures of the component polymers

Polymer blending is an effective and economic way for the combination of the properties of different polymers. Although specific interaction between the polymers give rise to miscible blends, miscible blends without any interaction are also possible. Miscible blends are not preferred for industrial applications due to their averaged properties. Immiscible blends give poor mechanical properties due to poor adhesion between the components. The application of a compatibilizer modifies the interface and results in a synergism in characteristics of blends. The change in size of the dispersed phase domains is related with the compatibilizer efficiency. It may give an idea about the effect of dispersed phase on compatibilizer activity [74].

2.6.1 Immiscible Polymer Blends

The majority of blends are fully immiscible. They have a coarse phase morphology, the interface is sharp, and the adhesion between both blend phases (each exhibiting the T_g , of the pure blend components) is not high, so that these blends should be used in compatibilized form [153].

Examples of fully immiscible blends are PA/ABS, PA/EPDM, PA/PPO and PP/PA to a certain extent. All of these blends have become successful in the market, but this was followed by being compatibilized in an efficient manner. In PA6/ABS, the polyamide provides heat and chemical resistance, tensile properties and paintability. ABS lowers the moisture absorption, increases the dimensional stability, and provides a more economical price and good low temperature impact. PA6,6 (or 6)/EPDM blends are the so-called “supertough nylons”. In PA6 or 6,6/PPO blends, the polyamide provides good processability (as such, PPO is intractable) and also paintability and good chemical resistance, as the PPO exhibits low moisture absorption, good dimensional stability and stiffness at higher temperatures. In PA6/PP blends, the contribution of PA is as described above, and PP lowers both moisture absorption and price [153].

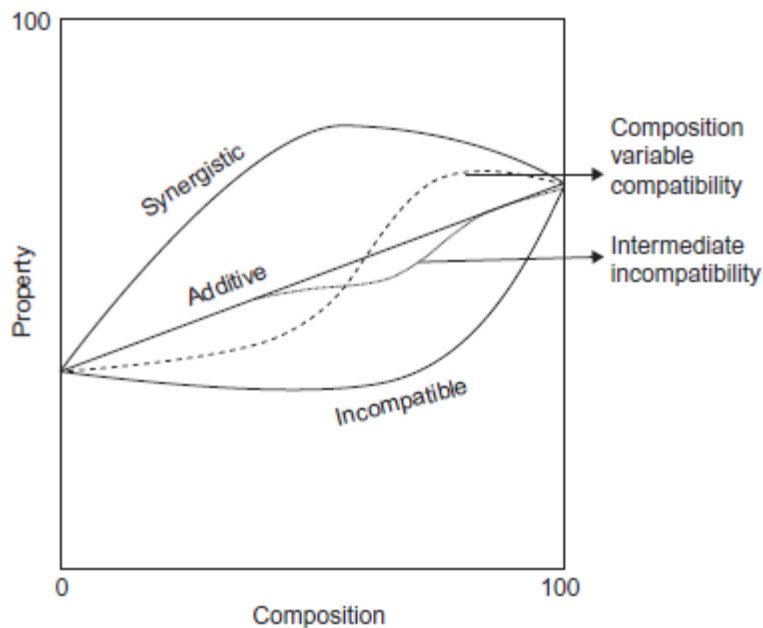


Figure 2.10 Variation of polymer blend property as a function of composition [152].

Compatibility and incompatibility in polymer blends are very important from the side of industrial applications. Large phase separation and weak interface determine incompatibility of polymer blends. Thus, they demonstrate poor mechanical properties as given property-composition figure, Figure 2.10. Wening et al. studied the impact properties of a PP and PE blend system and suggested that when PP is melt blended with PE an improvement in impact properties was experienced [154].

2.6.2 Miscible Polymer Blends

Miscibility in polymer blends is invariably the result of specific interactions between the blend components. These interactions consist of hydrogen bonding interactions, dipole-dipole interactions and Van der Waals interactions (such as dispersion forces). There existed some miscible polymer pairs even without any specific interactions. For example, blends of poly(vinyl ethylene) and poly(cis-1,4-isoprene) are thermodynamically miscible, as evidenced by many experimental techniques. There existed

no specific interaction between the blend components and it was confirmed by Fourier transform infrared (FTIR) spectroscopy. [155]. An explanation in a more detailed way for the effect of hydrogen bonding on miscibility is given in the classical work of Coleman and Painter [156]. Miscible polymer blends form one phase and by that the properties are inclined to an average level [152].

Averaging of properties is not the target of polymer blending; blending is intended to obtain desirable properties of every component into the blend. Retention of properties needs each component to be in a separate phase. The continuous phase contributes the main properties and the dispersed phase adds additional properties such as toughness, where the stress is transferred from the continuous phase to the dispersed phase [152].

2.6.3 Compatible Polymer Blends

While analyzing phase-separated systems, the properties brought about by the interfacial region defines the mechanical characteristics. Therefore, a phase-separated system where the phases are adhered with each other at a low level gives rise to a reduction of ultimate properties, for example, strength and toughness. Therefore, a blend with poor interface will represent the incompatible region in Figure 2.10. An original approach for modification of the compatibility of PE-PP blend was put forth by Longworth et al., in which an acidic monomer was grafted onto one polymer and a basic monomer to the other one was included. The blends so prepared were found to have ductile properties and mechanical properties were improved [157].

Impact modified polymer blends such as high impact poly(styrene) (HIPS), poly(methyl methacrylate) (PMMA), poly(acrylonitrile-*co*-butadiene-*co*-styrene) (ABS), or PVC each have a dispersed elastomer phase whose adhesion to the matrix phase is excellent. It is a frequent practice to blend of elastomeric block or graft copolymers with brittle polymers [157].

A variation in the size of the phase domains from macro to micro provides information regarding efficiency of compatibilizers. The contribution will be even better when nanophase separation is obtained. Leibler et al. investigated nanophase separation using copolymers as compatibilizers [158]. Modified polyolefins comprise a major share of polymeric compatibilizers while styrenic block copolymers with elastomers constitute the second largest group.

2.7 Characterization Methods

Firstly, analysis of Nuclear Magnetic Resonance (NMR) is used in order to confirm the structures of synthesized cyclic phosphazenes which are HPACTP and HPCTP. Moreover, numerous test methods are used for evaluating the fire retardant and thermal properties of polymer blends. In this investigation, Underwriters Laboratory UL 94 Test (UL-94), Limiting Oxygen Index (LOI), Thermal Gravimetric Analysis (TGA), Differential Scanning Calorimeter (DSC) and Cone Calorimeter tests are used for polymer blends. Tensile Test is also used for understanding the tensile properties of blends. Scanning Electron Microscopy (SEM) is applied in order to determine the morphologies of blends.

2.7.1 Nuclear Magnetic Resonance (NMR)

NMR includes the positioning of an atomic nucleus in an external magnetic field to produce two spin states at different levels of energies. Low and high energy spin states nuclei absorb energy of radio frequency range to change its spin orientation as per applied magnetic field direction. As long as the development in processing techniques continues to abstract more and meaningful information from the experiments, NMR takes a place in one of the most powerful tools to give a clarifying explanation about the structure of small as well as large molecules [159].

Numerous types of experiments such as 1D-NMR (^1H DEPT, NOE, ^{13}C , ^{15}N , ^{19}F , ^{31}P , ^{29}Si etc.), 2D-NMR (COSY, DQFCOSY, TQF COSY, MQF COSY, HETCOR, HSQC, HMQC, HMBC, TOCSY, NOESY, EXSY etc.) and 3DNMR (Homonuclear and Heteronuclear) were developed [159].

1D-Nuclear Magnetic Resonance spectroscopy was applied in this thesis in order to confirm the structures of synthesized cyclic phosphazenes. ^1H , ^{13}C and ^{31}P NMR spectroscopies were the techniques applied in this investigation [159].

In proton NMR (^1H NMR), spin transitions of different types of Hydrogen nuclei in different electronic environments were pragmatically observed. An interpretation of ^1H NMR data on the basis of chemical shifts is well clarified and reported [159].

^{13}C NMR is the other spectroscopic technique applied: Among the three isotopes of carbon, ^{12}C accounts for 98.9% and due to the absence of a nuclear magnetic moment, it is not a proper nucleus for NMR and that is the reason that it is taken as an NMR inactive nucleus. ^{13}C isotope with 1.1% abundance and nuclear magnetic moment $\frac{1}{2}$, just like a proton, is used to provide structural information for the organic compounds. Owing to 100% isotopic abundance of ^{31}P and relatively high gyromagnetic ratio, ^{31}P NMR is a routine NMR technique, which helps in structure elucidation of phosphorous containing organic, inorganic compounds and metabolites [159].

2.7.2 Underwriters Laboratory Test, UL-94

UL-94 is a facile test method to practice and apply as well as a very frequently applied method for measurements of the issues of ignition and flame spreading in polymers. A small flame exposes at a vertical location while application of the method. The illustrated set of the UL-94 test is demonstrated in Figure 2.11 [160].

The bottom of the specimen is the place where the flame ignites it and the top of the burner has to be positioned from a distance of 10 mm at the lowest border of the

sample. Exerting of flame continues during a time period of 10 seconds and then flame is removed. The after flame time t_1 (the time required for the flame to extinguish) is noted. Following the disappearance of the flame, it is again applied for another duration of 10 seconds. The after flame time t_2 is noted, along with the afterglow time t_3 , which is the time required for the fire glow for disappearance. Over the test, the presence of burning drops, resulting in a piece of cotton located under the sample to ignite, must be taken into consideration and noted. With respect to facts, the distinctive flammable property of compound consists of three essential groups which are V0, V1 and V2. The properties depend on their performance concerning time values during which individual specimens prolong to burn. Burning time totally for each specimen is determined as well as with dripping nature of the sample whether it is present or absent [161-163]. Criteria for classified groups of UL-94 test are briefly stated in Table 2.2.

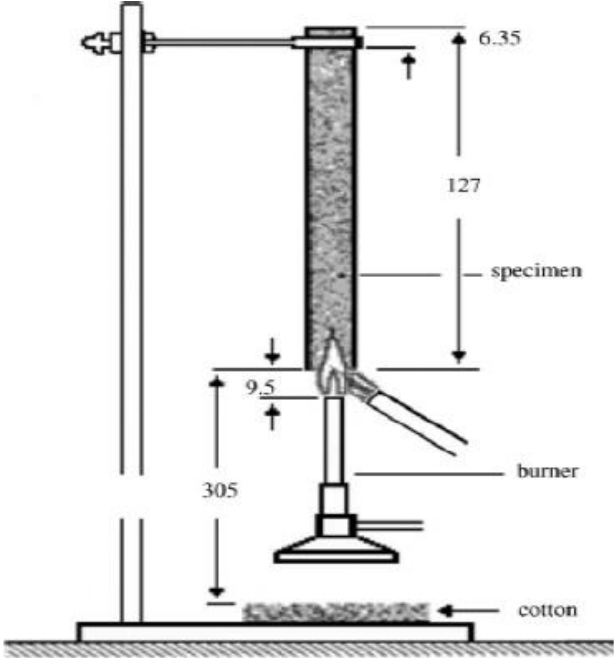


Figure 2.11 The schematic view of the UL-94 test [161].

Table 2.2 Criteria for UL-94 classifications (time in seconds) [162].

<u>Time (s)</u>	<u>V0</u>	<u>V1</u>	<u>V2</u>
t ₁	<10	<30	<30
t ₂	<10	<30	<30
t ₁ + t ₂ (for five samples)	<50	<250	<250
t ₂ + t ₃	<30	<60	<60
Cotton ignited by burning drips	No	No	Yes
After glow or after flame up to the holding clamp	No	No	No

2.7.3 Limiting Oxygen Index (LOI)

LOI is largely applied for measurements to quantify flammable properties of polymeric materials. Test firstly was put forwards within the year of 1966 then the test was standardized as with the documents which are, ISO 4589, NF T 51-071 and ASTM D 2863 [160]–[162]. Scheme of LOI test is represented in Figure 2.12. In a very slow manner of streaming of mixture composing of oxygen and nitrogen is realized at the lower part of the duct. Oxygen and nitrogen ratios are varied through during test as aiming to fix the oxygen content that will assist the burning of the sample for a minimum duration of 3 minutes or having 50 mm portion of the specimen combusted. The LOI value is found in Equation 2.1.

$$\text{LOI} = \frac{\text{O}_2}{\text{O}_2 + \text{N}_2} \times 100$$

Equation 2.1 Limiting oxygen index calculation

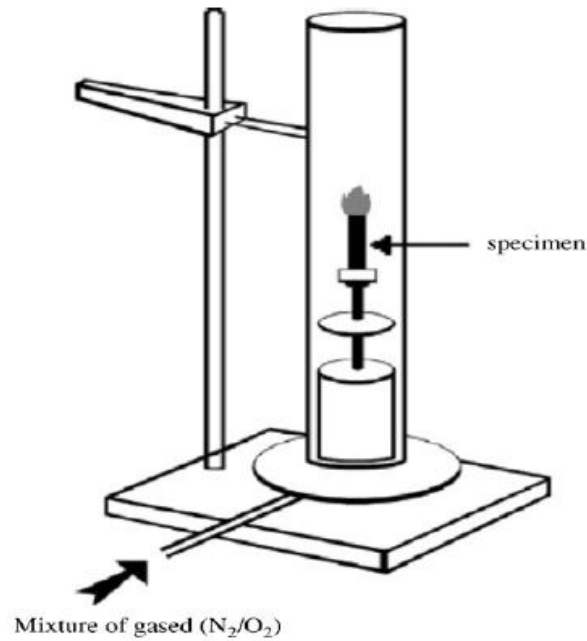


Figure 2.12 The schematic view of the LOI test [161].

Since air comprises 21% oxygen, compounds with values of LOI under 21 are defined as ignitable, the ones with LOI value over 21 are identified as quenching or self-extinguishable. While LOI values increase, flame retardant property becomes improved [160]–[162]. Despite the fact that the method is in use widely, the method exhibits many drawbacks. Firstly, the test environment has not been associated with any particular status of complete fires. Secondly, the application of flame expansion in downward direction for 50 mm for finding out the oxygen index of a material is not, since in real fire scenarios, highly significant. Finally, LOI experiment is carried out in an environment at which concentration of oxygen appears over the ordinary levels of oxygen portion within air. This situation hardly takes place in majority of fires [14].

2.7.4 Thermal Gravimetric Analysis (TGA)

Variations in the weight of a sample are recorded by application of TGA while heating of the sample progressively. Evaporation and decomposition of the constituents of polymer and additives happen at varying temperatures. This gives rise to be monitored as a progress of weight losing stages in TGA plot. Significant data about a polymeric material can be revealed by TGA analysis. The volatile portion, the starting point of thermal decomposition, portion of inorganic filler, the volatile additives and the effective level of flame retardants can be given under the list of this meaningful information. TGA device can be applied along with options of Fourier Transform Infrared Spectroscopy, FTIR device and Mass Spectroscopy, MS instrument for gaining extra information of the degrading thermally of polymeric materials [163], [164].

2.7.5 Differential Scanning Calorimetry (DSC)

DSC is a widespread technique for the analysis of polymers thermally. Within the instrument there are two tiny metal vessels one of which is allocated for the polymer specimen to be inspected and the other container is taken as the reference. Temperatures of both reference and sample containers are conserved at same temperature by means of separate heaters operating electrically throughout the duration of experiment.

The variation in electrical power provided to the two containers is measured with respect to temperature and thus, also as a function of time. Heats of transition, glass transition temperature, heat capacity, temperature for crystallization, heats of reaction for polymers and temperature of melting can be found out by using of DSC devices [163], [164].

2.7.6 Cone Calorimeter

Shape of heater in cone used to heat specimen throughout test is responsible for naming of cone calorimetry device. Cone calorimetry can determine large number of the properties regarding reaction of fire in one set applying a small size of a sample. The combustion surroundings created throughout experiment is a well designed demonstration of the most of fire environment represented as actual conditions. Therefore, cone calorimeter test has its own popularity through the scientists and the method is standardized as the documents of ISO 5660 and ASTM E 1354 [14].

The cone calorimeter working depends on the principle that the specimen is exposed to a heat flux incidentally by using a unit of heater. Illustration of the device is drawn in Figure 2.13 [162]. While heating progresses, the sample decomposes as well as evolution of combustive gases from the specimen is observed. Combustion of the gases is started by ignition effect of electric spark. The gases follow a route of the heating cone and a tube system used for exhausting with a fan working centrifugally and hood captures these gases. Gas flowing and concentration of oxygen are measured and the results of measurement is employed to quantify fire properties of the material. Heat Release Rate (HRR), Time of Combustion (TOC), Mass Loss Rate (MLR), Total Heat Rate (THR), Peak Heat Release Rate (PHRR), Time to Ignition (TTI), amount of lost masses of CO and CO₂ and total smoke emissions can be attained by application of cone calorimetry [14], [161], [162], [165], [166].

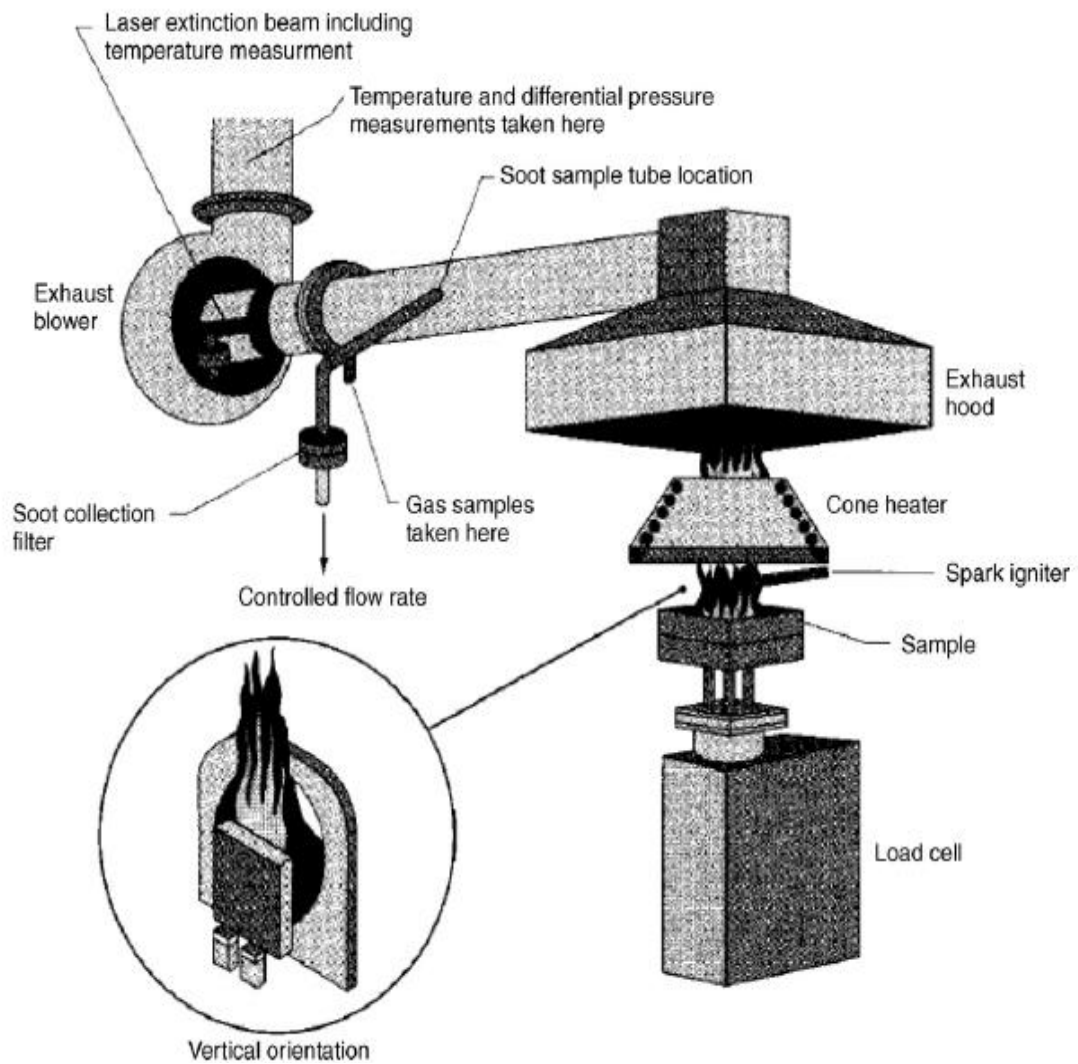


Figure 2.13 Schematic representation of cone calorimeter [161].

Peak heat release rate (PHRR) with the standard unit of kW/m^2 , is taken into consideration as the most significant parameter while dealing with a performance of a material in an artificially created fire environment. Also, PHRR is used as a mean for determination of the material contribution the harsh conditions of severity of fire flash point.

Total heat evolved (THE) after gaining the information of area under the heat release rate versus time plot as a representation of whole amount of fire loading of a specimen, also information of total heat evolved (THE) is obtained in its own unit of MJ/m².

Time to ignition (TTI) in seconds, is time passed before guided ignition of a material as an exertion of irradiation to material is realized. Between these two points of, time to ignition is defined, TTI, in units of seconds. When onset of sustained flaming is observed, ignition timer is started manually. Total mass loss (TML), which aims to find weight percentage of fire remains is variation in specimen mass against burning. It is in grams. Total-heat-evolved / total-mass-loss ratio (THE/TML) uses the standard unit of MJ/m²g.

Concerning cone calorimetry, heat flow range is between 10 and 100 kWm⁻². 35 and 50 kWm⁻² are amounts of fluxes of heat, which are in accordance with heat flux values determined in the development of fires, are the widespread applied values in the tests. Horizontal or vertical positions of the heater can be in operation. Experiments are mainly completed in the horizontal direction since heat transfer element related with convection is almost negligible. The location of the specimen is 2.5 cm under the heater placed in horizontal direction. Sample coordinates should be 10 x 10 cm² with different thicknesses up to 50 mm. The thickness dimension of the material has a very critical role. The results are highly dependent on thickness. Thin sample shows smaller values of time to ignition and larger values peak heat release rate in comparison with the same specimen with major thickness values [14], [161], [162], [165], [166].

Varying types of combustion behaviour as a result of different polymers and polymeric composites give various kinds of Heat Release Rate vs. time curves. The burning properties of polymeric materials are exhibited on various shapes of HRR vs. time curves. Some typical examples of these plots are drawn in Figure 2.14 [166].

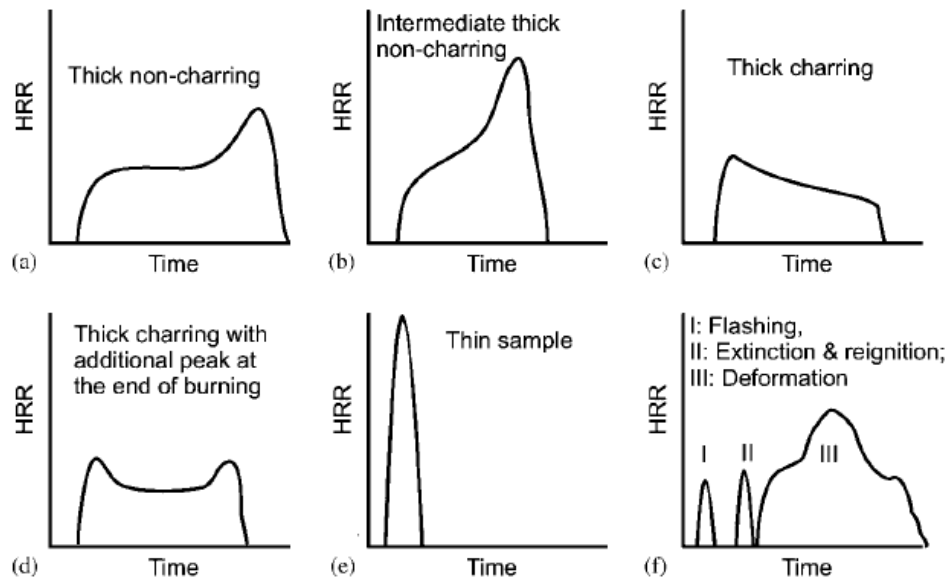


Figure 2.14 Characteristic HRR curves for different typical burning behaviours [166].

2.7.7 Tensile Tests

ASTM D 638 procedures are applied for the aims of characterizing of mechanical properties of the polymers specimen in dog bone shape. The specimen is fastened from the two tips by clamps and stretched at a rate of elongation constantly till to the failure point of the specimen. Gauge distance between the two ends is the dimension of central part initially with the narrow part of the dog bone, L_0 . Force depends on elongation while the sample deforms. The tensile response plot is generally obtained as engineering stress σ , vs. engineering strain ϵ , where A_0 is the initial, in other words undeformed, cross sectional area of the gauge region and ΔL is the variation in specimen gauge length ($L-L_0$) owing to the deforming. In Figure 2.15, the stress-strain graph is plotted for the whole range of strain of a regular polymeric substance [167].

$$\sigma = \frac{F}{A_0}$$

Equation 2.2 Engineering stress

$$\varepsilon = \frac{\Delta L}{L_0}$$

Equation 2.3 Engineering strain

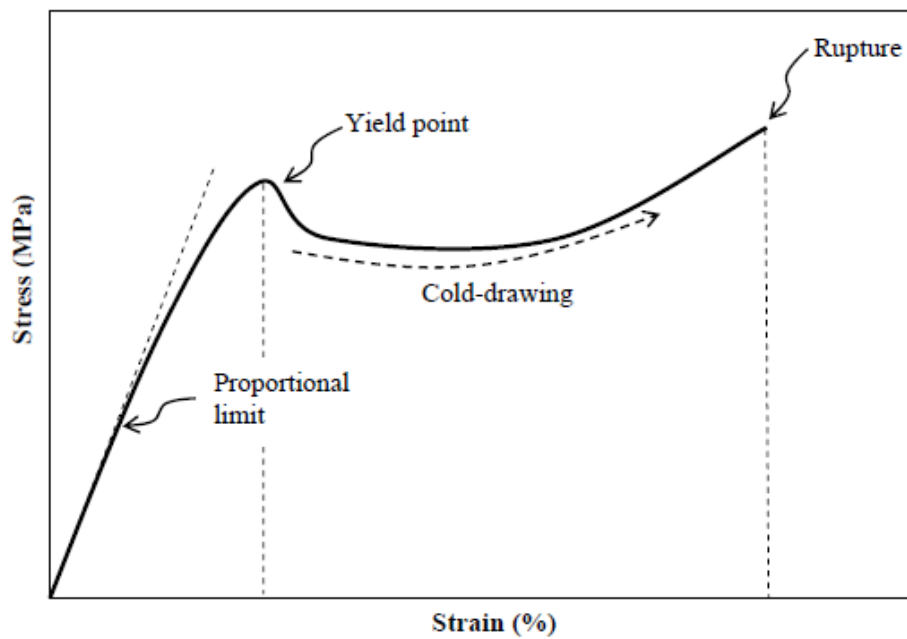


Figure 2.15 Stress-strain curve for a typical crystalline polymeric material [168].

Tensile strength, σ (Eq. 2.2) is the greatest value of tensile stress that the specimen keeps up as the tensile test is performed. Tensile strength at yield is noticed when the maximum stress, in other words, tensile strength at yield, is notified at the point of yield. Greatest stress happening at break is termed as tensile strength at break [167].

Tensile strain (ϵ) is the variation in length of sample with respect to earliest value of length, also defined, briefly, as the ratio of the extension to the length of specimen, (gauge length) (Eq. 2.3).

Modulus of elasticity, E is the ratio of stress to strain below proportional limit and it is the measure of the stiffness of the elastic material. It is also named as elastic modulus or Young's modulus or tensile modulus and expressed in force per unit area (Eq. 2.4) [169].

$$E = \frac{\sigma}{\epsilon}$$

Equation 2.4 Modulus of elasticity

2.7.8 Scanning Electron Microscopy (SEM)

Among various electron microscopes SEM is a sort of microscope that operates on a principle based on scanning the test specimen sample with means of a targeted electron beams. Then, images of the material are created. The electrons emitted from the device interact with the atoms within the substrate then signals are produced providing information concerning the topographical properties of surface and the constituents of the specimen. Beams of electron usually prompt to scan in a rapid mode of scanning, and beam and signal detected combine in order to present the visual representation [170].

It is necessary that the surface of the substance is electrically conductive although it is not critical whether the material surface planned to be scanned may be prepared by polishing or etching processes. Hence, it requires to be in conductive form with help

of metal coating on surface with a very low thickness before test is performed. A scale of magnifying from 10 to beyond 50000 diameters can be achieved [170].

2.8 Production Methods of Polymer Blends

The synthesized cyclic phosphazene additives are blended with polyolefins by using twin screw extruder for the production of the targeted polymer blends. After extrusion, polymer pellets are obtained. Then they are injected into molds for tensile tests. Compression molding is applied in order to shape them into proper forms for flammability tests. The detailed information about extrusion, injection molding and compression molding is given in the following section.

2.8.1 Extrusion

Extrusion is a widespread technique applied in plastic industry. It is used for melting the polymer and blending it with the other substances of a composite, For example, colorants, fillers and other types of additives are mixed with polymers for obtaining desired blends. In spite of the fact that the mostly extruded plastics comprise thermoplastics, some thermosets, such as rubbers are also obtained by using extrusion process. Plastics are extruded into various forms like fibers coating on wire, pipes, cables, sheets and long thin rods. All these various shapes can be attained by extrusion [171], [172].

During extrusion, polymers as pellets or in granule forms and other ingredients of the composite are located in the hopper part of the extruder. Then the blend in hopper follows a route to a hole positioned at the top of the screw. The material mixture is pulled by the screw. Then, it approaches to die which is a hole positioned at the bottom part of the extruder barrel. The blend leaves from die.

The plastic is molten by screw by the means of both external heat and heat evolved as a result of the friction of polymers. The molten plastic gains its shape by the die, becomes solid by instantaneous cooling; therefore it holds its shape [171], [172].

2.8.2 Injection Molding

Injection molding is another polymer processing method in which parts are molded by injecting molten material. Injection molding is applied for various types of materials, including thermoplastics and thermoset polymers. Firstly a barrel is prepared by preheating then the material is send to the barrel. It is mixed and driven into a cavity of mold. This process is carried out at a high pressure. Finally the material is cooled, hardened and takes the form of the mold. In this study the samples in dog-bone shapes were produced with laboratory scale injection molding in order to apply tensile tests [173].

2.8.3 Compression Molding

Compression molding is a widespread applied technique for the aim of polymer molding, especially thermosets. The working principle of compression molding is quite simple. Firstly, the material to be molded is preheated in an open molding cavity. Then the mold is closed. Pressure is applied. The material is forced into contact with all areas of the cavity. While pressure is employed, heat is conserved to the point at which the material is completely molded. In this study, stainless steel plates are applied as molds. The inner parts of these plates are cut out into desired shape. Teflon film is employed for preventing polymer melts adhering onto the both upper and lower plates of the hydraulic press. [172].

CHAPTER 3

EXPERIMENTAL

Experimental part of this study comprises two main parts which are focussed on synthesis and characterization of hexachlorocyclotriphosphazene derivatives and the preparation of flame retardant polymer blends, respectively. In the first part, materials, synthesis and characterization methods of hexaphenoxycyclotriphosphazene and hexakis(propyl amino)cyclotriphosphazene are explained. The reactive chlorines of HCTP were replaced by nucleophilic displacement both in these two alternatives [52].

In the second part, blends of polyolefins with derivatives of hexachlorocyclotriphosphazene (HPCTP and HPACTP) are mentioned and preparation details of these blends are explained.

3.1 Materials

PE was obtained from PETKIM A.S. (Turkey) under the trade name LDPE F2-12. The density was 0.92 g/cm^3 and the melt flow index was 2-3.5 g/10 min (2.16 kg, 190 °C) as provided by the supplier. PP was purchased from Borealis (Austria) under the trade name HE125MO. The density was 0.905 g/cm^3 and the melt flow index was 12 g/10 min (2.16 kg, 230 °C) as provided by the supplier. HPCTP and HPACTP were synthesized by using hexachlorocyclotriphosphazene as the base material. The synthesis details and the properties of HPCTP and HPACTP are given in Section 3.2 and 3.3 respectively. The properties of the chemicals used for the synthesis of the cyclophosphazene derivatives and polymers used for the preparation of the blends are listed in Table 3.1 below.

Table 3.1 The properties of materials

Material	Supplier	Specifications
PE	PETKIM	Density: 0.92 g/cm ³ Melt Flow Index: 2-3.5 g/10 min %Crystallinity: %50-53
PP	Borealis	Density: 0.905 g/cm ³ Melt Flow Index: 12 g/10 min
HCTP	Sigma-Aldrich	Appearance: Colorless Molecular Weight: 347.66 g/mol Density: 1.98 g/mL
Tetrahydrofuran	Sigma-Aldrich	Appearance: Colorless Molecular Weight: 72.11 g/mol Purity (GC): ≥ 99.90 %
Sodium	Sigma-Aldrich	Appearance: Silvery Molecular Weight: 22.99 g/mol Purity: Conforms
Phenolic Resin	Sigma-Aldrich	Molecular Weight: 94.11 g/mol
Triethylamine	Sigma-Aldrich	Appearance: Colorless Molecular Weight: 101.19 g/mol Purity (Titration by HClO ₄): ≥ 99.0 %
Propylamine	Sigma-Aldrich	Appearance: Colorless Molecular Weight: 59.11 g/mol Purity (GC): ≥ 99.0 %
Acetone	Sigma-Aldrich	Appearance: Colourless Molecular Weight: 58.08 g/mol

3.2 Synthesis of Hexaphenoxycyclotriphosphazene (HPCTP)

HCTP was used as the starting material for the synthesis of hexaphenoxycyclotriphosphazene (Figure 2.7(a)). The synthesis of HPCTP was performed according to the literature [52]. The synthesis route of HPCTP is given in Figure 3.1 below.

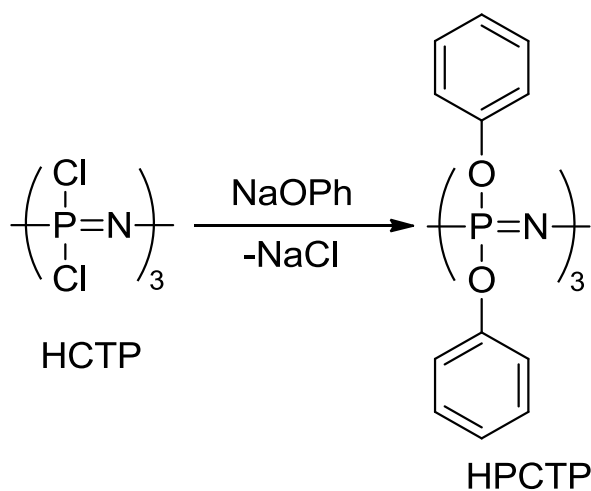


Figure 3.1 Synthesis route of hexaphenoxycyclotriphosphazene (HPCTP).

HCTP is a colorless crystalline materials with a molecular weight of 347.66 g/mol. Due to high activity of the P-Cl bonds on the structure it should be handled carefully and must be protected from moisture. Thus, all the manipulations were performed in either a Glove box or using shlenk line techniques under an inert atmosphere of argon. The glass equipments were assembled hot and dried under vacuum using a heat gun. All the chemicals are used as received without further purifications unless otherwise is stated. Tetrahydrofurane was dried and purified over sodium-benzophenone technique [174] . The synthesis was done as explained below;

A solution of sodium phenoxide in tetrahydrofuran with a volume of 500 mL was prepared from phenol (94.11 g, 1 mole) and sodium (20.7 g, 0.9 mole) in an atmosphere of dry argon. A solution of hexachlorocyclotriphosphazene (52.2 g, 0.15 mole) in tetrahydrofuran (500 ml) was added drop by drop to the stirred solution of sodium phenoxide in tetrahydrofuran. The mixture was then boiled with reflux for 12 hours and then allowed to stand at 25 °C for 24 hours. The mixture yielding sodium chloride (55 g, 100% based on HCTP) was filtered, and the filtrate was evaporated, then, the residue was dissolved in acetone and poured into a large excess of water yielding 88.5 g of a white solid precipitate. This was then recrystallized twice from n-heptane and n-heptane-benzene mixtures, and was exhaustively dried in vacuum oven at 60 °C to give HPCTP (83.2 g, with 93% yield), m.p. 112 °C – 112.5 °C. Characterization was carried out by ¹H, ¹³C, and ³¹P NMR spectroscopy as given in Appendix and in accordance with the literature [52]. HPCTP exhibits, in fact, an excellent high-temperature mass spectroscopy standard because of its high mass (MW = 693 g/mol) and its high stability. The compound is a white, crystalline solid, which is soluble in benzene or tetrahydrofuran. It is highly resistant to hydrolytic degradation.

3.3 Synthesis of Hexakis(propyl amino) cyclotriphosphazene (HPACTP)

HPACTP was also synthesized from the initial starting material of HCTP. The synthesis of HPACTP was carried out according to the report of Bickley et al. [4] In Figure 3.2 below, the synthesis route of HPACTP is shown.

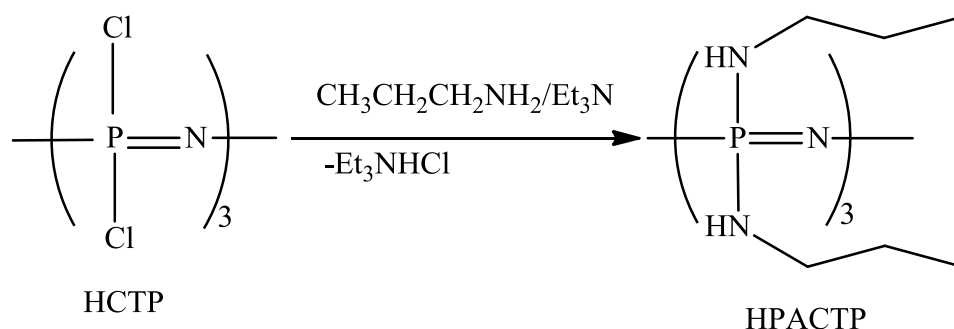


Figure 3. 2 Synthesis route of hexakis(propyl amino) cyclotriphosphazene (HPACTP).

HCTP was used as a starting material for the synthesis of hexakis(propyl amino) cyclotriphosphazene. All the manipulations were here also performed in either a Glove box or using shlenk line techniques under an inert atmosphere of argon. The glass equipments were assembled hot and dried under vacuum using a heat gun. The amines were All the chemicals are used as received without further purifications unless otherwise is stated. Tetrahydrofurane was dried and distilled over sodium-benzophenone. The amines were dried and stored over molecular sieve. The detail of the synthesis is given as below;

57 mL (0.69 mol) of propyl amine was added to a stirred solution of 10 g (28.8 mmol) hexachlorocyclotriphosphazene in 200 mL toluene and 100 mL triethylamine at room temperature. The formation of a white precipitate indicated the onset of the reaction. The solution was heated with reflux until substitution was completed (^{31}P NMR control) and cooled prior to filtration. The solvent and excess amines were removed under reduced pressure yielding the hexakis(propyl amino)cyclotriphosphazene. After 2 hours of reflux period, filtration, solvent removal and drying steps were completed. Product of hexakis(propyl amino)cyclotriphosphazene was stirred with finely ground potassium hydroxide of 96.9 g in 1 L of ether for 24 hours [4]. The isolated product was checked by ^1H , ^{13}C , and ^{31}P NMR spectroscopy and the spectra are given in Appendix.

3.4 Characterization Methods

3.4.1 NMR

The structure of the synthesized cyclophosphazene derivatives (HPCTP and HPACTP) were characterized using Bruker-Instrument, (DPX-400) model Nuclear Magnetic Resonance Spectrometer (NMR) in deuteriochloroform (CDCl₃). Molecular structure of the targeted phosphazenes was checked by ¹H NMR, ¹³C NMR and ³¹P NMR analysis and the NMR spectra of them were given in Appendix.

3.4.2 Differential Scanning Calorimetry (DSC)

DSC was carried out with Mettler Toledo DSC 1 Star System at a heating rate of 10 °C/min up to 400°C under nitrogen flow of 50ml/min.

3.4.3 Thermal Gravimetric Analysis (TGA)

TGA was conducted with a thermal analyser (Perkin Elmer Diamond TG/DTA) from RT to 800 °C at 10 °C/min ramp rate under flowing nitrogen and atmospheric conditions, respectively.

3.4.4 Underwriters Laboratory UL-94 Test

UL-94 rating was obtained according to ASTM D3801 where V0 indicates the best flame retardancy and V2 is the worst. The dimensions of bar specimens were 130 mm × 13 mm × 3.25 mm.

3.4.5 Limiting Oxygen Index (LOI)

LOI value was determined by using LOI instrument (Oxygen Index, Fire Testing Technology Limited, England) instrument using test bars of size 130 mm × 6.5 mm × 3.25 mm, according to the standard oxygen index test ASTM D2863.

3.4.6 Thermal Gravimetric Analysis (TGA)

TGA was carried out by using Perkin Elmer Pyris 1 TGA at a heating rate of 10 °C/min up to 800 °C under nitrogen flow of 50 ml/min.

3.4.7 Differential Scanning Calorimetry (DSC)

DSC was carried out by using Mettler Toledo DSC 1 Star System at a heating rate of 10 °C/min up to 400°C under nitrogen flow of 50mL/min.

3.4.8 Cone Calorimeter

The cone calorimeter test was carried out without replication following the procedures in ISO 13927 using Mass Loss Cone with thermopile attachment (Fire testing Technology, U.K). Square specimens (100 mm × 100 mm × 4 mm) were irradiated at a heat flux of 35 kW/m², corresponding to a mild fire scenario.

3.4.9 Tensile Tests

Tensile test was carried out by using Lloyd LR 30 K universal tensile testing machine, represented in Figure 3.3, with load cell of 5 kN at crosshead speed of 5 cm/min according to the standard of ASTM D-638. Tension tests were conducted on dog-bone shaped samples (7.4 mm × 2.1 mm × 80 mm). Tensile strength, percentage

elongation at break and tensile modulus values were recorded. All the results represent an average value of five samples with standard deviations.



Figure 3.3 The photograph of tensile test machine used in this study.

3.4.10 Scanning Electron Microscopy

The morphology of fractured surfaces of test samples obtained after tensile tests were examined with SEM (LEO 440 computer controlled digital, 20 kV). All specimens were sputter-coated with gold before examination.

3.5 Preparation of PE and PP Blends with Phosphazene Derivatives and Their Characteristics

10%, 20% and 30% weight HPCTP and HPACTP were added to PE and PP matrices in melt, respectively. Then, PE-HPCTP, PE-HPACTP, PP-HPCTP and PP-HPACTP blends were prepared. The characteristics of the combustion and thermal degradation were investigated by applying UL-94, LOI, TGA, DSC and cone calorimeter. Tensile tests were applied in order to determine mechanical characteristics of these blends. SEM gave information on the test samples of the blends.

3.5.1 Sample Preparation for the Characterization of the Blends

Blends were prepared by melt mixing in a counter rotating twin screw microextruder (15 mL microcompounder, DSM Xplore, Netherlands) at a screw speed of 100 rpm at 200°C for 5 minutes (Figure 3.4). HPCTP loadings were 10%, 20% and 30% by weight.



Figure 3.4 The twin screw extruder used in this study for the production of blends.

Test samples were prepared by injection molding instrument (Microinjector, Daga Instruments) at a barrel and mold temperature of 210 °C and 40 °C, respectively (Figure 3.5). Injection pressure of 5 bar were applied. Injection molded dog-bone shape specimens with dimensions of 7.4 mm × 2.1 mm × 80 mm were prepared for tensile testing.



Figure 3.5 The laboratory scale injection-molding machine.

The samples for flammability and thermal characterization testing were prepared by compression molding at 230 °C. A laboratory scale hot-press machine (Rucker PHI) was used.

CHAPTER 4

RESULTS AND DISCUSSION

The thermal and flame retardant properties of synthesized cyclic phosphazenes derivatives namely hexaphenoxycyclotriphosphazene and hexakis(propyl amino)cyclotriphosphazene and as well as their polyolefin blends were studied.

Thermal gravimetric analysis (TGA) and differential scanning calorimetry (DSC) were applied to obtain thermal information about the synthesized compounds and related blends under focus. In the related sections given below, conclusions were reached for each of the phosphazenes and remarks were presented elaborately.

In the rest of the results and discussion part, the mechanical, physical, thermal and flame retardant properties of polyolefin blends are presented in separate sections with their own conclusions. Mechanical properties of blends were evaluated by application of tensile test. SEM micrographs of broken surfaces were obtained in order to examine the dispersion nature of cyclic phosphazenes in PE and PP matrices. UL-94 and LOI tests were discussed from the point of view of the flame retardancy effect of the synthesized cyclic phosphazenes on these blends. TGA and DSC tests were performed to observe the thermal behaviour of PE and PP blends. Finally, cone calorimeter results were presented for discussion of flame retardant characteristics of selected blends in conjunction with the results of UL-94 and LOI tests. In the light of all the results of these tests performed through the investigation, mechanical, physical, thermal and flame retardant properties of polyolefin blends were discussed.

4.1 The Thermal Properties of Cyclic Phosphazenes

In this sub chapter, the results of thermal gravimetric analysis and differential scanning calorimetry tests of cyclic phosphazenes, which are hexaphenoxycyclotriphosphazene (HPCTP) and hexakis(propyl amino)cyclotriphosphazene (HPACTP), are represented.

4.1.1 Hexaphenoxycyclotriphosphazene (HPCTP)

Results of thermogravimetric analysis and differential scanning calorimetry are presented in order to evaluate thermal nature of HPCTP.

4.1.1.1 Thermogravimetric Analysis (TGA) for HPCTP

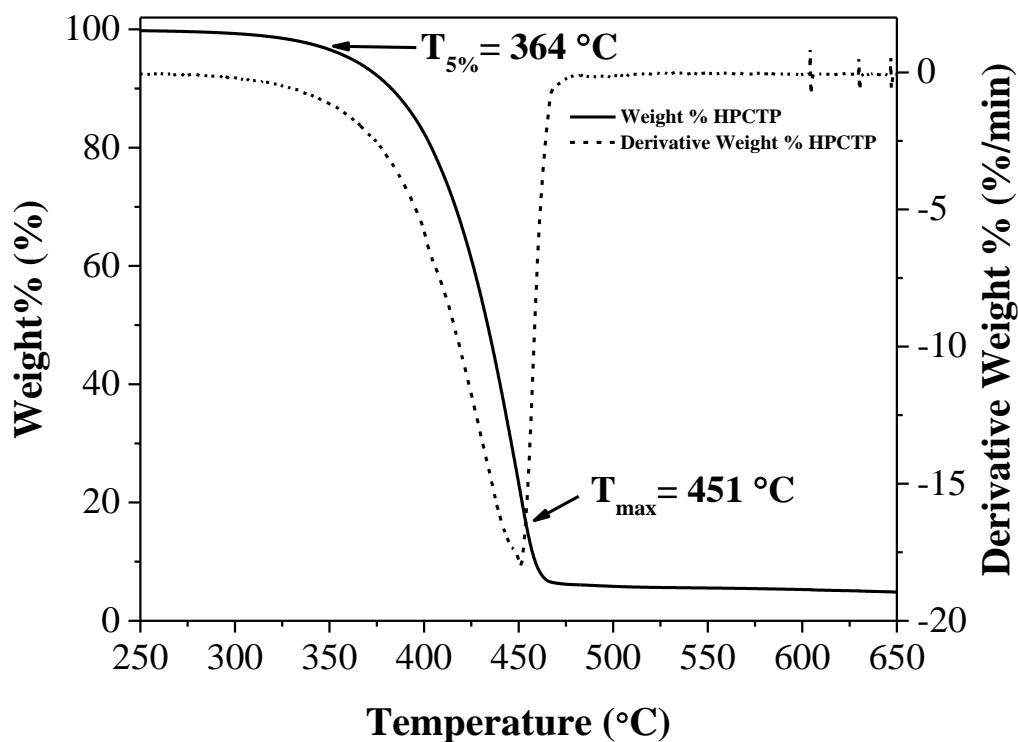


Figure 4.1 TG and DTG Curve of Hexaphenoxycyclotriphosphazene (HPCTP) under the conditions of N₂ atmosphere.

When flammability is considered, thermal gravimetric analysis (TGA) acts as a useful tool by indicating thermal characteristics of the substance. In Figure 4.1 and Table 4.1, thermal gravimetric data of HPCTP are shown. HPCTP demonstrated single step weight loss, with a maximum weight loss at a temperature of 451°C.

Table 4.1 $T_{5\%}$, $T_{50\%}$ and T_{\max} values of Hexaphenoxycyclotriphosphazene (HPCTP) under the conditions of N_2 atmosphere

Sample	$T_{5\%}$	$T_{50\%}$	T_{\max} ($^{\circ}C$)
HPCTP	364	433	451

$T_{5\%}$: 5% decomposition temperature; $T_{50\%}$: 50% decomposition temperature;
 T_{\max} : Maximum decomposition temperature

According to TGA results, sample of HPCTP is stable up to the temperature values around 360 $^{\circ}C$. In range between 300 $^{\circ}C$ and 500 $^{\circ}C$, a significant weight loss was observed. $T_{5\%}$, $T_{50\%}$ and T_{\max} values are determined on TG and DTG curves based on the temperature values corresponding to 5%, 50% and the maximum weight losses. It is reported in literature that HPCTP has thermal stability at 350 $^{\circ}C$ for a long lasting time [175]. This property offers HPCTP to be used as a high temperature standard for the experiments of mass spectrometry [3]. At the end of the thermal decomposition of the sample, there remains almost no char residue at 900 $^{\circ}C$.

According to Shan et al., 2% decomposition temperature of HPCTP is reported as 331 $^{\circ}C$ [31]. This result tends to coincide with temperature values in Figure 4.1. Similar aromatic side group substituted cyclic phosphazenes are reported with $T_{5\%}$ values of 276 $^{\circ}C$ and 201 $^{\circ}C$ [176], [177]. Higher $T_{5\%}$ -values of HPCTP make it a good candidate for applications needing thermal stability.

4.1.1.2 Differential Scanning Calorimetry (DSC) for HPCTP

DSC curves and data related with HPCTP are given in Figure 4.2 and Table 4.2. One endothermic peak resulting from melting of HPCTP crystals is observed.

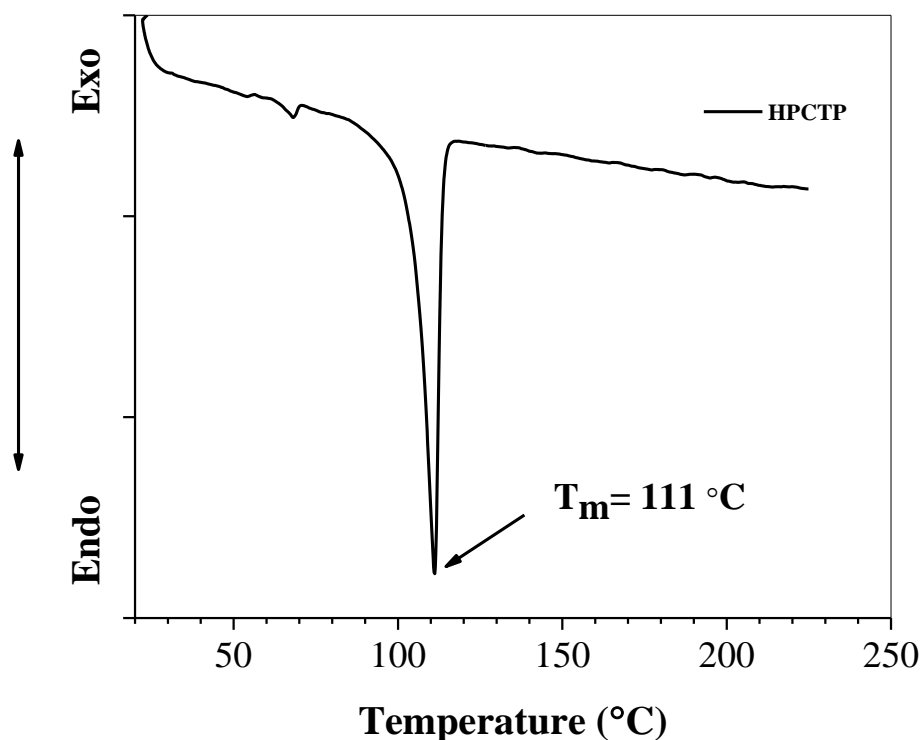


Figure 4.2 DSC Curve of hexaphenoxycyclotriphosphazene (HPCTP) under the conditions of N₂ atmosphere

There is only one endothermic single peak observed around 111 °C indicates that HPCTP does not have a decomposition path within the range of 20°C and 225°C but directly melts as seen in Figure 4.2. The melting point determined by DSC is in accordance with the value reported in the literature [103]. The thermal stability of HPCTP is rather high as expected as this is the characteristics of various aryloxyphosphazenes [52].

Table 4.2 T_m and ΔH_m values of hexaphenoxycyclotriphosphazene (HPCTP) under the conditions of N_2 atmosphere

Sample	T_m ($^{\circ}C$)	ΔH_m (J/g)
HPCTP	111	46.4

T_m : Melting Temperature, ΔH_m : Enthalpy of melting

4.1.2 Hexakispropylaminocyclotriphosphazene (HPACTP)

Thermal and flame retardancy properties of hexakispropylaminocyclotriphosphazene (HPACTP) are evaluated by examining the results of thermogravimetric analysis and differential scanning calorimetry.

4.1.2.1 Thermogravimetric Analysis (TGA) for HPACTP

In Figure 4.3, HPACTP undergoes two steps of weight loss and it may be concluded that a decomposition process occurred. When the bond dissociation energies of the chemical bonds in HPACTP's structure are taken into consideration, the weakest bond strength belongs to the N-C bond with a value of around 305 kJ mol^{-1} . Thus, the detachment of propyl groups of HPACTP is expected to be responsible for the first weight loss step in the TGA curve [178]. Then the second weight loss may be attributed to decomposition of the remaining substituents on the phosphazene ring. However, the first step of the weight loss in Figure 4.3 corresponds to approximately 55 % and this value very well coincide with the calculated value of 56 % for propylamine weight percent in the chemical composition of HPACTP. Therefore, it may be speculated that the first weight loss is due to the propylamine groups in spite of the fact that P-N bond does not have the weakest bond strength. Then the fragmentation continues to some extent with phosphorous nitrogen ring to end up

with around 27 % char residue. The two step weight loss is more clearly observable from DTG data showing two inflection points in Figure 4.3.

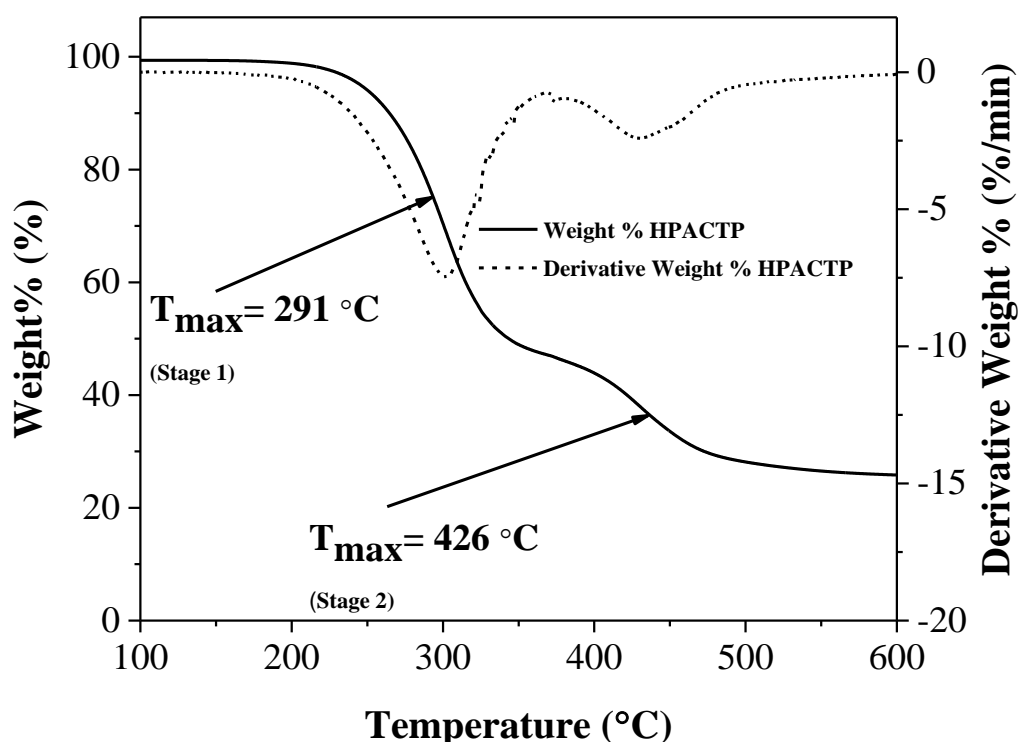


Figure 4.3 TG and DTG Curve of Hexakispropylaminocyclotriphosphazene (HPACTP) under the conditions of N₂ atmosphere

In Table 4.3 thermal characteristics of HPACTP are presented. T_{\max} is observed before 50% decomposition temperature at around 291 °C. Separation of propyl amine groups from the backbone of phosphorus and nitrogen is assumed to be the driving factor for having the first maximum temperature of HPACTP. Further decomposition gives rise to the second maximum temperature at 426 °C, approximately.

Table 4.3 TGA of Hexakispropylaminocyclotriphosphazene (HPACTP) under the conditions of N₂ atmosphere

Sample	T _{5%}	T _{50%}	T _{max} (°C)	
			Stage 1	Stage 2
HPCTP	246	344	291	426

T_{5%}: 5% decomposition temperature; T_{50%}: 50% decomposition temperature;

T_{max}: Maximum decomposition temperature

4.1.2.2 Differential Scanning Calorimetry (DSC) for HPACTP

DSC curve is plotted in Figure 4.4 for HPACTP and the data is presented in Table 4.4. One main and two small endothermic peaks are observed in the thermogram. The main endothermic peak is attributed to the melting of HPCTP crystals with a melting point of around 67 °C on DSC curve. This melting value for HPACTP is in accordance with the value of 68 °C reported by Bickley et al [4].

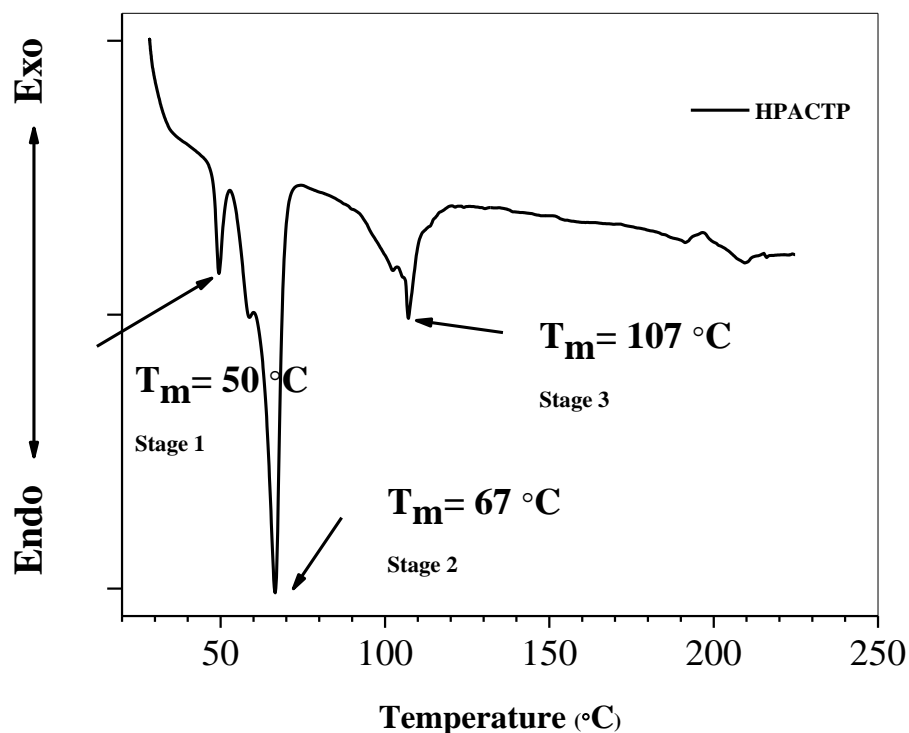


Figure 4.4 DSC Curve of Hexakispropylaminocyclotriphosphazene (HPACTP) under the conditions of N₂ atmosphere

Table 4.4 DSC Data of Hexakispropylaminocyclotriphosphazene (HPACTP) under the conditions of N₂ atmosphere

Sample	T _m (°C)			ΔH _m (J/g)		
	Stage 1	Stage 2	Stage 3	Stage 1	Stage 2	Stage 3
HPACTP	50	67	107	5.1	72.3	34

T_m: Melting Temperature, ΔH_m: Enthalpy of melting

4.2 The Mechanical Properties of Polyolefins and Cyclic Phosphazenes Blends

The mechanical properties of polyolefin blends with cyclic phosphazenes, PE and PP are presented in this section. Mechanical testing results and SEM analysis were also presented.

4.2.1 Tensile Properties of PE-HPCTP and PE-HPACTP Blends

The stress-strain graphs are plotted in Figure 4.5 and the tensile properties covering tensile strength, elongation at break and Young's Modulus are shown in Table 4.5. Tensile strength of PE-HPCTP blends decreases with higher concentrations of HPCTP, whereas elongation at break values have an increasing trend. However, the tensile strength does not decrease while concentration of HPCTP increases from 20% to 30%. Homogeneous dispersion of HPCTP through PE matrix may be responsible for having a value 8.4 MPa of tensile strength. In a similar way, Young's modulus firstly decreases when the concentration of HPCTP increases to 20 %. Then, it reaches a level of 83.4 MPa while moving from 20 % to 30 % of HPCTP concentrations.

Table 4.5 Tensile Test Results of PE-HPCTP and PE-HPACTP Blends

Samples	Tensile Strength (MPa)	Elongation at Break (%)	Young's Modulus (MPa)
Pure PE	14.7± 0.7	115.2±1.6	60.6±8.0
HPCTP10PE	11.6±1.4	86.2±10.1	93.9±6.1
HPCTP20PE	7.9 ±0.3	82.2±16.6	83.2±4.7
HPCTP30PE	8.4±0.7	100.2±17.1	83.4±13.7
HPACTP10PE	12.0±0.9	107.1±4.4	82.9±28.6
HPACTP20PE	10.4±0.6	96.2±14.2	84.2±19.1
HPACTP30PE	7.5±0.1	90.0±4.5	95.5±13.5

Tensile strength and elongation at break decrease while concentrations of HPACTP increases. This reduction may be a result of incompatibility between HPACTP and PE matrix. It is reported that aliphatic cyclic phosphazene additions to the polymer blends exhibit similar reductions. This is attributed directly to the compatibility of additive with polymer matrix [36]. Increases in Young's modulus values may indicate that the rigidity of blends increases due to the filler effect of HPACTP crystals. In section 4.2.3, SEM micrographs indicate dispersion of HPACTP particles through PE matrix. Well dispersion of HPACTP is observed. Filler effect at bulk level resulted in rigid PE-HPACTP blends.

It is known that the stress is transferred from continuous phase to dispersed phase [152]. Regarding PE blends in this study, dispersed phase was not able to give higher mechanical properties. Mechanical properties of blends show decrease in both ultimate stress and strain. But the results are rather acceptable for the use.

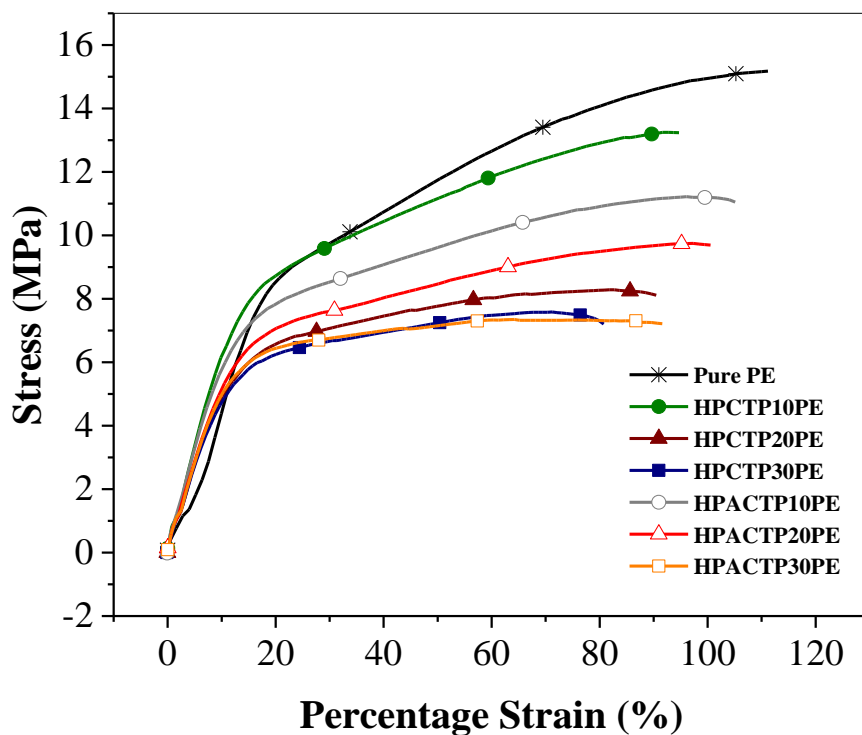


Figure 4.5 Stress-strain Curve of PE-HPCTP and PE-HPACTP Blends.

4.2.2 Tensile Properties of PP-HPCTP and PP-HPACTP Blends

The stress-strain curves of PP-HPCTP and PP-HPACTP blends are demonstrated in Figure 4.6 and Table 4.6.

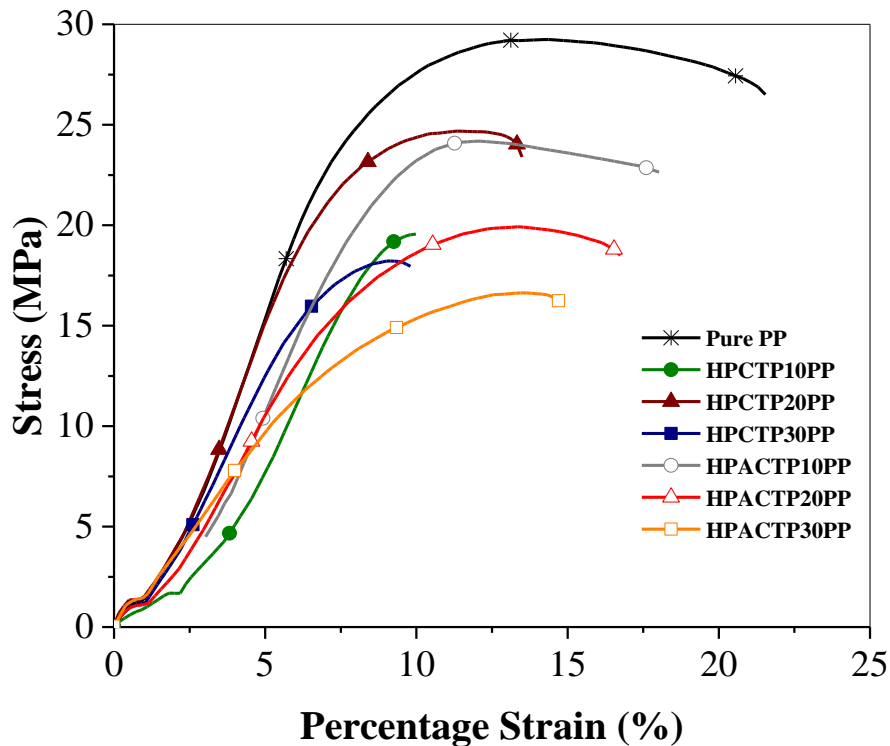


Figure 4.6 Stress-strain Curve of PP-HPCTP and PP-HPACTP Blends.

Tensile strength of PP-HPCTP blends decreases while loading increases up to 30%. Whereas, the increase at 20% loading may be an indication that homogeneous dispersion occurred in addition to good compatibility. Also, higher stiffness character is observable in increasing Young's modulus value for 20 % loading. Then, all tensile property values decrease with increasing HPCTP content up to 30 %. Detailed observations are given in the next section.

In the case of PP-HPACTP blends, tensile properties have a decreasing trend while the concentration of HPACTP increases in blends. Filler effect is responsible for having lower values of tensile strength and Young's modulus. It can be discussed that HPCTP acts as an inert filler through PP matrix. Polymer chain interactions may be interrupted by HPCTP. In section 4.2.4, layers of PP are easily observed for

HPCTP20PP and HPCTP30PP. As a result of HPCTP generated effects, mechanical stress is reduced. This reduction is within acceptable region for application purposes of HPCTP according to Höhne et al. [179]. They also reported a similar decreasing trend in tensile strength values for PA6-HPCTP blends [179]. Additionally, HPCTP does not decompose at process temperatures as well as indicated in section 4.1.1.1. This indicates that the thermal stability of a blend is important for flame retardant applications [180]. Processability of PP-HPCTP blends appears as tensile tests and thermal stability are combined.

Table 4.6 Tensile Test Results of PP-HPCTP and PP-HPACTP Blends

Samples	Tensile Strength (MPa)	Elongation at Break (%)	Young's Modulus (MPa)
Pure PP	29.5±0.4	20.8±0.9	453.6±17.1
HPCTP10PP	21.2±1.7	16.6±6.3	363.5±27.3
HPCTP20PP	24.3±0.5	16.0±2.3	415.3±19.3
HPCTP30PP	19.4±1.4	11.8±2.1	341.9±18.5
HPACTP10PP	23.6±0.6	29.1±15.4	342.1±23.9
HPACTP20PP	20.5±0.5	32.9±28.0	294.9±19.7
HPACTP30PP	16.0±0.9	15.9±2.2	243.6±26.7

4.2.3 SEM Analysis of PE-HPCTP and PE-HPACTP Blends

Representative SEM micrographs belonging to surface of fractured PE blends are demonstrated in Figure 4.7. For the blend of HPCTP10PE (image1), there existed homogeneous dispersion through the matrix and particles of cyclic phosphazenes. Probably this situation may result from good adhesion between PE and HPCTP

particles. Other alternatives of aromatic phosphazene applications are studied in literature. Fracture morphology of aromatic phosphazene additives indicates enhancements in interfacial adhesion and well dispersion behaviour [181].

Crystal structures of HPCTP particles are observed in all SEM micrographs. In higher concentrations, the boundaries of crystals become more clear due to the agglomerations (image 2 and 3). HPACTP particles also have a crystal structure and wetted particles are dispersed through the matrix in all concentrations (images 4, 5 and 6) at a good condition except some local points of HPACTP clusters in image (6). Similar aliphatic phosphazene additives demonstrate homogeneous coverage through matrix [182] Also, other alternatives of aromatic phosphazene applications are studied. Fracture morphology of aromatic phosphazene additives indicates enhancements in interfacial adhesion

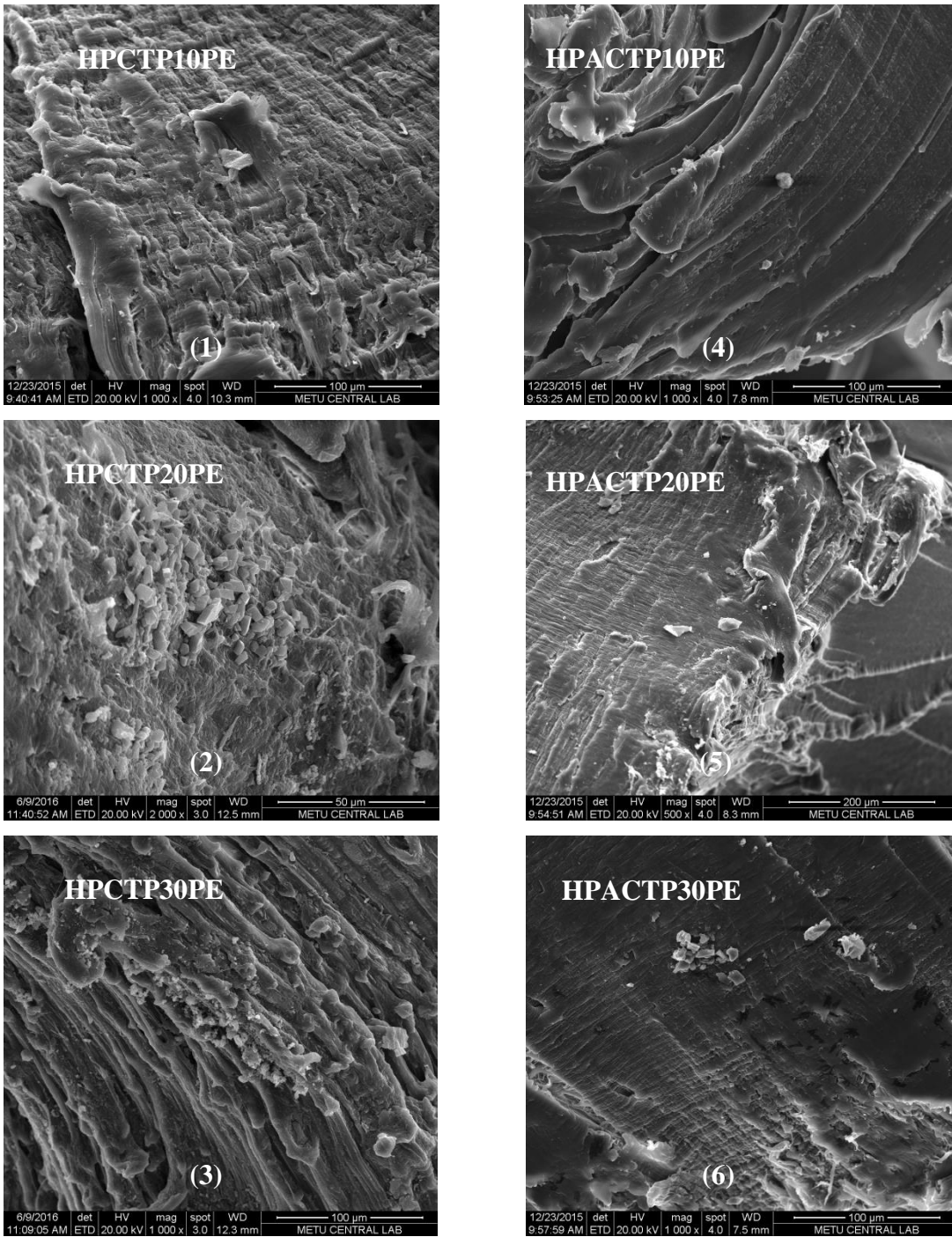


Figure 4.7 SEM micrographs of fractured surfaces of PE-HPCTP and PE-HPACTP blends.

Agglomeration of cyclic phosphazene particles through the matrix may be the result of a condition that an optimum level of dispersion was lost after the loading of 20 %. PE blends undergoes strain hardening. It can be claimed that the cyclic phosphazenes do not affect the crystallinity. As a result of this, melting point temperature does not vary as discussed in the section of 4.3.1.2.

4.2.4 SEM Analysis of PP-HPCTP and PP-HPACTP Blends

In Figure 4.8, representative SEM micrographs of PP Blends are shown. There existed a good adhesion through the matrix for 10 % concentration of HPCTP (image 1). Well dispersed particles give rise to homogeneous appearance for HPCTP10PP. On the other hand, plates and layers are observed for HPCTP20PP and HPCTP30PP (images 2 and 3). As indicated in section 4.2.4, morphology of fracture indicated good adhesion and favourable dispersion according to Cai et al [181]. Well dispersion and good adhering of HPCTP HPCTP20PP indicate enhanced mechanical properties through other two types PP-HPCTP blends in section 4.2.2. After stress relief, there existed curly structures at fractured surfaces. For HPACTP blends, sponge structures are observed (images 4, 5 and 6). Especially in HPACTP10PP and HPACTP20PP blends, there existed a homogeneous dispersion and wetted particles through the matrix are easily observed (images 4 and 5). Crystals of HPACTP adhered to the PP matrix in a good condition at the concentration of 30% and agglomerations did not exist.

Strain orientation is observed for PP blends as well as for PE blends discussed earlier. Fibril structures are observed in SEM micrographs. Melting point temperatures do not change which will be discussed in the next section of 4.3.2.2.

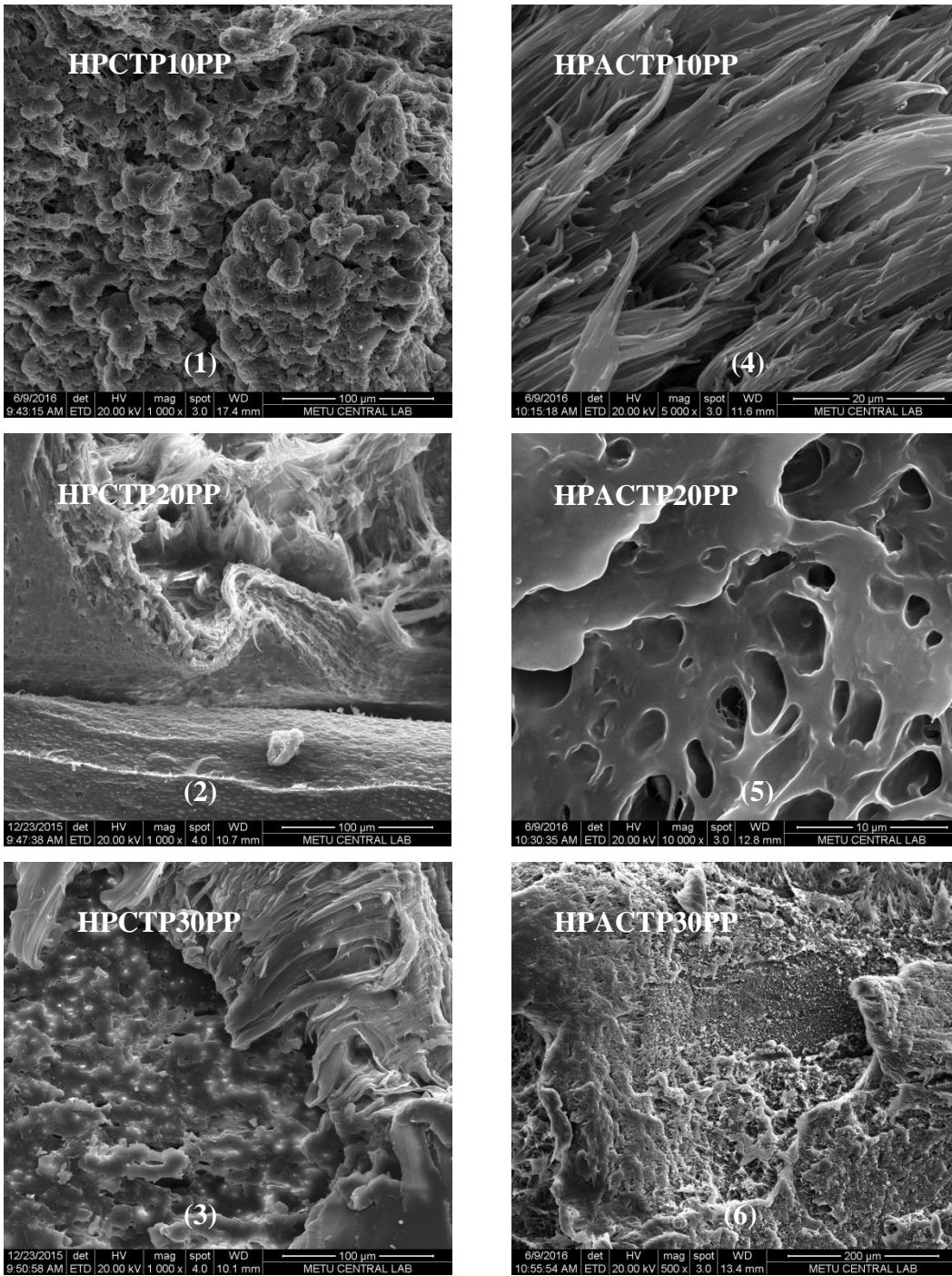


Figure 4.8 SEM micrographs of fractured surfaces of PP-HPCTP and PP-HPACTP blends.

4.3 Thermal Properties of Polyolefins and Cyclic Phosphazenes Blends

Within the context of this part, thermal properties of blends are analyzed by using the results of TGA and DSC. Prepared blends of polyolefins and cyclic phosphazenes were studied elaborately in order to understand the thermal nature of these blends.

4.3.1 PE-HPCTP and PE-HPACTP Blends

In this part, TGA and DSC results are presented for PE-HPCTP and PE-HPACTP Blends. It is aimed to demonstrate thermal nature of PE blends.

4.3.1.1 Thermogravimetric Analysis (TGA) for PE-HPCTP and PE-HPACTP Blends

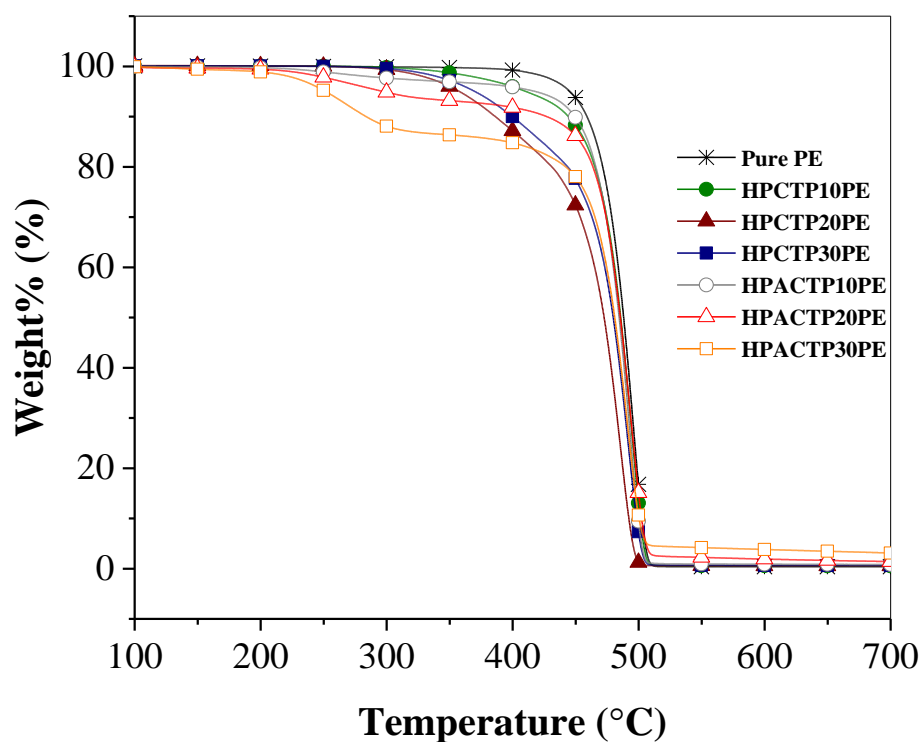


Figure 4.9 TG Curve of PE-HPCTP and PE-HPACTP Blends under the conditions of N₂ atmosphere.

From Figure 4.9, it is observable that nearly all PE blends prepared with HPCTP have one maximum weight loss point whereas PE-HPACTP blends have a tendency to have two steps of weight loss. Similar aromatic phosphazene additives show similar behaviours in T_{5%} values in literature. According to Kawahara et al., T_{5%} values are reported around 330 °C [183]. Phosphazenes start to decompose before the main matrix starts to deteriorate as seen in Figures 4.9 and 4.10. It is more clearly seen in Figure 4.10 that HPACTP30PE undergoes two steps of decomposition. First

one occurs at 275 °C. The first decomposition points for HPACTP10PE and HPACTP20PE do not appear in Figure 4.9 and 4.10. This may result from dispersion of HPACTP through PE matrix is more homogeneous in HPACTP30PE. The other data covering all the blends are presented in Table 4.7. Considering T_{max} data, all blends converge a value of maximum temperature around 490°C. There does not exist a large difference between the values of pure PE and PE blends of cyclic phosphazenes.

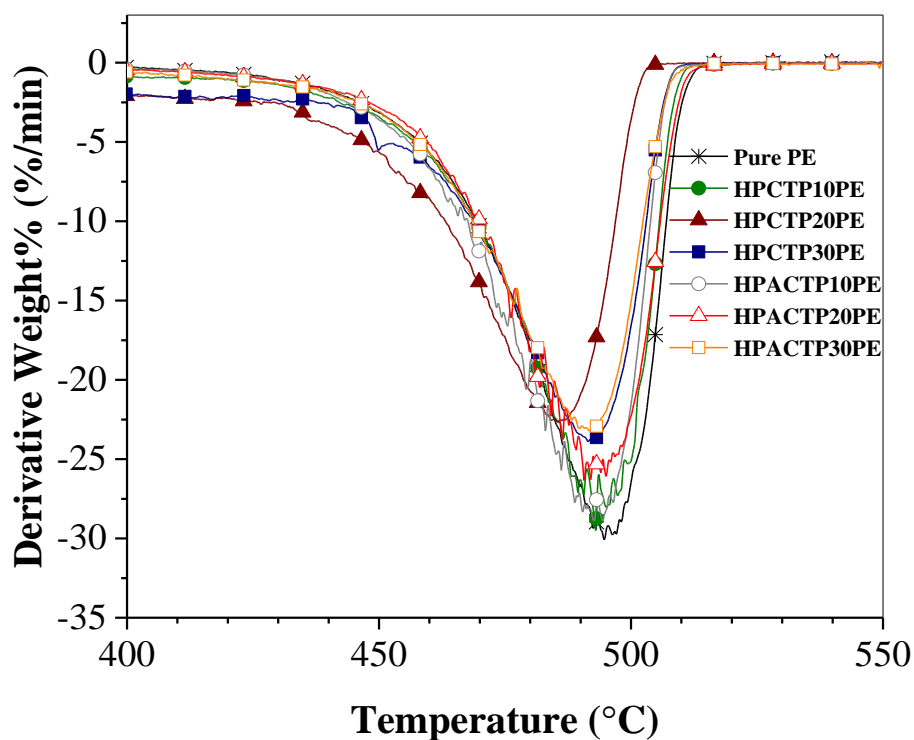


Figure 4.10 DTG Curves of PE-HPCTP and PE-HPACTP Blends.

On the other hand, it can be easily observed that 5% decomposition temperature of all blends exhibit large drops compared to pure PE and within the group while concentration of cyclic phosphazenes increases. Similar aliphatic structures are

studied in literature and $T_{5\%}$ values exhibited a decreasing trend with increasing aliphatic cyclic phosphazene concentration likewise to PE-HPACTP blends [109], [184].

El Gouri et al. studied a similar type of aliphatic phosphazene additives and found a decreasing increasing behaviour in $T_{5\%}$ values [180]. While HPACTP content increases $T_{5\%}$ values decrease in Table 4.7. This may indicate degradation takes place predominantly within HPACTP concentrated segments.

Table 4.7 TGA of PE-HPCTP and PE-HPACTP Blends under the conditions of N_2 atmosphere

Sample	$T_{5\%}$	$T_{50\%}$	T_{max} ($^{\circ}C$)
Pure PE	446	488	495
HPCTP10PE	411	486	493
HPCTP20PE	358	473	486
HPCTP30PE	370	480	492
HPACTP10PE	418	485	493
HPACTP20PE	297	486	491
HPACTP30PE	252	481	492

$T_{5\%}$: 5% decomposition temperature; $T_{50\%}$: 50% decomposition temperature;

T_{max} : Maximum decomposition temperature

HPCTP has a good thermal stability [31]. Decomposition temperature values exhibit increases for PE-HPCTP blends with 20% and 30% loadings by weight. As indicated in section 4.2.1, a similar trend for tensile strength values is also observed. Homogeneous dispersion of HPCTP particles may be the reason of these increases

both in thermal and mechanical properties. When SEM micrographs are observed in section 4.2.3 again, well dispersed HPCTP particles can be easily seen.

Based on literature data, HPCTP particles disperse through other types of matrices homogeneously; Shan et al. reported onset temperature for blends of HPCTP and poly(lactic acid) around 300 °C [31]. In this study, T_{5%} values for PE-HPCTP blends show higher temperatures than the temperature values for 2% mass loss by weight of HPCTP with different type of matrix.

Similar aliphatic phosphazenes to HPACTP are studied in literature and homogeneous dispersion through different types of matrices is reported [180]. In section 4.2.3, SEM micrograph of HPACTP30PE indicates some local agglomerations. These local points show their effect in tensile strength values for HPACTP20PE and HPACTP30PE as decreases in section 4.2.1. Then T_{50%} values can be correlated with these decreasing values results with tensile tests and SEM. In brief, agglomerated particles of HPACTP are responsible for lowering T_{50%}.

4.3.1.2 Differential Scanning Calorimetry (DSC) for PE-HPCTP and PE-HPACTP Blends

Regarding DSC data, enthalpy of melting (ΔH_m), melting temperature (T_m) and percent crystallinities ($\chi\%$) are listed in Table 4.8. Percent crystallinity is calculated by using Equation 4.1. In the formula, Φ corresponds to mass fraction of cyclic phosphazene additives in the blends. ΔH_m° represents enthalpy of melting value for 100 % crystalline PE with a value of 290 J/g [185].

$$\chi\% = \left[\frac{\Delta H_m}{\Delta H_m^\circ \times (1-\Phi)} \right] \times 100$$

Equation 4.1 Percent Crystallinity Calculation

In Figure 4.13, it is observable that only one peak occurs on the plot and it indicates that cyclic phosphazenes are compatible within PE matrix. Enthalpy of melting decreases with increasing HPCTP amount for PE blends, generally. From 10% to 20% of HPCTP concentration, it is observable in Table 4.8 that ΔH_m decreases from the value of 130.90 J/g to 87.76 J/g. On the other hand, an increase happens in HPCTP30PE, it may be a result of exiting optimum loading level of HPCTP crystals or agglomerations of HPCTP within PE matrix.

Single endothermic peaks observed for PE-HPCTP blends. Similar result is obtained in literature for a similar type of aromatic group substituted cyclic phosphazene [186]. It is clear that a single peak indicates an enhancement in compatibility between additive and polymer matrix. Also, melt processing would be another factor for having improved interfacial adhesion.

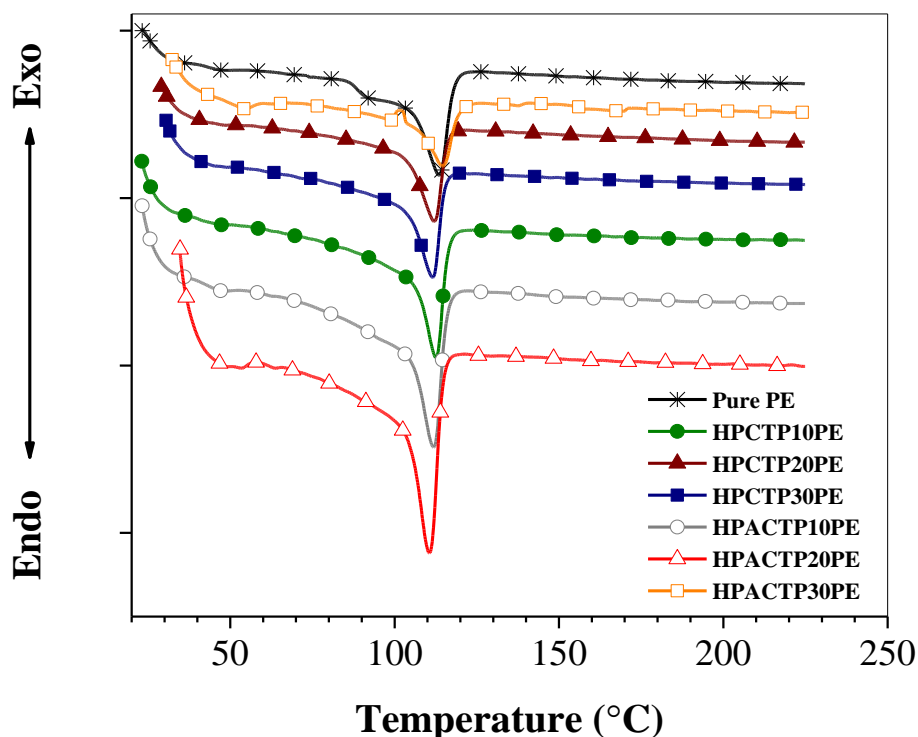


Figure 4.13 DSC Curve of PE-HPCTP and PE-HPACTP Blends under the conditions of N₂ atmosphere.

In Figure 4.14, the melting points of PE blends do not vary much with the amount of HPACTP. While T_m of HPACTP30PE increases, ΔH_m decreases and so $\chi\%$ does. As indicated in previous paragraph, decomposed crystals of HPACTP may be responsible for this situation.

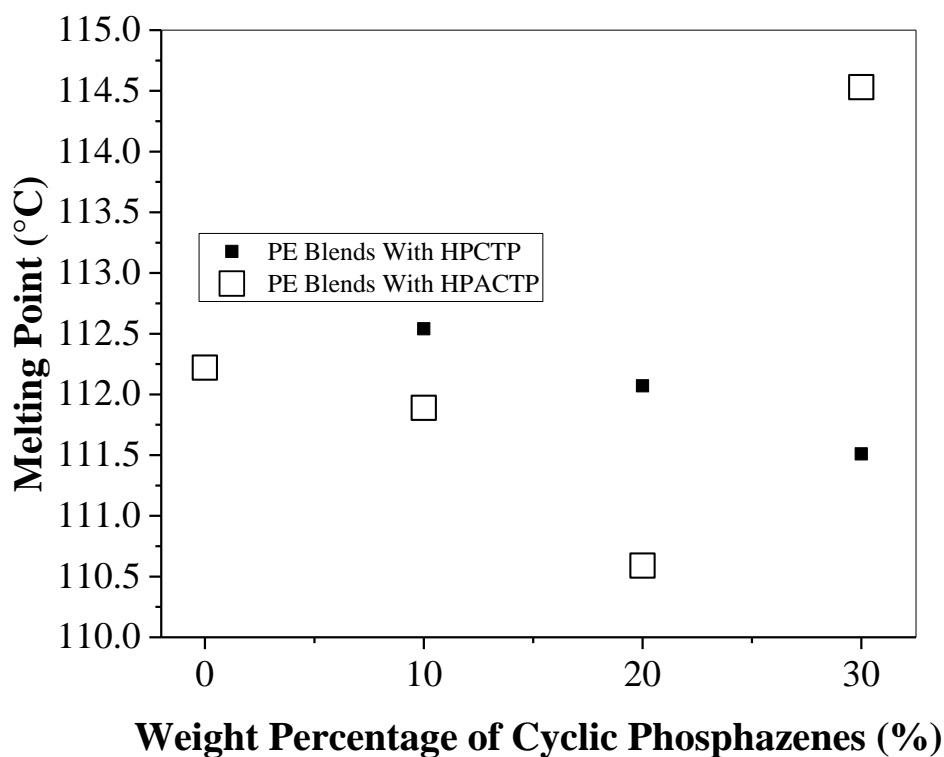


Figure 4.14 The variation of Melting Point of PE Blends versus Cyclic Phosphazene Concentration

In the case of HPCTP30PE, T_m decreases while ΔH_m increases. It is generally expected the T_m and ΔH_m values increase with each other. In Figure 4.15, $\chi\%$ of HPCTP30PE demonstrates a rise.

Percent crystallinities have a decreasing trend with loading of HPACTP and this reflects its effect in decreasing ultimate stress and strain values indicated in section 4.2.1. For HPACTP30PE, percent crystallinity value dropped and it complies with SEM micrograph of the blend as seen in picture (6) in Figure 4.7. Some local agglomerated HPACTP domains are observed. Agglomerations of HPACTP particles are formed as their concentration increases. It is also reported in literature that when HPCTP content of polymer matrix augments, percent crystallinity values demonstrate a decreasing trend and a decline is observed for mechanical properties [179].

HPCTP dispersion through PE matrix is homogeneous as clearly seen in section 4.2.3. It is supported by DSC result in Figure 4.13 by having single melting points. Furthermore literature studies of HPCTP in PA6 matrix indicates that the polymer blends with HPCTP have no signals for HPCTP. This result indicates HPCTP particles are distributed in amorphous form or they exhibit molecular coordination through polymer matrix. HPCTP may not be dispersed in crystalline form [179].

Table 4.8 DSC Data of PE-HPCTP and PE-HPACTP Blends

Sample	T_m (°C)	ΔH_m (J/g)	χ (%)
PE	112.2	94.1	32.4
HPCTP10PE	112.5	130.9	50.2
HPCTP20PE	112.1	87.8	37.8
HPCTP30PE	111.5	106.5	52.5
HPACTP10PE	111.9	163.3	62.6
HPACTP20PE	110.6	174.8	75.4
HPACTP30PE	114.5	36.5	18.0

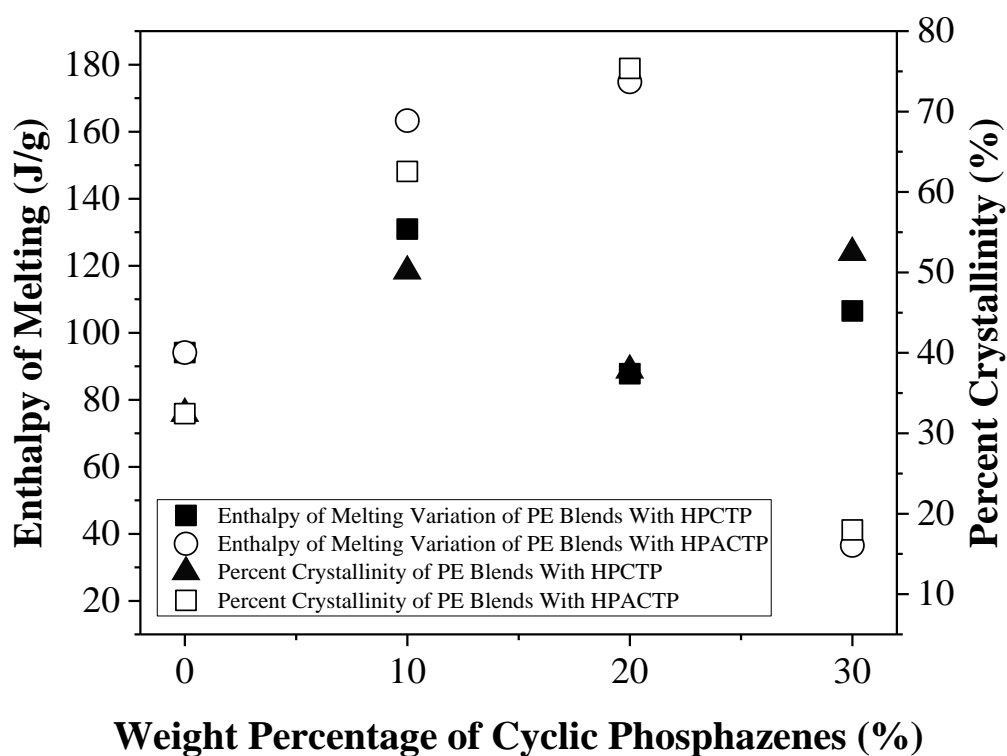


Figure 4.15 The Variation of Enthalpy of Melting and Percent Crystallinity of PE Blends versus Cyclic Phosphazene Concentration

4.3.2 PP-HPCTP and PP-HPACTP Blends

TGA and DSC results were obtained and discussed for PP-HPCTP and PP-HPACTP Blends. Results are compared with each other. It can be seen that no char residue formed for PP blends in a similar manner presented for PE blends in previous sections.

4.3.2.1 Thermogravimetric Analysis (TGA) for PP-HPCTP and PP-HPACTP Blends

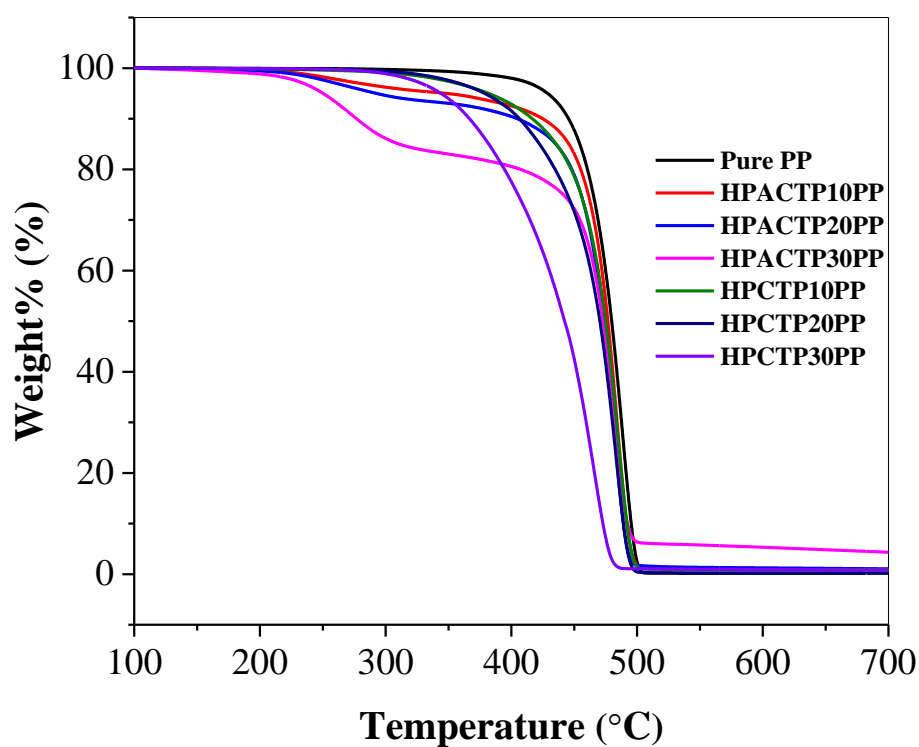


Figure 4.17 TG Curve of PP-HPCTP and PP-HPACTP Blends under the conditions of N₂ atmosphere.

In Figures 4.17 and 4.18, single weight loss points are observed for PP-HPCTP blends, whereas PP-HPACTP blends demonstrate two stages of decomposition. The first stage maximum temperature of HPACTP reaches a value of 275 °C.

T_{5%} values of PP blends decrease with higher contents of HPCTP and HPACTP. On the contrary to the findings of PE-HPCTP blends, PP-HPCTP blends have decreasing elongation at break values with increasing concentration. The reason for having

lower $T_{5\%}$ for PP blends may suggest that degradation of both HPCTP and HPACTP in the PP matrix occur firstly.

Li et al. studied another type of aliphatic cyclic phosphazene which is used as a coating for cotton fabrics. They reported $T_{5\%}$ values around 250 °C, especially for higher loadings of 30% by weight [109]. These values of $T_{5\%}$ coincide well with the ones for HPACTP20PP and HPACTP30PP. Decomposition temperature values follow a decreasing trend while loadings increase. It is clear that $T_{5\%}$ values of PP-HPACTP decrease as a result of increasing aliphatic cyclic phosphazene content.

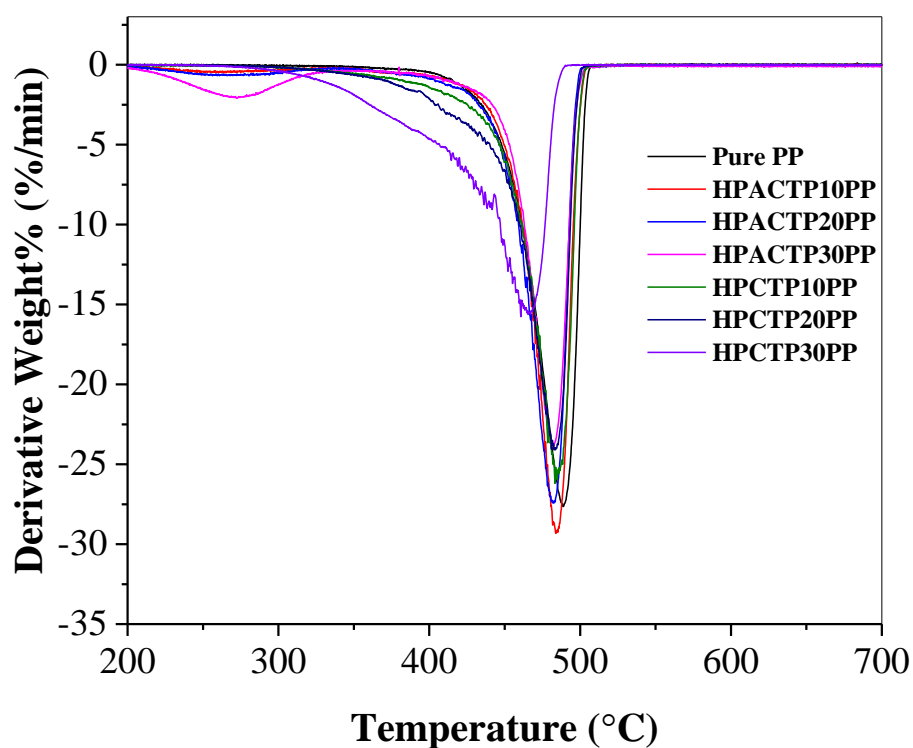


Figure 4.18 DTG Curve of PP-HPCTP and PP-HPACTP Blends.

However, the values of $T_{50\%}$ and T_{\max} are nearly the same, except for HPCTP30PP. There may exist an optimum value of concentration for PP blends with HPCTP between 20% and 30% values of concentration. Then, agglomerations of HPCTP may start to form through PP matrix and this may result in a decrease in the T_{\max} value.

Table 4.9 TGA of PP-HPCTP and PP-HPACTP Blends under the conditions of N_2 atmosphere.

Sample	$T_{5\%}$	$T_{50\%}$	T_{\max} ($^{\circ}C$)
Pure PP	429	480	489
HPCTP10PP	381	480	489
HPCTP20PP	379	475	483
HPCTP30PP	344	471	461
HPACTP10PP	348	477	483
HPACTP20PP	293	473	482
HPACTP30PP	250	473	482

4.3.2.2 Differential Scanning Calorimetry (DSC) for PP-HPCTP and PP-HPACTP Blends

Agglomerations are observed for these blends in SEM micrographs in section 4.2.4. Good adhesion of cyclic phosphazenes to PP matrix is observed. Then, it can be discussed that clusters of cyclic phosphazene crystals may act as filler. Percent crystallinity is calculated by using Equation 4.1. Enthalpy of melting for theoretical 100 % crystalline PP is taken as 207 J/g [187]. As seen in Table 4.10, T_m values for PP-HPACTP blends decrease, whereas $\chi\%$ values increase.

Table 4.10 DSC Data of PP-HPCTP and PP-HPACTP Blends under the conditions of N₂ atmosphere.

Sample	T _m (°C)	ΔH _m (J/g)	χ (%)
PP	164.9	70.6	34.1
HPCTP10PP	164.4	70.7	37.9
HPCTP20PP	163.9	89.2	53.9
HPCTP30PP	164.3	62.5	43.2
HPACTP10PP	164.4	73.7	38.5
HPACTP20PP	163.0	84.73	46.0
HPACTP30PP	161.9	107.11	59.5

In Figure 4.19, two peaks are observed for all PP blends except for HPCTP20PP. Cyclic phosphazenes generally act as incompatible filler for PP blends. On the other hand, PP-HPACTP blends exhibit larger enthalpy of melting with increasing HPACTP concentration, as clearly seen in Figure 4.21. Percent crystallinity has an increasing trend for PP-HPACTP blends.

Other types of aromatic and aliphatic phosphazenes in blends demonstrate their thermal properties separately [180], [188] HPCTP is studied in poly(lactic acid) blends and thermal properties of HPCTP is reported [31]. In Figure 4.19, thermal properties of both HPCTP and HPACTP in PP blends are observed. In accordance with the literature, aromatic and aliphatic phosphazenes exhibit their own thermal properties.

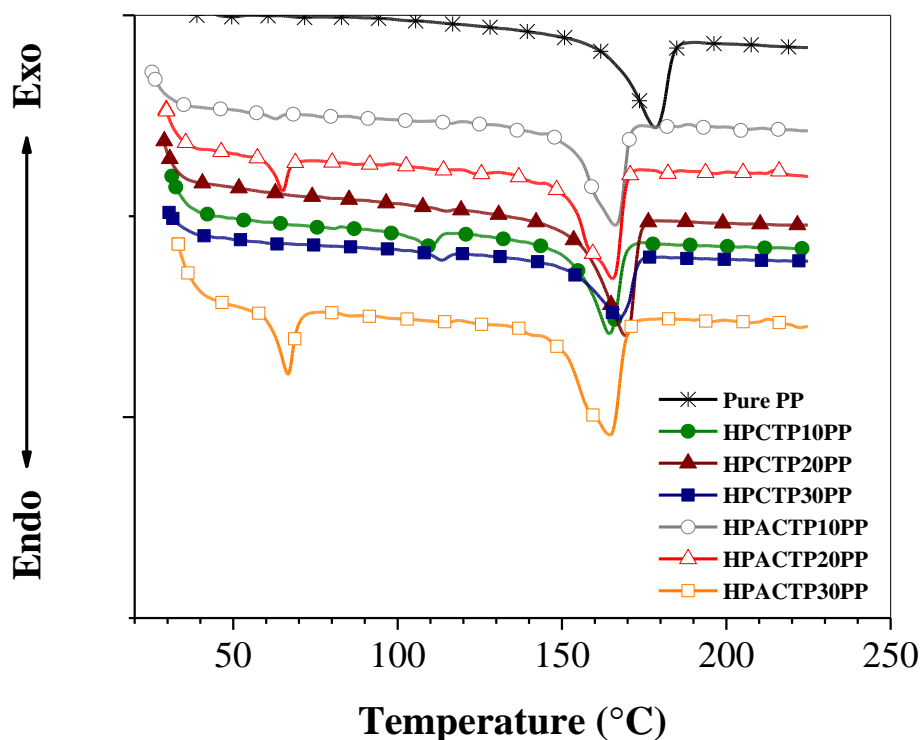


Figure 4.19 DSC Curve of PP-HPCTP and PP-HPACTP Blends under the conditions of N₂ atmosphere.

As seen in Figures 4.20 and 4.21, the reason that HPCTP20PP has higher values of ΔH_m and $\chi\%$ and a lower value of T_m in comparison to other two PP-HPCTP blends may be good dispersion of HPCTP crystals through PP matrix. In addition, it may be speculated that an optimum value of distribution for HPCTP crystals is around 20% concentration. Since, clusters of HPCTP started to form as seen in SEM micrographs in section 4.2.4. Incompatible blending may occur for HPCTP10PP and HPCTP30PP due to insufficient loading or overloading of HPCTP in PP.

Unlike the results presented in 4.3.1.2, HPCTP signals are present in Figure 4.19 and this observation indicates that distribution of HPCTP may be in crystalline form. Signals are more significant for aliphatic cyclophosphazenes for HPACTP20PP and HPACTP30PP.

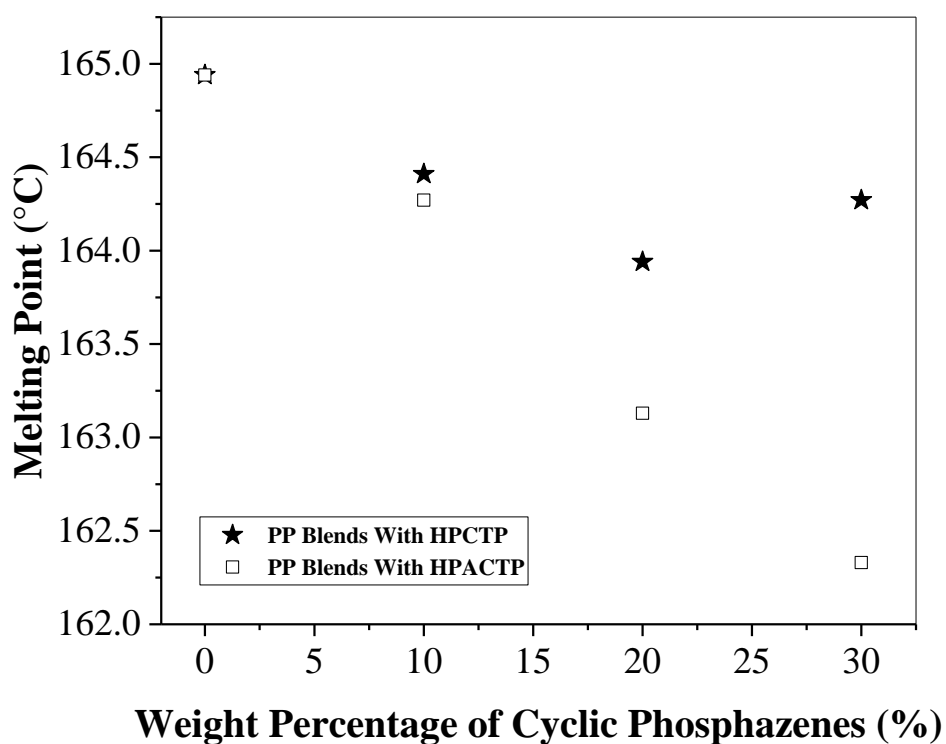


Figure 4.20 The Variation of Melting Point of PP Blends versus Cyclic Phosphazene Concentration

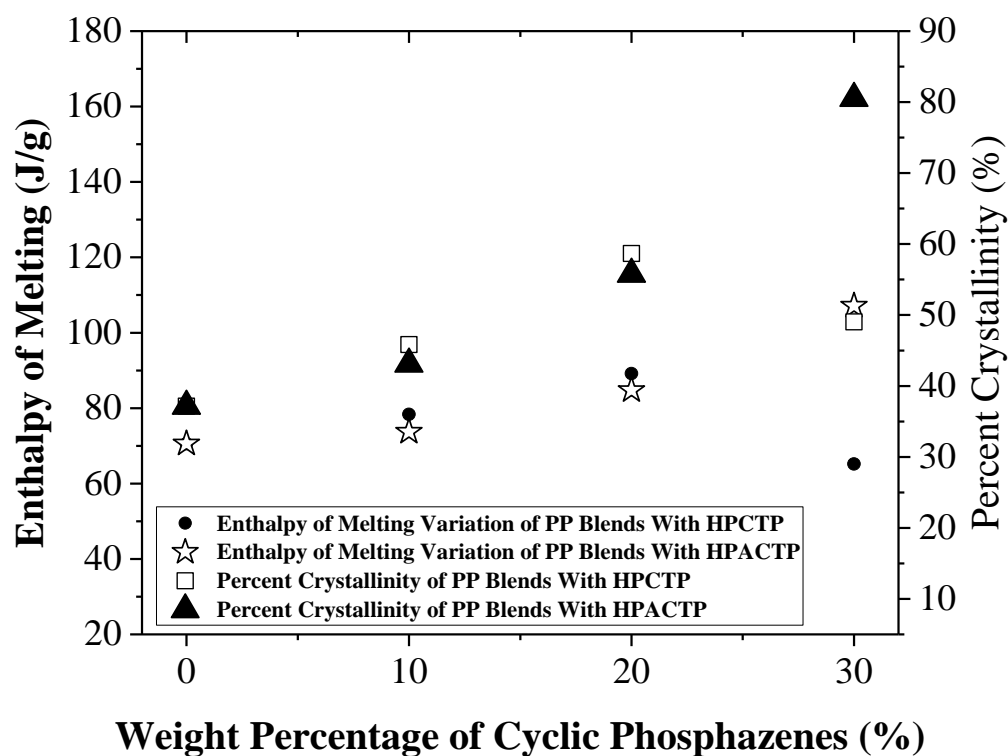


Figure 4.21 The Variation of Enthalpy of Melting and Percent Crystallinity of PP Blends versus Cyclic Phosphazene Concentration

It is clearly seen that increased percent crystallinity for HPCTP20PP shows its effect in its better mechanical performance reported in section 4.2.2. Crystalline domains give order and high cohesion to the blend. For PP-HPACTP blends, mechanical properties are dropped significantly, as a result of decreases in percent crystallinities. Two signals are observed for PP-HPACTP blends and they become clearer with increasing loading. This may be a result of amorphous dispersion of HPACTP through the matrix.

4.4 Flame Retardancy of Polyolefins and Cyclic Phosphazenes Blends

Flame retardancy of blends was studied by means of limiting oxygen index, UL-94 and cone calorimetry. Limiting oxygen index and UL-94 tests were applied for evaluation of flame retardant properties of materials. Cone calorimeter tests were also conducted in order to determine the time to ignition, heat release rate and total heat release rate.

4.4.1 PE-HPCTP and PE-HPACTP Blends

Test samples were prepared for PE blends for tests of flame retardancy. First of all, LOI and UL-94 tests were applied. Based on the results of these tests, especially UL-94 test results with V0, cone calorimeter tests were applied for selected blends.

4.4.1.1 Limiting Oxygen Index (LOI) for PE-HPCTP and PE-HPACTP Blends

According to LOI tests applied on test samples of PE blends, a sharp increase occurred while concentration of both HPCTP and HPACTP increases to 10%. The value of LOI was increased from 19.8 to 24.3 and then as seen in Figure 4.23, this increasing trend continues for concentrations of 20% and 30% of HPCTP in a smoother mode for PE-HPCTP blends. Regarding PE-HPACTP blends, the increase was only observed for 10% of HPACTP, then they followed a constant trend for higher concentrations of HPACTP.

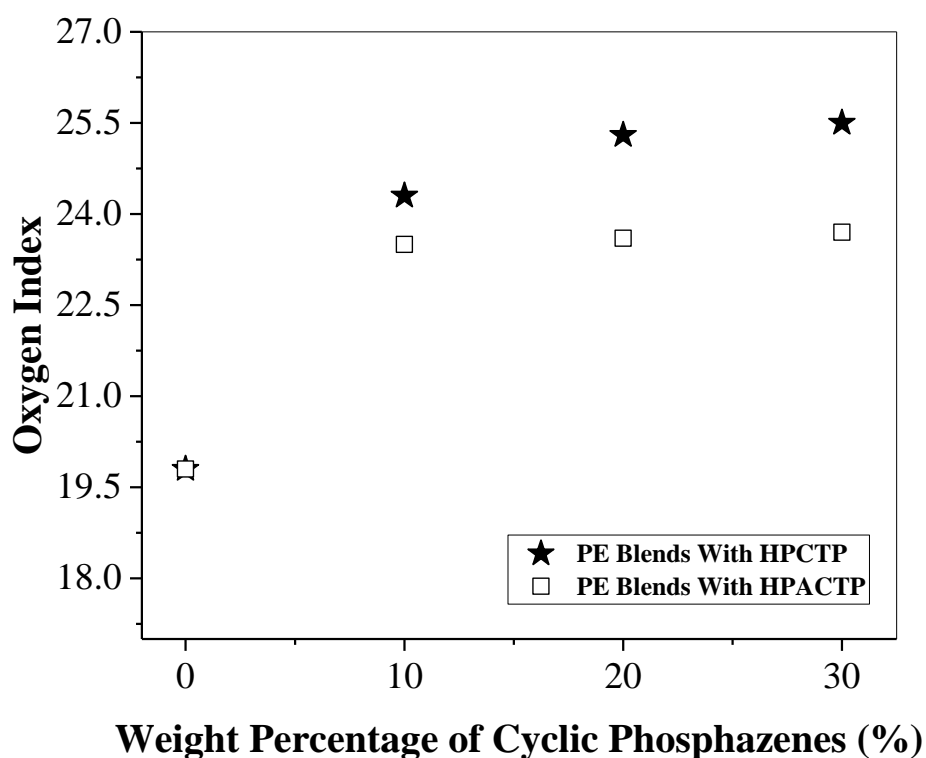


Figure 4.23 Oxygen Index versus Cyclic Phosphazene Concentration for PE-HPCTP and PE-HPACTP Blends

Aromatic structure of HPCTP may be responsible for having larger values of LOI for PE-HPCTP blends in comparison with PE-HPACTP ones. Flame retardancy effect of different kinds of aromatic cyclic phosphazenes are reported in literature with increasing effect in LOI values [189], [190]. In another article, Cao et al. reported good performance of non-flammability for thermoset resin blends prepared with HPCTP [191].

Incorporation of HPCTP through PE matrix results in higher LOI values. As seen in SEM micrographs, homogeneous dispersion of HPCTP as well as with aromatic structure are the main factors for improved LOI performance. Qian and co-workers

studied HPCTP in PU matrix and reported similar results in LOI performance [192]. First concentration increase of HPCTP in PU matrix has an improving effect in LOI. Then enhancements in PU follow a more stabilised manner in their studies. This behaviour is similar to PE matrix results obtained in this study. LOI value increased to 24.3 significantly. Then values do not increase substantially for 20 % and 30 % concentrations. More incorporation of HPCTP does not have a substantial increase. Only slight enhancements are observed. This may be related with bi-phase flame retardancy of HPCTP according to Qian et al [192].

In this study, 10% of HPCTP causes a distinguishable effect in LOI performance of PE blends. On the other hand, agglomerations at higher concentrations result in a stability of LOI values after 20% concentration. As seen in section 4.2.3. SEM micrographs indicate clusters of HPCTP particles. This may result in stable increasing trend of LOI from 25.3 to 25.5.

Aliphatic structure of HPACTP may have resulted in lower values of LOI and following a constant line around 23.5 value for 20% and 30% concentrations of HPACTP. However, it is obvious that LOI values of HPACTP increase from 19.8 to 23.7 with higher loading loadings. According to literature data, aliphatic structured cyclic phosphazenes shows significant effects by showing synergism with other types of flame retardants [36]. In this study, although HPACTP is used as a single additive, LOI values are increased. On the other hand, increments in LOI values are not distinguishable. In section 4.2.3, clustered particles of HPACTP are observed at 30% concentrations. Agglomerations may be the reason for having a constant line at higher concentrations.

4.4.1.2 UL-94 for PE-HPCTP and PE-HPACTP Blends

UL-94 test results are given in Table 4.12. There exist a great difference between the time values of PE-HPCTP and PE-HPACTP blends. Aromatic structures involved in PE-HPCTP blends have shorter t_1 values compared to PE-HPACTP blends. V0 is found for blends with HPCTP concentrations of 20% and 30%.

The results of both LOI in section 4.4.1.1 and UL-94 in this section support that dehalogenated cyclic phosphazenes may be good candidates for flame retardant applications. Aromatic cyclic phosphazenes perform better than the aliphatic ones based on V_0 evaluations indicating flame retardancy property. HPCTP is also reported as flame retardant additive for PA 6 in literature [179]. HPCTP also demonstrates sufficient flame retardancy for PE blends.

Table 4.12 UL-94 Evaluation of PE-HPCTP and PE-HPACTP Blends

Sample	t_1 (s)	t_2 (s)	Evaluation*
PE	Burned to the clamp	-	V2
HPCTP10PE	2	18	V1
HPCTP20PE	2	3	V0
HPCTP30PE	1	2	V0
HPACTP10PE	18	Burned to the clamp	V2
HPACTP20PE	20	Burned to the clamp	V2
HPACTP30PE	20	Burned to the clamp	V2

*V0 indicated Flame retardant performance whereas V1 and V2 means that sample does not have flame retardancy.

V2 is found for all the PE-HPACTP blends. Aliphatic structures may be responsible for the results of fast burning of PE-HPACTP blends. t_2 values could not be determined, since samples with HPACTP were burned to the clamp.

Similar to the results of LOI in section 4.4.1.1, improved performance of UL-94 test is observed for HPCTP20PE and HPCTP30PE. It should be discussed that mechanical properties do not demonstrate an improvement for these two blends with respect to pure PE. Although an enhancement is not observed, the results are within acceptable region similar to other studies in literature [179].

4.4.1.3 Cone Calorimetry for PE-HPCTP Blends

Cone calorimeter is applied in order to observe heat release rate (HRR) in the course of combustion. Generally, low values of peak heat release rate (PHRR) and total heat evolved (THE) demonstrate improved flame retardancy effect. Heat flux rate at 35 kW/m² is applied to the samples of pure PE, HPCTP20PE and HPCTP30PE.

Based on the data of Figure 4.24, polyethylene (Pure PE) burns in a fast manner following the ignition. Heat release peak at the point of 535.03 kW/m² is observed. After adding HPCTP with 20% to PE, HPCTP20PE blend is obtained and PHRR is increased to the value of 589.13 kW/m² while PHRR decreases to the point of 552.37 kW/m² for HPCTP30PE which has a composition of 30% . There also exists extended burning time for HPCTP20PE (440 s) as well as for HPCTP30PE (710 s) in comparison with pure PE (418 s). Detailed information is given in section 2.7.6. The higher concentration of HPCTP in the blend of HPCTP30PE results in extended burning time in comparison to HPCTP20PE.

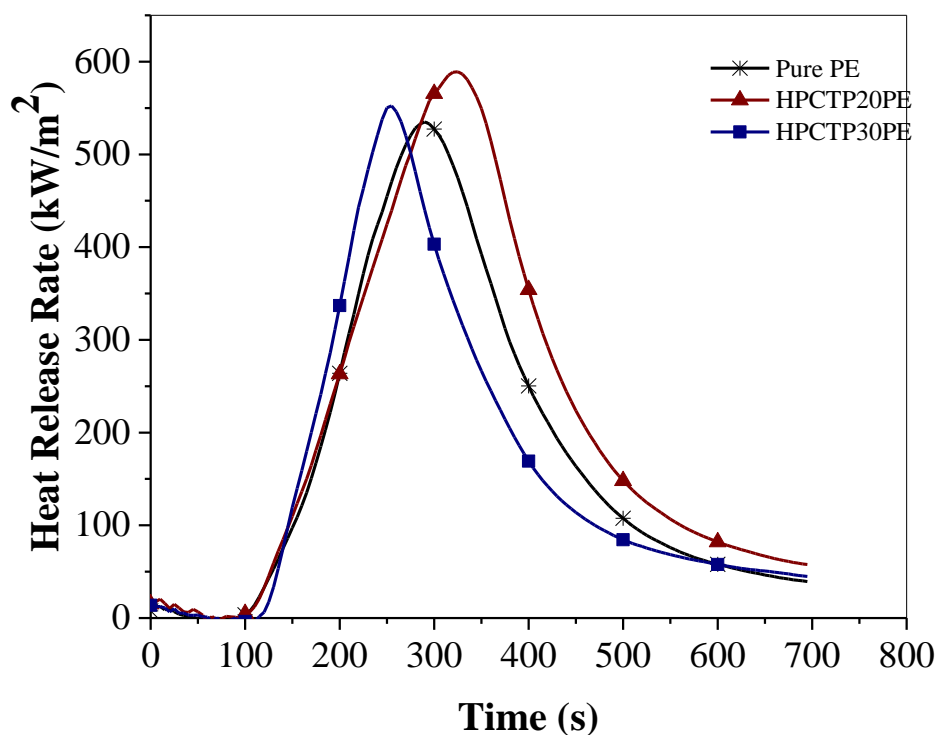


Figure 4.24 HRR curves of pure PE, HPCTP20PE and HPCTP30PE

HPCTP20PE and HPCTP30PE are selected depending of their results of LOI and UL-94 which were presented in sections 4.4.1.1 and 4.4.1.2. At first glance, increases in PHRR for HPCTP20PE and HPCTP30PE do not coincide with the results of LOI and UL-94 tests which indicate the flame retardant effect of HPCTP. Then, it should be advised to analyze the data of total heat evolved and total mass loss in order to search the flame retardant effect, whether it occurs in the gas phase. Then, in Table 4.13, necessary data is given for a more elaborate analysis. An improved flame retardant effect in the gas phase is observed as the concentration of HPCTP increases in the blend of HPCTP30PE.

Table 4.13 Cone calorimeter data of pure PE and the blends of HPCTP20PE and HPCTP30PE

Sample	PHRR (kW/m ²)	TTI (s)	Average HRR (kW/m ²)	THE (MJ/m ²)	THE/TML (MJ/m ² g)
Pure PE	535.03	93	267.46	112.17	5.02
HPCTP20PE	589.13	97	304.06	133.90	4.47
HPCTP30PE	552.37	114	163.89	116.61	4.80

PHRR: Peak Heat Release Rate, TTI: Time to ignition,

HRR: Heat Release Rate, THRR: Total Heat Release Rate, TML: Total Mass Loss

The ratio of total heat evolved (THE) to total mass loss (THE/TML) indicates the effective heat combustion, and it is clearly observed that the flame retardant effect of HPCTP occurs in the gas phase by flame inhibition [176]. The value of THE/TML ratio decreases for HPCTP20PE and HPCTP30PE blends by 11% and 4.4%, respectively. Reduction of THE/TML demonstrates the contributory effect of HPCTP in the gas phase.

It should be discussed that flame inhibition effect in the gas phase may be driving force for obtaining enhanced flame retardancy of PE and PP blends by HPCTP additive. Höhne et al. suggested that a radical scavenging effect results in an unfinished burning process [179]. Good performance of THE/TML ratios indicates that enhanced flame retardancy of PE-HPCTP blends and also PP-HPCTP blends which will be discussed in section 4.4.2.3.

In addition, decomposition products of phenoxy and free radicals have a quenching effect of flammable free radicals [192]. It is possible that burning chain reaction is inhibited and PE matrix burns at lower intensity. As THE/TML ratio demonstrates, pyrolysis products of HPCTP are effective in gas phase and flame retardancy is convincingly enhanced.

4.4.2 PP-HPCTP and PP-HPACTP Blends

LOI, UL-94 and cone calorimetry tests were applied for PP blends. Similar results to PE blends were found. With respect to the results of UL-94, samples of cone calorimetry were prepared.

4.4.2.1 Limiting Oxygen Index (LOI) for PP-HPCTP and PP-HPACTP Blends

PP-HPCTP blends demonstrated higher LOI values than the ones of PP-HPACTP blends in Figure 4.25.. Increases in LOI were found higher as HPCTP concentrations increased. LOI value reached to 22.5 at the concentration of 30% HPCTP. According to literature data, aromatic structures on cyclic phosphazenes demonstrated higher performance of LOI. Xu et al. reported high LOI performances of aromatic cyclic phosphazenes with synergistic agents [36]. In this study, HPCTP additives result in higher LOI values without any benefits of synergism. Well dispersion of HPCTP particles through PP matrix may be effective for having this performance. As seen in section 4.2.4, SEM micrographs indicate well dispersed particles of HPCTP.

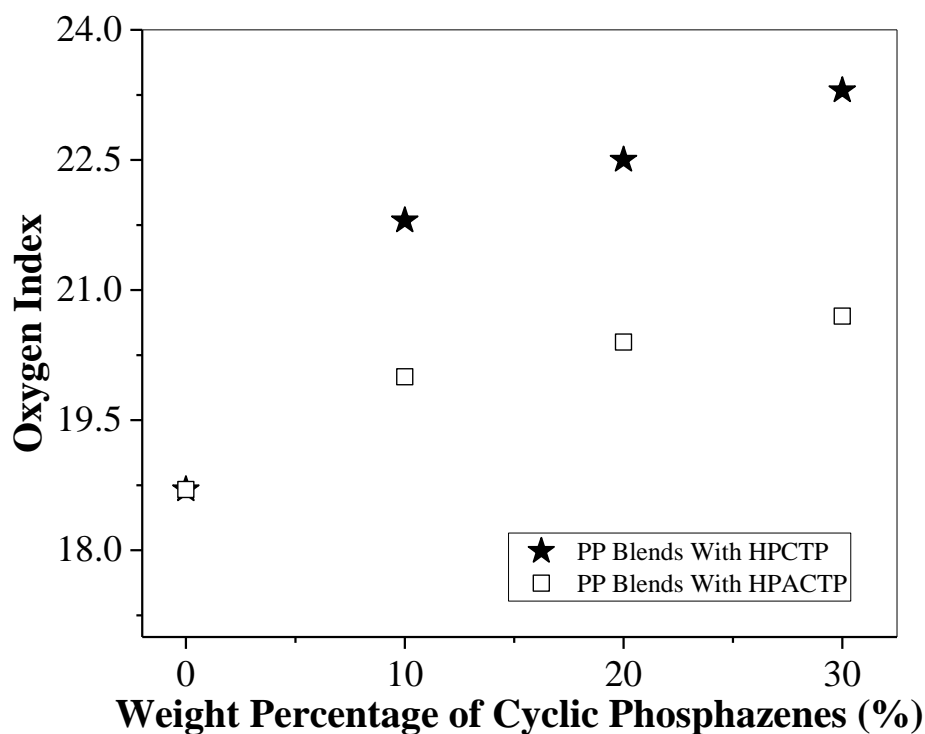


Figure 4.25 Oxygen Index versus Cyclic Phosphazene Concentration for PP-HPCTP and PP-HPACTP Blends

PP-HPACTP blends have LOI values around 20.5 for all compositions, 10%, 20% and 30% of HPACTP. Lower increases in LOI may result from compatible characteristics of HPACTP with PP matrix. HPACTP has an aliphatic structure. Different from PP blends with HPCTP, the increases in LOI were smaller with addition of HPACTP. These higher increases may also result from aromatic structure of HPCTP.

Good compatibility may not meet the requirements for mechanical improvement. In the literature, it is reported that aliphatic structures of cyclic phosphazenes have increasing effects in other types of polymer matrices with synergistic agents. They

also mentioned enhanced processability of flame retardants [36] whereas PE-HPACTP blends do not demonstrate improvements as seen in Table 4.6.

4.4.2.2 UL-94 for PP-HPCTP and PP-HPACTP Blends

Depending on the results of UL-94 tests, samples were evaluated in Table 4.15. PP-HPCTP blends with concentrations of 20% and 30% were evaluated as V0 likewise to the results of PE blends with HPCTP. Aromatic structure of HPCTP decreases time periods of t_1 and t_2 at a certain degree that HPCTP20PP and HPCTP30PP were grouped as V0. It is obvious that HPCTP has an effect on increased flame retardancy of PP blends. It is reported that aromatic phosphazenes achieve good performance of UL-94 test [188], [193] Incorporation of HPCTP within matrix is an advantage for reaching flame retardancy effect [179] Similarly, HPCTP particles adhered well through PP matrix in section 4.2.4. Thus, HPCTP20PP and HPCTP30PP are classified best, V0.

On the other hand, PP-HPACTP blends were evaluated as V2. All samples were burned to the clamp after ignition. Compatibility of HPACTP with PP may be active for burning to the clamp without having any t_1 value. Aliphatic structure of HPACTP gave rise to compatibility through PP matrix, whereas increased LOI values were found, UL-94 test results indicated an opposite result that the blends did not have even a t_1 value. It should be discussed that synergism with other types of additives may result in improvements of UL-94 test results. El Gouri and co-workers studied similar types of HPACTP additives [180]. They reported V0 rating for an epoxy blend with aliphatic group substituted phosphazene additives as well as with synergistic agents.

Table 4.15 UL-94 Evaluation of PP-HPCTP and PP-HPACTP Blends

Sample	t1 (s)	t2 (s)	Evaluation
PP	Burned to the clamp	-	V2
HPCTP10PP	17	30	V2
HPCTP20PP	2	7	V0
HPCTP30PP	1	3	V0
HPACTP10PP	Burned to the clamp	-	V2
HPACTP20PP	Burned to the clamp	-	V2
HPACTP30PP	Burned to the clamp	-	V2

4.4.2.3 Cone Calorimetry of PP-HPCTP Blends

For analysing of calorimeter results of polypropylene (Pure PP), it can be commented that its firing process occurs in a slower characteristic in comparison to pure PE with an HRR value of 550.91 at peak. Likewise to PE blends of HPCTP, HPCTP20PP and HPCTP30PP were selected depending of their results of LOI and UL-94 which were presented in sections of 4.4.2.1 and 4.4.2.2. With the addition of HPCTP in weight concentrations of 20% and 30%, blends of HPCTP20PP and HPCTP30PP were prepared. PHR values of these blends are 627.93 and 620.52 kW/m². TTI value of 68 sec is decreased to 64 and 57 seconds with addition of HPCTP. In Figure 4.26, plots of HPCTP20PP and HPCTP30PP blends are in almost an overlapping form. Loads of 20wt% and 30wt% HPCTP do almost the same effect in Table 4.16 when it is dealt with data obtained for these blends.

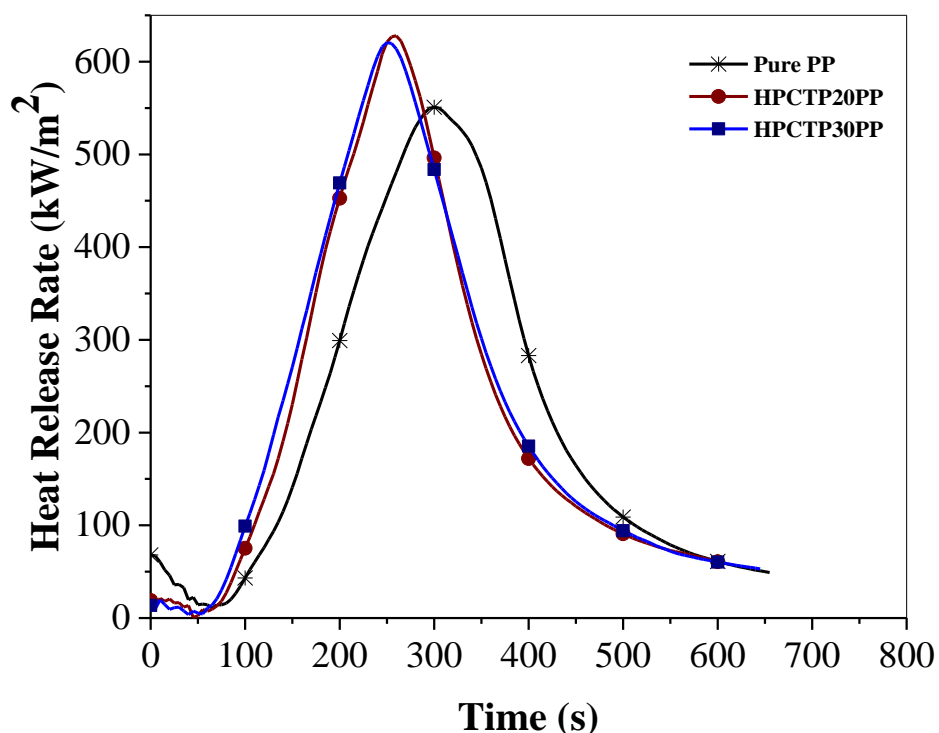


Figure 4.26 HRR curves of pure PP, HPCTP20PP and HPCTP30PP

In a very similar way to the former examples of PE blends that the THE/TML ratio is decreased from 4.81 to 3.84 and 4.22 MJ/m².g with reduction per cents of 20 and 12.3 for HPCTP20PP and HPCTP30PP blends. It is clearly an indication of gas phase flame retardancy effect of HPCTP. HPCTP20PP and HPCTP30PP blends benefits from scavenging effect of combustion products of HPCTP. Flammable radicals are effective for good cone calorimeter results [192]. It is clear that combustion intensity is inhibited by HPCTP additives. Cone calorimetry results are also satisfying when combining with LOI and UL-94 test results.

Liu et al. reported possible gas phase flame inhibition effect of aromatic phosphazenes and suggested free radical scavenging factor [194]. Enhanced values of THE/TML indicate flame retardancy of HPCTP20PP and HPCTP30PP. Also, it

should be discussed that homogeneous dispersion starts to disappear while HPCTP concentration increases from 20% to 30%. Agglomerations in HPCTP30PP may be responsible for lower performance of cone calorimetry test. Well adhered HPCTP particles in HPCTP20PP provides lower value of THE/TML ratio. When mechanical test results, SEM micrographs and flame retardancy test performances combine, HPCTP20PP blend is the best compatible blend in this study.

Table 4.16 Cone calorimeter data of pure PP and the blends of HPCTP20PP and HPCTP30PP

Sample	PHRR (kW/m²)	TTI (s)	Average HRR (kW/m²)	THE (MJ/m²)	THE/TML (MJ/m²g)
Pure PP	550.91	68	312.20	117.86	4.81
HPCTP20PP	627.93	64	352.17	103.41	3.84
HPCTP30PP	620.52	57	319.37	124.50	4.22

PHR: Peak Heat Release Rate, TTI: Time to ignition,

HRR: Heat Release Rate, THRR: Total Heat Release Rate, TML: Total Mass Loss

CHAPTER 5

CONCLUSIONS

Mechanical, physical, thermal and flame retardant properties of polyolefin blends with cyclic phosphazenes were analysed by using test results of thermal gravimetric analysis (TGA), differential scanning calorimetry (DSC), tensile tests, scanning electron microscopy (SEM), UL-94, limiting oxygen index (LOI) and cone calorimeter.

In TGA plots, single step weight loss was observed for HPCTP, whereas HPACTP demonstrated two steps. The first peak of HPCTP corresponds to decomposition. On the other hand, first peak of HPACTP may correspond to detachment of propyl groups and the second peak may indicate breaking down of cyclic phosphazene backbone. Based on the results of DSC, one endothermic peak resulting from melting of HPCTP crystals was observed, whereas three peaks were observed for HPACTP.

Depending on blend compositions, one maximum weight loss point was observed for PE-HPCTP and two steps of weight loss were observed for PE-HPACTP including char formation in TGA. However, T_{\max} values for pure PE and PE blends did not change extensively. Compatibility of cyclic phosphazenes through PE matrix may be the reason of this result. On the other hand, it should also be stated that agglomerations were observed at 30% concentration of HPCTP.

The existence of only one peak in DSC graph indicates that cyclic phosphazenes are compatible through the matrix of PE. ΔH_m has a decreasing trend while HPCTP concentration increases, probably owing to amorphous dispersion. In comparison with 20% and 30% of HPCTP concentrations, ΔH_m value increased. However, beyond 20%, ΔH_m value of PE-HPACTP blends demonstrates a sharp decrease.

Based on the results of TGA and DSC, there existed no char formation in PP-HPCTP and PP-HPACTP blends unlike the case of PE blends. PP-HPCTP and PP-HPACTP blends comply with single and double loss points, respectively. Considering $T_{5\%}$ values of PP blends, cyclic phosphazenes, presumably, exhibited a plasticizing effect then large differences between the temperature values of pure PP and PP blends are observed. It should also be taken into consideration that there may exist a certain point of HPCTP concentration between 20% and 30%, then agglomerations of HPCTP particles started to cluster resulting in a drop of T_{max} .

HPCTP20PP exhibits higher values of ΔH_m and $\chi\%$ and a lower value of T_m , then it may be concluded that around 20% concentration an optimum value of distribution for HPCTP crystals occur through the matrix with lowest agglomeration and highest effect of plasticizing. Continuous PP plates are also observed in SEM, and this phenomenon gives rise to protected crystalline zones (see Figure 4.8).

Within the frame of mechanical test results, tensile strength and elongation at break values of PE-HPCTP blends have a decreasing trend with increasing HPCTP amounts until 30% concentration of HPCTP. It should be stated that tensile strength and elongation at break values increased while concentration of HPCTP increases from 20% to 30% due to homogeneous dispersion of HPCTP through PE matrix observed in SEM analysis. HPCTP10PE has the best mechanical properties compared to the other two PE-HPCTP blends. However, HPCTP20PE and HPCTP30PE have flame retardant characteristics while HPCTP10PE is not flame retardant based on LOI and UL-94 tests.

Regarding PE-HPACTP blends, values of both tensile strength and elongation at break followed a decreasing trend with increasing concentrations of HPACTP. Incompatibility of HPACTP through PE matrix is the reason for reduction of these values. In addition, Young's modulus values increased due to the polymorphic characteristic of HPACTP crystals. HPACTP10PE is compatible mechanically among all PE blends prepared with aliphatic cyclic phosphazenes. However, all these blends do not demonstrate flame retardancy property.

In PP based blends homogeneous dispersion is observed up to 20% PP-HPCTP concentration and this resulted in higher tensile strength with increasing concentration. However, all tensile property values decreased at 30 % concentration of HPCTP due to agglomeration of cyclic phosphazene particles within the matrix. It may be concluded that there existed an optimum level of dispersion between the values of 20% and 30%. HPCTP20PP has better mechanical properties than PP blends prepared with 10% and 30% of HPCTP.

Concerning PP-HPACTP blends, tensile properties have a tendency to decrease with augmented concentration of HPACTP. This should be a result of both crystalline sites on HPACTP particles and insufficient dispersion. HPACTP10PP has the best mechanical properties through PP blends with aliphatic additives.

A sudden increase in LOI occurred by forming PE blends with 10% of HPCTP and HPACTP. At higher concentrations of HPCTP, the increasing effect of HPCTP follows a more moderate trend, probably, due to particle distribution in a clustered manner. LOI values of PE-HPACTP blends nearly remain at the same level for the concentrations of 20% and 30%. It can be concluded that aromatic structure of HPCTP is responsible for having larger values of LOI for PE-HPCTP blends in comparison to PE-HPACTP ones. Aliphatic structure of HPACTP is the main factor for having lower values of LOI unlike the effect of aromatic HPCTP.

UL-94 test results of PE blends are in accordance with LOI results. Effect of aromatic structures established shorter t_1 values than the ones obtained with aliphatic structures. Consequently, V0 is found for blends with HPCTP concentrations of 20% and 30%, and V2 is found for all the PE-HPACTP blends.

HPCTP20PE and HPCTP30PE are picked for cone calorimeter test based on the results of LOI and UL-94. The data of total heat evolved and total mass loss indicate that the flame retardant effect occurs in the gas phase. It should be concluded that flame retardant effect in the gas phase is ameliorated with increased concentration of HPCTP from 20% to 30%. In these blends, the reduction in the ratios of total heat evolved (THE) to total mass loss (THE/TML) points that the flame retardant effect of HPCTP occurs in the gas phase by flame inhibition. The contributory effect of HPCTP in the gas phase is one of the main effects giving a rise to flame retardant nature.

LOI and UL-94 results of PP blends coincide with PE blends. PP-HPCTP blends show clearly higher LOI values than the ones obtained for PP-HPACTP blends. Aromatic structures play a dominant role in realizing the flame retardancy observed in the data of LOI and UL-94. Aromatic structure of HPCTP has a decreasing effect in both the values of t_1 and t_2 . Therefore, HPCTP20PP and HPCTP30PP are denoted as V0. However, PP-HPACTP blends are listed under the group of V2. It should be concluded that aliphatic structure of HPACTP gives rise to compatibility through PP matrix. Main result in this study is that aromatic structures in the substituent groups on cyclic phosphazene additives give flame retardancy property to PE and PP blends. Aliphatic structured additives do not exhibit distinguishable flame retardancy.

In a resembling manner to the previous examples of PE blends, the THE/TML ratio is decreased while concentration of HPCTP increases from 20% to 30% and, repetitively, it is an indication of gas phase flame retardant effect of HPCTP.

It can be concluded that HPCTP20PP with a lower value of THE/TML, 3.84 MJ/m²·g, has a higher flame retardancy than HPCTP20PE whose THE/TML value is 4.47 MJ/m²·g. Furthermore, HPCTP20PP has the best compatibility in terms of mechanical properties through all the flame retardant blends of PE and PP prepared with HPCTP.

REFERENCES

- [1] Joel R Fried, *Polymer Science And Technology*. New Jersey: Prentice Hall PTR, 2003.
- [2] S. M. Lomakin and G. E. Zaikov, *Modern Polymer Flame Retardancy*. Boston: VSP, 2003.
- [3] H. Allcock, "Phosphorus-Nitrogen Compounds," in *Phosphorus-Nitrogen Compounds*, New York: Academic Press, 1972, p. 157.
- [4] J. Bickley *et al.*, "Supramolecular variations on a molecular theme: the structural diversity of phosphazenes (RNH)₆ P₃ N₃ in the solid state," *Dalt. Trans.*, no. 7, pp. 1235–1244, 2003.
- [5] D B Malpass, *Introduction to Industrial Polyethylene*. John Wiley and Sons, 2010.
- [6] J. C E Carraher, *Introduction to Polymer Chemistry*. Florida: CRC Press, 2010.
- [7] J. F W Billmeyer, *Textbook of polymer science*. New York: Wiley, 1984.
- [8] N Pasquini, *Polypropylene handbook, products, technologies and markets*. Cincinnati: Hanser/Gardner Publications, 2005.
- [9] V. Babrauskas *et al.*, "Fire hazard comparison of fire-retarded and non-fire-retarded products Special Publication #749," 1988.
- [10] A. F. Grand and A. C. Wilkie, *Fire Retardancy of Polymeric Materials*. New York: Marcel Dekker, Inc., 2000.
- [11] W. C. Kuryla and A. J. Papa, *Flame Retardancy of Polymeric Materials vol. 2*. New York: Marcel Dekker, 1973.
- [12] S. Zhang and A. R. Horrocks, "A Review of Flame Retardant Polypropylene Fibres," *Prog. Polym. Sci.*, vol. 28, pp. 1517–1538, 2003.
- [13] J Breil, *Multilayer Flexible Packaging*. Massachusetts: Elsevier, 2010.
- [14] A. P. Gibson and A. G. Mouritz, *Fire Properties of Polymer Composite Materials*. Dordrecht: Springer, 2006.
- [15] V. S. Levchik and E. D. Weil, "Featured Article Combustion and Fire Retardancy of Aliphatic Nylons," *Polym. Int.*, vol. 49, pp. 1033–1073, 2000.

- [16] S. Lu and I. Hamerton, "Recent Developments in the Chemistry of Halogen-free Flame Retardant Polymers," *Prog. Polym. Sci.*, vol. 27, pp. 1661–1712, 2002.
- [17] A. B. Morgan and J. W. Gilman, "An overview of flame retardancy of polymeric materials: application, technology, and future directions," *Fire Mater.*, vol. 37, pp. 259–279, 2013.
- [18] M. Xanthos, *Functional Fillers for Plastics*. Weinheim: Wiley-VCH, 2005.
- [19] A. B. Morgan and C. A. Wilke, *Flame retardant polymer nanocomposites*. New Jersey: Wiley- Interscience, 2007.
- [20] Q. Li, J. Pingkai, and P. Wei, "Thermal Degradation Behavior of Poly(propylene) with a Novel Silicon- Containing Intumescent Flame Retardant," *Macromol. Mater. Eng.*, vol. 290, pp. 912–919, 2005.
- [21] S. Bourbigot, M. Le Bras, S. Duquesne, and M. Rochery, "Recent Advances for Intumescent Polymers," *Macromol. Mater. Eng.*, vol. 289, pp. 499–511, 2004.
- [22] F. Xie, Y. Wang, B. Yang, and Y. Liu, "A Novel Intumescent Flame-Retardant Polyethylene System," *Macromol. Mater. Eng.*, vol. 291, pp. 247–253, 2006.
- [23] M. Doğan and E. Bayramlı, "Synergistic effect of boron containing substances on flame retardancy and thermal stability of intumescent polypropylene composites," *Polym. Adv. Technol.*, vol. 22, no. 12, pp. 1628–1632, 2011.
- [24] SpecialChem, "Techno Brief: Melamine Compounds as Flame Retardants," *Techno Brief: Melamine Compounds as Flame Retardants*, 2018. [Online]. Available: <https://polymer-additives.specialchem.com/selection-guide/melamine-compounds-as-flame-retardants/mechanism-of-action>. [Accessed: 08-Jun-2018].
- [25] S. V Levchik and W. E. D, "A review of recent progress in phosphorus-based flame retardants," *J. Fire Sci.*, vol. 24, pp. 345–364, 2006.
- [26] D. R. Lide, *Handbook of Chemistry and Physics*, 81st ed. Maryland, 2000.
- [27] K. H. Pawlowski and B. Scharrel, "Flame retardancy mechanisms of triphenyl phosphate, resorcinol bis(diphenyl phosphate) and bisphenol A bis(diphenyl phosphate) in polycarbonate/acrylonitrile-butadiene-styrene blends," *Polym. Int.*, vol. 56, pp. 1404–1414.
- [28] U. Braun *et al.*, "Influence of oxidation state of phosphorus on the decomposition and fire behavior of flame-retarded epoxy resin composites," *Polymer (Guildf)*, vol. 47, pp. 8495–8508, 2006.

- [29] U. Braun, H. Bahr, H. Sturm, and B. ScharTEL, "Flame retardancy mechanisms of metal phosphinates and metal phosphinates in combination with melamine cyanurate in glass-fiber reinforced poly(1,4-butylene terephthalate): the influence of metal cation," *Polym. Adv. Technol.*, vol. 19, pp. 680–692, 2008.
- [30] B ScharTEL, R. Kunze, D. Neubert, and U. Braun, "Mechanistic studies on PA-66 fire retarded with red phosphorus," *Recent Adv. Flame Retard. Polym. Mater.*, vol. 13, pp. 93–103, 2002.
- [31] X. Shan, L. Song, W. Xing, Y. Hu, and S. Lo, "Effect of nickel-containing layered double hydroxides and cyclophosphazene compound on the thermal stability and flame retardancy of poly(lactic acid)," *Ind. Eng. Chem. Res.*, vol. 51, no. 40, pp. 13037–13045, 2012.
- [32] W. J. Liang, B. Zhao, C. Y. Zhang, R. K. Jian, D. Y. Liu, and Y. Q. Liu, "Enhanced flame retardancy of DGEBA epoxy resin with a novel bisphenol-A bridged cyclotriphosphazene," *Polym. Degrad. Stab.*, vol. 144, pp. 292–303, 2017.
- [33] S. Bourbigot and S. Duquesne, "Fire retardant polymers: recent developments and opportunities," *J. Mater. Chem.*, vol. 17, pp. 2283–2300, 2007.
- [34] S. Duquesne, R. Delobel, M. Le Bras, and G. A. Camino, "A comparative study of the mechanism of action of ammonium polyphosphate and expandable graphite in polyurethane," *Polym. Degrad. Stab.*, vol. 77, pp. 333–344, 2002.
- [35] M. M. M, A. Lorenzetti, F. Simioni, and G. Camino, "Expandable graphite as an intumescent flame retardant in polyisocyanurate–polyurethane foams," *Polym. Degrad. Stab.*, vol. 77, pp. 195–202, 2002.
- [36] C. Wu, W. Wu, H. Qu, and J. Xu, "Synthesis of a novel phosphazene derivative and its application in intumescent flame retardant-EVA copolymer composites," *Mater. Lett.*, vol. 160, pp. 282–285, 2015.
- [37] S. S. Ray and M. Okamoto, "Polymer/layered silicate nanocomposites: a review from preparation to processing," *Prog. Polym. Sci.*, vol. 28, pp. 1539–1641, 2003.
- [38] M Moniruzzaman and K. I. Winey, "Polymer nanocomposites containing carbon nanotubes," *Macromolecules*, vol. 39, pp. 5194–5205, 2006.
- [39] L. A. Utracki, M. Sepehr, and E. Boccaleri, "Synthetic, layered nanoparticles for polymeric nanocomposites (PNCs)," *Polym. Adv. Technol.*, vol. 18, pp. 1–37, 2007.
- [40] R A Vaia and J. F. Maguire, "Polymer nanocomposites with prescribed morphology: going beyond nanoparticle-filled polymers," *Chem. Mater.*, vol. 19, pp. 2736–2751, 2007.

- [41] J Zhu, F. M. Uhl, A. B. Morgan, and C. A. Wilkie, "Studies on the mechanism by which the formation of nanocomposites enhances thermal stability," *Chem. Mater.*, vol. 13, pp. 4649–4654, 2001.
- [42] J W Gilman *et al.*, "Flammability properties of polymer-layered silicate nanocomposites. polypropylene and polystyrene nanocomposites," *Chem. Mater.*, vol. 12, pp. 1866–1873, 2000.
- [43] J. W. Gilman, R. H. Harris, J. R. Shields, T. T. Kashiwagi, and A. B. Morgan, "A study of the flammability reduction mechanism of polystyrene-layered silicate nanocomposite: layered silicate reinforced carbonaceous char," *Polym. Adv. Technol.*, vol. 17, pp. 263–271.
- [44] M Bartholmai and B. Scharrel, "Layered silicate polymer nanocomposites: new approach or illusion for fire retardancy? Investigations of the potentials and the tasks using a model system," *Polym. Adv. Technol.*, vol. 15, pp. 355–364, 2004.
- [45] A. B. Morgan and M. Bundy, "Cone calorimeter analysis of UL-94 V-rated plastics," *Fire Mater.*, vol. 31, pp. 257–283, 2007.
- [46] A B Morgan, "Flame retarded polymer layered silicate nanocomposites: a review of commercial and open literature systems," *Polym. Adv. Technol.*, vol. 17:, 2006.
- [47] G Beyer, "Flame retardancy of nanocomposites – from research to technical products," *J. Fire Sci.*, vol. 23, pp. 75–87, 2005.
- [48] W. Xie, Z. Gao, W. P. Pan, D. Hunter, A. Singh, and R. Vaia, "Thermal degradation chemistry of alkyl quaternary ammonium montmorillonite," *Chem. Mater.*, vol. 13, pp. 2979–2990, 2001.
- [49] D Dharaiya D and S. C. Jana, "Thermal decomposition of alkyl ammonium ions and its effect on surface polarity of organically treated nanoclay," *Polymer (Guildf.)*, vol. 46, pp. 10139–10147, 2005.
- [50] R. K. Shah and D. R. Paul, "Organoclay degradation in melt processed polyethylene nanocomposites," *Polymer (Guildf.)*, vol. 47, p. 4084, 2006.
- [51] A. B. Morgan, "A review of transition metal-based flame retardants: transition-metal oxide/salts, and complexes," in *In ACS Symposium Series 1013 – Fire and Polymers V: Materials and Concepts for Fire Retardancy*, 2009, pp. 312–328.
- [52] H. R. Allcock, *Phosphorus-Nitrogen Compounds Cyclic, Linear and High Polymeric Systems*. New York: Academic Press, 1972.
- [53] H. R. Allcock, "Recent advances in phosphazene (phosphonitrilic) chemistry," *Chem. Rev.*, vol. 72, no. 4, pp. 315–356.

- [54] H. R. Allcock, W. J. Cook, and D. P. Mack, "Phosphonitrilic compounds. XV. High molecular weight poly[bis(amino)phosphazenes] and mixed-substituent poly(aminophosphazenes)," *Inorg. Chem.*, vol. 11, no. 11, pp. 2584–2590, 1972.
- [55] H. R. Allcock and S. R. Pucher, "Polyphosphazenes with glucosyl and methylamino, trifluoroethoxy, phenoxy, or (methoxyethoxy)ethoxy side groups," *Macromolecules*, vol. 24, no. 1, pp. 23–34, 1991.
- [56] H. R. A. et Al., "Synthesis of poly[(amino acid alkyl ester)phosphazenes]," *Macromolecules*, vol. 10, no. 4, pp. 824–830, 1977.
- [57] H. R. Allcock, S. R. Pucher, and A. G. Scopelianos, "Poly[(amino acid ester)phosphazenes]: synthesis, crystallinity, and hydrolytic sensitivity in solution and the solid state," *Macromolecules*, vol. 27, no. 5, pp. 1071–1075, 1994.
- [58] L. S. Nair, D. S. Katti, and C. T. Laurencin, "Biodegradable polyphosphazenes for drug delivery applications," *Adv. Drug Deliv. Rev.*, vol. 55, no. 4, pp. 467–482, 2003.
- [59] H. R. Allcock, *Heteroatom Ring Systems and Polymers*. New York: Academic Press, 1967.
- [60] S. Kumbar, C. Laurencin, and M. Deng, *Natural and Synthetic Biomedical Polymers*. Boston: Elsevier, 2014.
- [61] J. Liebig and F. Wöhler, "TAPC preparation from NH₄Cl and POCl₃," *Justus Liebigs Ann. Chem.*, vol. 11, no. 139, p. 407., 1834.
- [62] C. Gerhardt, "Recherches Sur les combinaisons du phosphore avec l'azote," *Ann. Chim. Phys.*, vol. 18, p. 188, 1846.
- [63] C. Gerhardt, "Recherches Sur les combinaisons du phosphore avec l'azote," *Acad. SC*, vol. 22, p. 858, 1846.
- [64] J. H. Gladstone and J. D. Holmes, "On chlorophosphuret of nitrogen and its products of decomposition," *J. Chem. Soc.*, vol. 17, no. 225, 1864.
- [65] J. H. Gladstone and J. D. Holmes, "Sur le chlorophosphure d'azote et ses produits de décomposition," *Ann. Chim. Phys.*, vol. 3, p. 465, 1864.
- [66] J. H. Gladstone and J. D. Holmes, "Sur le chlorophosphure d'azote et ses produits de décomposition," *Bull. Soc. Chim. Paris*, vol. 3, p. 113, 1865.
- [67] A. C. R. Laurent, "Sur diverses combinaisons organique," *C. R. Acad. Sci.*, vol. 31, p. 349, 1850.
- [68] H. Wichelhaus, "Ueber Chlorphosphorstickstoff," *Berichte der Dtsch. Chem.*

- Gesellschaft*, vol. 3, no. 163, p. 414, 1870.
- [69] A. C. R. Besson, "Sur la combinaison du gaz ammoniac avec les chlorures et bromures de phosphore," *R. Acad. Sci.*, vol. 111, p. 972, 1890.
- [70] A. C. Besson, "Sur la décomposition sous l'action de la chaleur du pentachlorure de phosphore ammoniacal: chlorazoture de phosphore et phospham," *C. R. Acad. Sci.*, vol. 114, no. 1264, 1892.
- [71] J. H. Gladstone, "On chlorophosphuret of nitrogen, and its products of decomposition," *J. Chem. Soc.*, vol. 3, no. 4, p. 353, 1851.
- [72] J. H. Gladstone, "Ueber den Chlorphosphorstickstoff und seine Zersetzungsproducte," *Justus Liebig Ann. Chem.*, vol. 77, p. 314, 1851.
- [73] H. N. Stokes, "Handbuch der stereochemie. Unter mitwirkung von Dr. Paul Walden, Professor der physikalischen und analytischen chemie am polytechnikum zu Riga herausgegeben von Dr. C.A. Bischoff, Professor der allgemeinen chemie daselbst.," *Am. Chem. J.*, vol. 17, no. 6, p. 497, 1895.
- [74] H. N. Stokes, "Ueber Chlorphosphorstickstoff und zwei seiner homologen Verbindungen," *Ber.*, vol. 28, p. 437, 1895.
- [75] H. N. Stokes, "Trimetaphosphimic acid and its decomposition products," *Am. Chem. J.*, vol. 18, p. 629, 1896.
- [76] H. N. Stokes, "Tetrametaphosphimic acid," *Am. Chem. J.*, vol. 18, p. 780, 1896.
- [77] N. S. Stokes, "Chloronitrides of phosphorus," *Am. Chem. J.*, vol. 19, p. 782, 1897.
- [78] A. C. Besson, "Sur un bromazoture de phosphore," *C. R. Acad. Sci.*, vol. 114, p. 1479, 1892.
- [79] A. Besson and G. Rosset, "Sur le chlorazoture de phosphore," *C. R. Acad. Sci.*, vol. 143, p. 37, 1906.
- [80] A. Besson and G. Rosset, "Action de l'ammoniac sur le chlorazoture de phosphore," *C. R. Acad. Sci.*, vol. 146, p. 1149, 1908.
- [81] W. Couldridge, "Some interactions of nitrogen chlorophosphide," *J. Chem. Soc.*, vol. 53, p. 398, 1888.
- [82] W. Couldridge, "Réactions du chlorazoture de phosphore," *Bull. Soc. Chim.*, vol. 50, p. 534, 1888.
- [83] J. H. Gladstone, "Ueber Chlorphosphorstickstoff und seine Zersetzungsproducte," *Justus Liebig Ann. Chem.*, vol. 76, p. 74, 1850.

- [84] J. H. Gladstone, "On the compounds containing phosphorus and nitrogen," *J. Chem. Soc.*, vol. 2, p. 121, 1850.
- [85] J. H. Gladstone, "On chlorophosphuret of nitrogen and its products of decomposition," *J. Chem. Soc.*, vol. 3, p. 135, 1851.
- [86] R. Steinman, F. B. Schriener, and L. F. Audrieth, "The Preparation and Physical Properties of Trimeric Phosphonitrilic Chloride," *J. Am. Chem. Soc.*, vol. 64, p. 2377, 1942.
- [87] J. D. Teja and R. A. Peters, "Phosphonitrile chloride polymers for coating glass fabrics," *Chem. Abstr.*, no. 51, p. 17239g, 1957.
- [88] M. Yokoyama, "Studies on Triphosphonitrilic Chloride and its Derivatives. I-II. I. Synthesis of Triphosphonitrilic Chloride from Phosphorus Pentachloride and Ammonium Chloride," *Chem. Abstr.*, vol. 55, p. 4341h, 1961.
- [89] L. G. Lund, N. L. Paddock, J. E. Proctor, and H. T. Searle, "Phosphonitrilic derivatives. Part I. The preparation of cyclic and linear phosphonitrilic chlorides," *J. Chem. Soc.*, p. 2542, 1960.
- [90] S. M. Zhivukhin and V. B. Tolstoguzov, "Phosphonitrile chloride, its preparation, properties, and use. III. Practical utilization of the phosphonitrile chloride polymers," *Chem. Abstr.*, vol. 55, p. 15200d, 1961.
- [91] S. M. Zhivukhin, V. B. Tolstoguzov, and M. M. Levitskii, "Reaction of phosphonitrile chlorides with silanols, silanolates, and hexaalkyl disiloxanes," *Chem. Abstr.*, vol. 56, p. 8278f, 1962.
- [92] V. B. Tolstoguzov and S. M. Zhivukhin, "The production of phosphonitrile chloride," *Khimicheskaya Promyshlennost*, pp. 19–23, 1962.
- [93] S. M. Zhivukhin and V. B. Tolstoguzov, "Reaction of phosphonitrile chlorides with silanols, silanolates, and hexaalkyl disiloxanes," *Chem. Abstr.*, vol. 57, p. 8184d, 1962.
- [94] H. Saito and M. Kajiwara, "Phosphonitrile chloride. I. Reactions of phosphonitrile chloride," *Kogyo Kagaku Zasshi*, vol. 66, no. 5, pp. 618–620, 1963.
- [95] I. Haiduc, *The Chemistry of the Inorganic Ring Systems Vol. 2*. London: Wiley-Interscience, 1970.
- [96] S. Krishnamurthy and A. C. Sau, "Cyclophosphazenes," *Adv. Inorg. Chem. Radiochem.*, vol. 21, p. 41, 1978.
- [97] J. F. Labarre, "Up-to-date improvements in inorganic ring systems as anticancer agents," *Top. Curr. Sci.*, vol. 102, p. 1, 1982.

- [98] J. F. Labarre, "Natural polyamines-linked cyclophosphazenes. Attempts at the production of more selective antitumorals," *Top. Curr. Sci.*, vol. 129, p. 173, 1985.
- [99] C. W. Allen, *The Chemistry of Inorganic Homo- and Hetero-Cycles Vol. 2*. London: Academic Press, 1987.
- [100] H. R. Allcock, J. L. Desorcie, and G. H. Riding, "The organometallic chemistry of phosphazenes," *Polyhedron*, vol. 6, p. 119, 1987.
- [101] V. Chandrasekhar and K. R. J. Thomas, "Coordination and organometallic chemistry of cyclophosphazenes and polyphosphazenes," *Appl. Organomet. Chem.*, vol. 7, p. 1, 1993.
- [102] H. R. Allcock and R. L. Kugel, "Phosphonitrilic Compounds. VII. High Molecular Weight Poly(diaminophosphazenes)," *Inorg. Chem.*, vol. 5, p. 1716, 1966.
- [103] H. R. Allcock, R. L. Kugel, and K. J. Valan, "Phosphonitrilic Compounds. VI. High Molecular Weight Poly(alkoxy- and aryloxyphosphazenes)," *Inorg. Chem.*, vol. 5, p. 1709, 1966.
- [104] H. R. Allcock and R. L. Kugel, "Synthesis of High Polymeric Alkoxy- and Aryloxyphosphonitriles," *J. Am. Chem. Soc.*, vol. 87, p. 4216, 1965.
- [105] H. R. Allcock, "Poly(organophosphazenes)—Unusual New High Polymers," *Angew. Chem. Int. Ed. Engl.*, vol. 16, p. 147, 1977.
- [106] H. R. Allcock, "Developments at the interface of inorganic, organic, and polymer chemistry," *Chem. Eng. News*, vol. 63, p. 22, 1985.
- [107] T. Yvernault and G. Casteignau, "Transistorized electronic timer," *Bull. Soc. Chim. Fr.*, no. 7, p. 2116, 1965.
- [108] R. A. Shaw, "Reactions of Halogenocyclophosphazenes with Nitrogenous Bases," *Z. Naturforsch.*, vol. 31b, p. 641, 1976.
- [109] Y. Li *et al.*, "Durable flame retardant and antibacterial finishing on cotton fabrics with cyclotriphosphazene/polydopamine/silver nanoparticles hybrid coatings," *Appl. Surf. Sci.*, vol. 435, pp. 1337–1343, 2018.
- [110] A. P. Carroll and R. A. Shaw, "Mercaptophosphazenes," *Chem. Ind.*, p. 1908, 1962.
- [111] E. Niecke, O. Glemser, and H. W. Roesky, "Ethylmercaptofluorotriphosphazenes," *Z. Naturforsch.*, vol. 24b, p. 1187, 1969.
- [112] R. De Jaeger and M. Gleria, "Poly(Organophosphazene)s And Related

Compounds: Synthesis, Properties And Applications,” *Prog. Polym. Sci.*, vol. 23, pp. 119–216, 1998.

- [113] C. W. Allen, “Regio- and stereochemical control in substitution reactions of cyclophosphazenes,” *Chem. Rev.*, vol. 91, no. 2, p. 119, 1991.
- [114] H. R. Allcock, “Recent advances in phosphazene (phosphonitrilic) chemistry,” *Chem. Rev.*, vol. 72, no. 4, p. 315, 1972.
- [115] C. W. Allen, “Linear, cyclic and polymeric phosphazenes,” *Coord. Chem. Rev.*, vol. 130, no. 1–2, p. 137, 1994.
- [116] E. J. Walsh, E. Derby, and J. Smegal, “Nucleophilic substitutions on hexachlorocyclotriphosphazene using 18-crown-6 ether complexes,” *Inorg. Chim. Acta*, vol. 16, p. L9, 1976.
- [117] P. E. Austin, G. H. Riding, and H. R. Allcock, “Improved method for the synthesis of poly(organophosphazenes) and hindered cyclophosphazenes,” *Macromolecules*, vol. 16, no. 5, p. 719, 1983.
- [118] D. Dell, B. W. Fitzsimmons, and R. A. Shaw, “Phosphorus–nitrogen compounds. Part XIII. Phenoxy- and p-bromophenoxy-chlorocyclotriphosphazatrienes,” *J. Chem. Soc.*, p. 4070, 1965.
- [119] E. T. McBee, K. Okuhara, and C. Morton, “Reactions of Hexachloro- and 2,2,4,4-Tetrachloro-6,6-diphenylcyclotriphosphazatrienes with Sodium Phenoxide,” *Inorg. Chem.*, vol. 5, no. 3, p. 450, 1966.
- [120] J. J. Beres, N. S. Schneider, C. R. Desper, and R. E. Singler, “Crystalline Poly(organophosphazene) Blends and Copolymers,” *Macromolecules*, vol. 12, no. 4, p. 566, 1979.
- [121] F. Minto, L. Flamigni, P. Bortolus, and M. Gleria, “Photochemical behavior of poly(organophosphazenes). IX. Internal photostabilization effects in (4-benzoylphenoxy) x (β-naphthoxy)2–x phosphazene copolymers,” *J. Inorg. Organomet. Polym.*, vol. 1, no. 1, p. 53, 1991.
- [122] H. R. Allcock, A. A. Dembeck, M. N. Mang, G. H. Riding, and M. Parvez, “Synthesis and structure of small-molecule cyclic phosphazenes bearing ortho-substituted aryloxy and phenoxy substituents,” *Inorg. Chem.*, vol. 31, no. 13, p. 2734, 1992.
- [123] H. R. Allcock, D. C. Ngo, M. Parvez, and K. Visscher, “Cyclic and short-chain linear phosphazenes with hindered aryloxy side groups,” *J. Chem. Soc. Dalton Trans.*, p. 1687, 1992.
- [124] H. R. Allcock, D. J. Brennan, B. S. Dunn, and M. Parvez, “Cyclotriphosphazenes with geminal (trimethylsilyl)methyl and alkyl or aryl side groups,” *Inorg. Chem.*, vol. 27, no. 18, p. 3226, 1988.

- [125] H. R. Allcock, D. J. Brennan, and D. S. Dunn, "Synthesis of polyphosphazenes bearing geminal (trimethylsilyl)methylene and alkyl or phenyl side groups," *Macromolecules*, vol. 22, no. 4, p. 1534, 1989.
- [126] H. Bode and H. Bach, "Über Phosphornitril-Verbindungen, I. Mitteil.: Phenylderivate des Triphosphornitrilchlorides," *Chem. Ber.*, vol. 75, p. 215, 1942.
- [127] M. Becke-Goehring and K. Z. John, "Zur Kenntnis der Phosphornitrilchloride. III. Die Phenylierung des trimeren Phosphornitrilchlorids und die Reaktionen des Diphenylderivats," *Anorg. Allg. Chem.*, vol. 304, p. 126, 1960.
- [128] R. G. Feistel, K. M. Feldt, L. R. Dieck, and T. Moeller, "Phosphorus compounds. Amido(phosphonitrilic chloride-cyclic trimer) and 1,1-diamido(phosphonitrilic chloride-cyclic trimer)," *Inorg. Synth.*, vol. 14, p. 23, 1973.
- [129] L. J. Carr, G. M. Nichols, and S. H. Rose, 131. Carr, L. J. and Rose, S. H. (*Borg-Warner Chemical, Inc.*), DTNSRDC/SME-CR-18-84, Navy Contract No. N0167-82-C-0168, November (1984). 132. Carr, L. J. and Nichols, G. M., *European Patent Application EP 145 002 (1985)*; *Chem. Abstr.*, 103, 178459q (1985),. Borg-Warner Chemical, Inc.
- [130] A. F. Popov, A. E. Shumieko, A. A. Afon'kin, and Z. P. Piskunova, "Catalytic effect of water in the phase-transfer synthesis of poly(nitrophenoxy) phosphazenes," *Chem. Abstr.*, vol. 116, p. 59621v, 1992.
- [131] Y. W. Chen-Yang and B. D. Tsai, "Preparation and characterization of (aryloxy)chlorocyclotriphosphazenes by phase transfer catalysis," *Polyhedron*, vol. 12, no. 1, p. 59, 1993.
- [132] L. J. Carr and S. H. Rose, "Navy Contract No. N0167-82-C-0168, November," Borg-Warner Chemical, Inc., 1984.
- [133] L. J. Carr and G. M. Nichols, "Phosphazine esters by using a phase transfer catalyst," *Chem. Abstr.*, vol. 103, p. 178459q, 1985.
- [134] S. Kamiyama, K. Fujikawa, Y. Yoshikawa, T. Okamoto, and T. Nishikawa, "Preparation of aryloxy-substituted phosphazenes as materials for fireproofing agents, lubricating oils, and electric insulators," *Chem. Abstr.*, vol. 111, p. 233197v, 1989.
- [135] M. L. Wang and H. S. Wu, "Kinetic study of the substitution reaction of hexachlorocyclotriphosphazene with 2,2,2-trifluoroethanol by phase-transfer catalysis and separation of the products," *Ind. Eng. Chem. Res.*, vol. 29, no. 10, p. 2137, 1990.
- [136] M. Wang and H. S. Wu, "Effects of mass transfer and extraction of quaternary salts on a substitution reaction by phase-transfer catalysis," *J. Org. Chem.*, vol.

55, no. 8, p. 2344, 1990.

- [137] M. L. Wang and H. S. Wu, "Kinetics of the reaction of hexachlorocyclotriphosphazene with 2,2,2-trifluoroethanol by phase-transfer catalysis," *J. Chem. Soc., Perkin Trans. 2*, vol. 841, no. 6, 1991.
- [138] M. L. Wang and H. S. Wu, "Kinetic and mass transfer studies of a sequential reaction by phase transfer catalysis," *Chem. Eng. Sci.*, vol. 46, p. 509, 1991.
- [139] Y. W. Chen-Yang, S. J. Cheng, and B. D. Tsai, "Preparation of the partially substituted (phenoxy)chlorocyclotriphosphazenes by phase-transfer catalysis," *Ind. Eng. Chem. Res.*, vol. 30, p. 1314, 1991.
- [140] A. J. Deome and D. A. Bulpett, "NOO02485WR10446/AC (NAVY), MTL TR 86-35," Watertown, MA.
- [141] R. E. Singler and M. J. Bieberich, "Synthetic Lubricants and High Performance Functional Fluids," in *Synthetic Lubricants and High Performance Functional Fluids*, New York: (R. L. Shubkin, Ed.), Marcel Dekker, 1992, p. 215.
- [142] R. E. Singler, A. J. Deome, D. A. Dunn, M. J. Bieberich, and I. E. C. P. R. Dev, "Preparation and properties of phosphazene fire-resistant fluids," *Ind. Eng. Chem. Prod. Res. Dev.*, vol. 25, no. 1, p. 46, 1986.
- [143] R. Rätz, H. Schroeder, H. Ulrich, E. Kober, and C. Grundmann, "A New Class of Stable Phosphonitrilic Acid Esters. Polyfluoroalkyl Phosphonitrilates," *J. Am. Chem. Soc.*, vol. 84, p. 551, 1962.
- [144] E. Kober, H. Lederle, and G. Ottmann, "Fluoroalkylphosphonitrilates: A New Class of Potential Fire-Resistant Hydraulic Fluids and Lubricants. I.," *Am. Soc. Lubric. Eng. Trans.*, vol. 7, no. 4, p. 389, 1964.
- [145] H. Lederle, E. Kober, and G. Ottmann, "Fluoroalkyl Phosphonitrilates: A New Class of Potential Fire-Resistant Hydraulic Fluids and Lubricants," *J. Chem. Eng. Data*, vol. 11, no. 2, p. 221, 1966.
- [146] G. Ottmann, H. Lederle, and E. Kober, "Arylamino Polyfluoroalkoxy Phosphonitriles. New Class of Potential Fire-Resistant Hydraulic Fluids and Lubricants," *Ind. Eng. Chem. Prod. Res. Dev.*, vol. 5, no. 2, p. 202, 1966.
- [147] R. E. Singler *et al.*, "AD A1 17 298 Defence Technical Information Center," 1982.
- [148] J. L. White and S. H. Bumm, "Polymer blend compounding and processing," *Polymer Blends Volume 2 Processing*. 2011.
- [149] W. E. Baker, C. E. Scott, and G. H. Hu, *Reactive polymer blending*. Hanser Verlag, 2001.

- [150] L. Utracki, "History of commercial polymer alloys and blends (from a perspective)," *Polym. Eng. Sci.*, vol. 35, no. 1, p. 217, 1995.
- [151] H. B. Eitouni and N. P. Balsara, *Thermodynamics of polymer blends. Physical properties of polymers handbook*. Springer, 2007.
- [152] S. Thomas, R. Shanks, and C. Sarathchandran, *Nanostructured Polymer Blends*. Massachusetts: Elsevier, 2014.
- [153] C. Koning, M. V. D. C. P. Jerome, and R. Jerome, "Strategies For Compatibilization Of Polymer Blends," *Prog. Polym. Sci.*, vol. 23, pp. 707–757, 1998.
- [154] E. M. Woo and Y. C. Tseng, "Glass transition and miscibility in blends of two semicrystalline polymers: Poly(arylether ketone) and poly(ether ether ketone)," *J. Polym. Sci. Part B Polym. Phys.*, vol. 37, no. 13, p. 1485, 1999.
- [155] W. Wenig and T. Schöller, "Phase separation in incompatible polymer blends: polypropylene-polyethylene system," in *Frontiers in polymer science*, W. Wilke, Ed. Steinkopff, 1985, p. 113.
- [156] M. Coleman and P. Painter, "Hydrogen bonded polymer blends," *Prog. Polym. Sci.*, vol. 20, no. 1, p. 159, 1995.
- [157] Z P Fang Z, G. W. Ma, Y. Z. Xu, and L. F. Tong, "Synergistic modification of EPDM and crosslinking agent in immiscible blends of polyvinyl chloride with low density polyethylene," *Chin. J. Polym. Sci.*, vol. 24, no. 02, p. 147, 2006.
- [158] O. Olabis, *Polymer-polymer miscibility*. Elsevier Science, 1979.
- [159] D. Krishnarao, *Nuclear Magnetic Resonance (NMR) Theory, Applications and Technology*. New York: Nova Publishers, 2014.
- [160] *UL-94-Test for Flammability of Plastic Materials for Parts in Devices and Appliances*. Northbrook IL: Underwriters Laboratories Inc., 1997.
- [161] P Kiliaris and C. D. Papaspyrides, "Polymer/Layered Silicate (Clay) Nanocomposites: An Overview of Flame Retardancy," *Prog. Polym. Sci.*, vol. 35, pp. 902–958, 2010.
- [162] F Laoutid, L. Bonnaud, M. Alexandre, J. M. Lopez-Cuesta, and P. Dubois, "New Prospects in Flame Retardant Polymer Materials: From Fundamentals to Nanocomposites," *Mater. Sci. Eng. R Reports*, vol. 63, pp. 100–125, 2009.
- [163] V. Shah, *Handbook of Plastics Testing Technology*. New York: John Wiley & Sons, Inc., 1998.
- [164] J. Scheirs, *Compositional and Failure Analysis of Polymers*. New York: John Wiley & Sons, Inc., 2000.

- [165] B. Schartel, M. Bartholmai, and U. Knoll, "Some Comments on the Use of Cone Calorimeter Data," *Polym. Degrad. Stab.*, vol. 88, pp. 540–547, 2005.
- [166] B. Schartel and T. R. Hull, "Development of Fire-Retarded Materials – Interpretation of Cone Calorimeter Data," *Fire Mater.*, vol. 31, pp. 327–354, 2007.
- [167] G. Özkoç, "Abs/Polyamide-6 Blends, Their Short Glass Fiber Composites and Organoclay Based Nanocomposites: Processing and Characterization," METU, 2007.
- [168] M. Kılınç, "Processing and Characterization of Poly(ethylene terephthalate) Based Composites," Middle East Technical University, 2004.
- [169] *Annual Book of ASTM Standards*. Philadelphia, 1993.
- [170] "Scanning Electron Microscope." [Online]. Available: http://en.wikipedia.org/wiki/Scanning_electron_microscope. [Accessed: 17-Jan-2018].
- [171] H. F. Giles, J. R. Wagner, and E. M. Mount, *Extrusion The Definitive Processing Guide and Handbook*. New York: William Andrew Publishing, 2005.
- [172] A. B. Strong, *Plastics Materials and Processing*. New Jersey: Prentice Hall, 2006.
- [173] "Injection Moulding." [Online]. Available: http://en.wikipedia.org/wiki/Injection_molding/last. [Accessed: 31-May-2014].
- [174] A. I. Vogel, A. R. Tatchell, B. S. Furnis, A. J. Hannaford, and P. W. G. Smith, *Vogel's Textbook of Practical Organic Chemistry*, 5th ed. Essex: Pearson Education Limited, 1989.
- [175] H. Allcock and R. Best, "Phosphonitrilic compounds: Part I. The mechanism of phosphonitrilic chloride polymerization capacitance, conductance, and electron-spin resonance studies," *Can. J. Chem.*, vol. 42, no. 2, p. 447, 1964.
- [176] B. Zhao, W. J. Liang, J. S. Wang, F. Li, and Y. Q. Liu, "Synthesis of a novel bridged-cyclotriphosphazene flame retardant and its application in epoxy resin," *Polym. Degrad. Stab.*, vol. 133, pp. 162–173, 2016.
- [177] R. Yang, W. Hu, L. Xu, Y. Song, and J. Li, "Synthesis, mechanical properties and fire behaviors of rigid polyurethane foam with a reactive flame retardant containing phosphazene and phosphate," *Polym. Degrad. Stab.*, vol. 122, pp. 102–109, 2015.
- [178] Y.-R. Luo, *Handbook of Bond Dissociation Energies in Organic Compounds*.

Florida: CRC Press, 2002.

- [179] C. Höhne, R. Wendel, B. Käbisch, T. Anders, F. Henning, and E. Kroke, “Hexaphenoxycyclotriphosphazene as FR for CFR anionic PA6 via T-RTM: a study of mechanical and thermal properties,” no. July 2016, pp. 291–306, 2016.
- [180] M. El Gouri, A. El Bachiri, S. E. Hegazi, M. Rafik, and A. El Harfi, “Thermal degradation of a reactive flame retardant based on cyclotriphosphazene and its blend with DGEBA epoxy resin,” *Polym. Degrad. Stab.*, vol. 94, no. 11, pp. 2101–2106, 2009.
- [181] W. Cai *et al.*, “A novel strategy to simultaneously electrochemically prepare and functionalize graphene with a multifunctional flame retardant,” *Chem. Eng. J.*, vol. 316, pp. 514–524, 2017.
- [182] M. Dutkiewicz, M. Przybylak, R. Januszewski, and H. Maciejewski, “Synthesis and flame retardant efficacy of hexakis(3-(triethoxysilyl)propyloxy)cyclotriphosphazene/silica coatings for cotton fabrics,” *Polym. Degrad. Stab.*, vol. 148, no. August 2017, pp. 10–18, 2018.
- [183] T. Kawahara, A. Yuuki, K. Hashimoto, K. Fujiki, T. Yamauchi, and N. Tsubokawa, “Immobilization of flame-retardant onto silica nanoparticle surface and properties of epoxy resin filled with the flame-retardant-immobilized silica (2),” *React. Funct. Polym.*, vol. 73, no. 3, pp. 613–618, 2013.
- [184] S. Wang *et al.*, “Durable flame retardant finishing of cotton fabrics with organosilicon functionalized cyclotriphosphazene,” *Polym. Degrad. Stab.*, vol. 128, pp. 22–28, 2016.
- [185] H. Shan, J. L. White, and A. Willem, “International Journal of Polymer Analysis and Comparison of Crystallization and Melting Characteristics of Quiescent and Melt-Spun Poly (ethylene-co-octene) Copolymers Comparison of Crystallization and Melting,” vol. 5341, no. May, 2007.
- [186] X. Zhang, L. P. Zhang, Q. Wu, and Z. P. Mao, “The influence of synergistic effects of hexakis (4-nitrophenoxy) cyclotriphosphazene and POE-g-MA on anti-dripping and flame retardancy of PET,” *J. Ind. Eng. Chem.*, vol. 19, no. 3, pp. 993–999, 2013.
- [187] J. Brandrup, E. H. Immergut, E. A. Grulke, A. Abe, and D. R. Bloch, *Polymer handbook*, 4th ed. Canada: John Wiley & Sons, 2005.
- [188] P. Jiang *et al.*, “Flammability and thermal degradation of poly (lactic acid)/polycarbonate alloys containing a phosphazene derivative and trisilanollsobutyl POSS,” *Polym. (United Kingdom)*, vol. 79, pp. 221–231, 2015.

- [189] Y. J. Shin *et al.*, “Application of cyclophosphazene derivatives as flame retardants for ABS,” *J. Ind. Eng. Chem.*, vol. 16, no. 3, pp. 364–367, 2010.
- [190] K. R. Fontenot *et al.*, “The thermal degradation pathway studies of a phosphazene derivative on cotton fabric,” *Polym. Degrad. Stab.*, vol. 120, pp. 32–41, 2015.
- [191] T. Cao, L. Yuan, A. Gu, and G. Liang, “Fabrication and origin of new flame retarding bismaleimide resin system with low dielectric constant and loss based on microencapsulated hexaphenoxycyclotriphosphazene in low phosphorus content,” *Polym. Degrad. Stab.*, vol. 121, pp. 157–170, 2015.
- [192] L. Qian, F. Feng, and S. Tang, “Bi-phase flame-retardant effect of hexaphenoxy-cyclotriphosphazene on rigid polyurethane foams containing expandable graphite,” *Polym. (United Kingdom)*, vol. 55, no. 1, pp. 95–101, 2014.
- [193] W. jun Liang, B. Zhao, P. hua Zhao, C. yun Zhang, and Y. qing Liu, “Bisphenol-S bridged penta(anilino)cyclotriphosphazene and its application in epoxy resins: Synthesis, thermal degradation, and flame retardancy,” *Polym. Degrad. Stab.*, vol. 135, pp. 140–151, 2017.
- [194] R. Liu and X. Wang, “Synthesis, characterization, thermal properties and flame retardancy of a novel nonflammable phosphazene-based epoxy resin,” *Polym. Degrad. Stab.*, vol. 94, no. 4, pp. 617–624, 2009.

APPENDIX

NMR SPECTRA OF HPCTP AND HPACTP

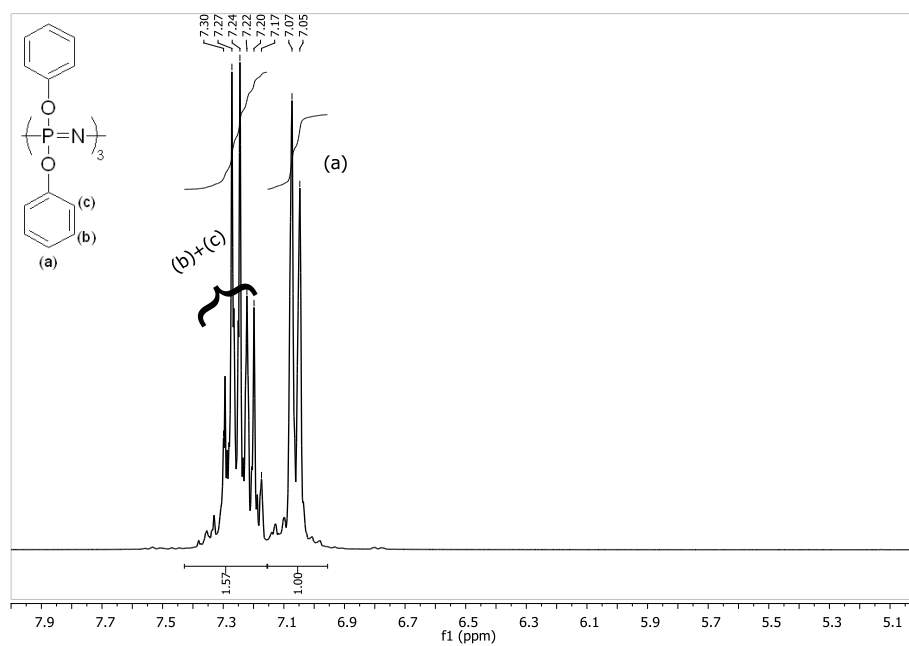


Figure A.1 ^1H NMR spectrum synthesized hexaphenoxycyclotriphosphazene (HPCTP).

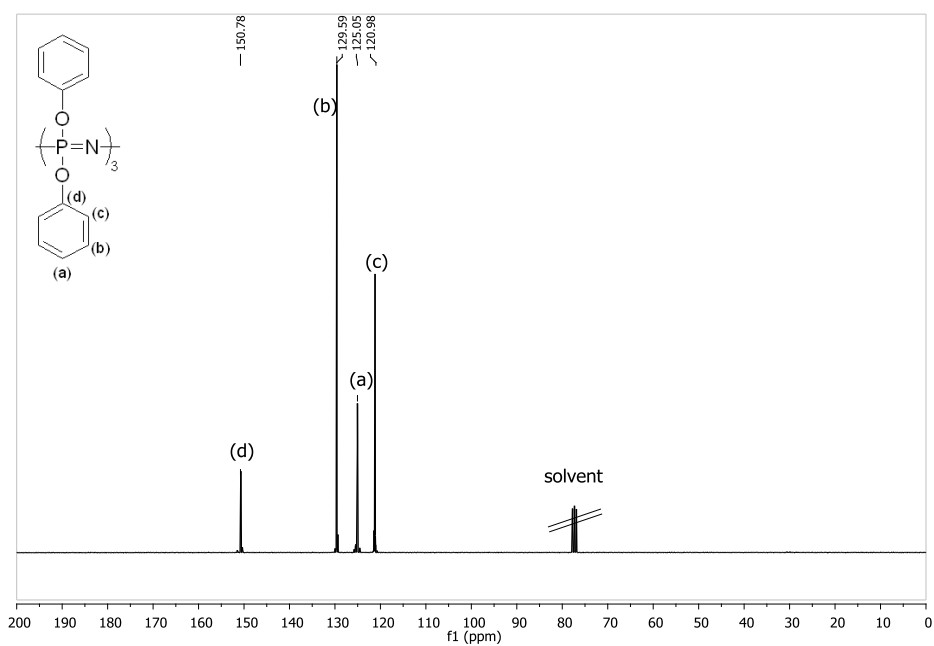


Figure A.2 ^{13}C NMR spectrum synthesized hexaphenoxycyclotriphosphazene (HPCTP).

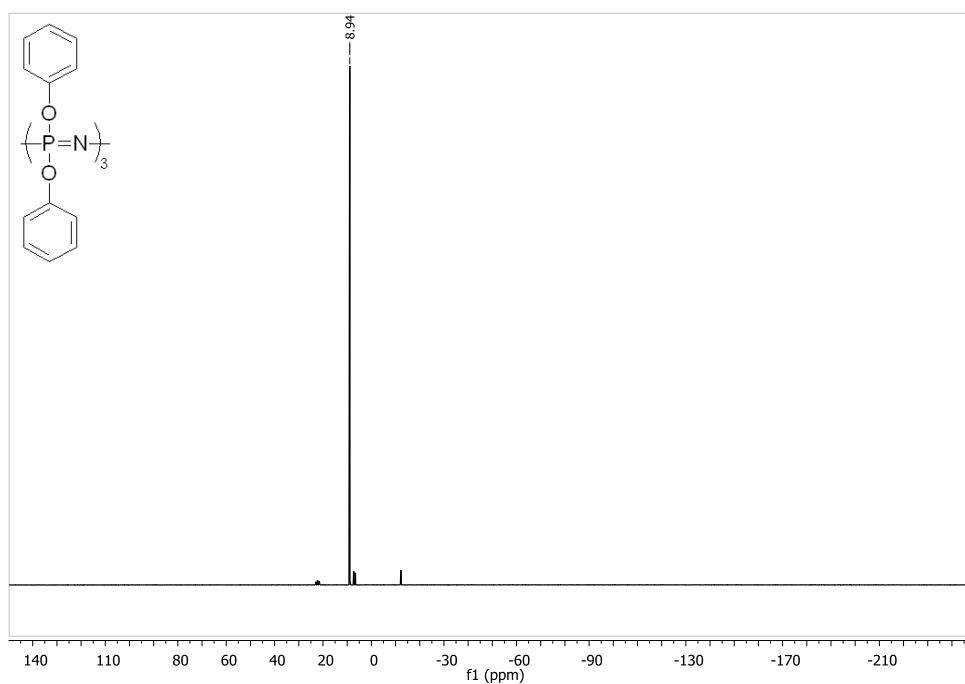


Figure A.3 ^{31}P NMR spectrum synthesized hexaphenoxycyclotriphosphazene (HPCTP).

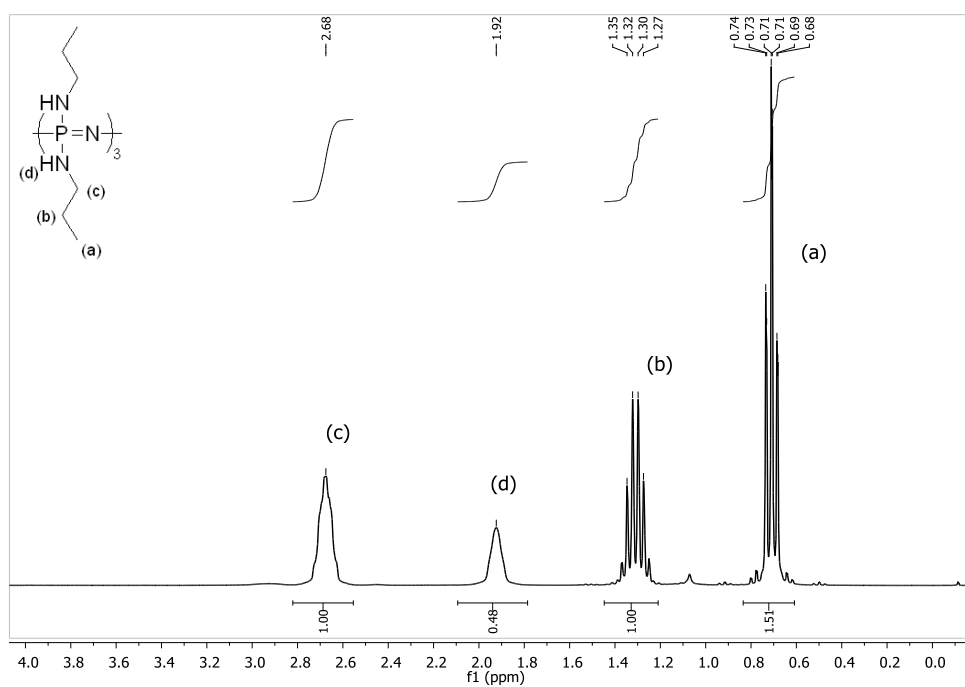


Figure A.4 ^1H NMR spectrum synthesized Hexakispropylaminocyclotriphosphazene (HPACTP).

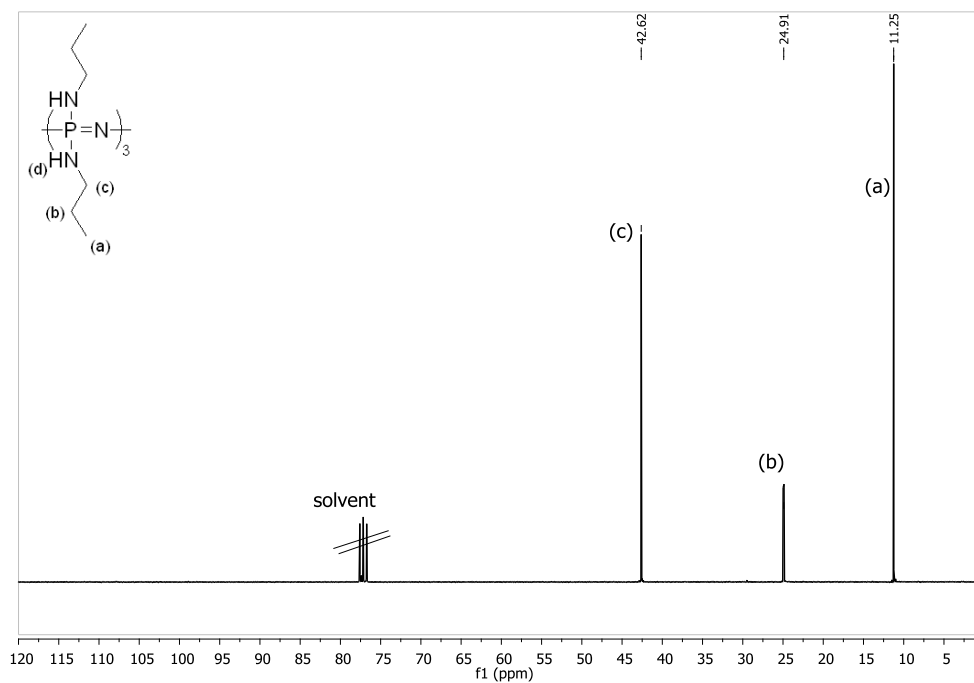


Figure A.5 ^{13}C NMR spectrum synthesized Hexakispropylaminocyclotriphosphazene (HPACTP).

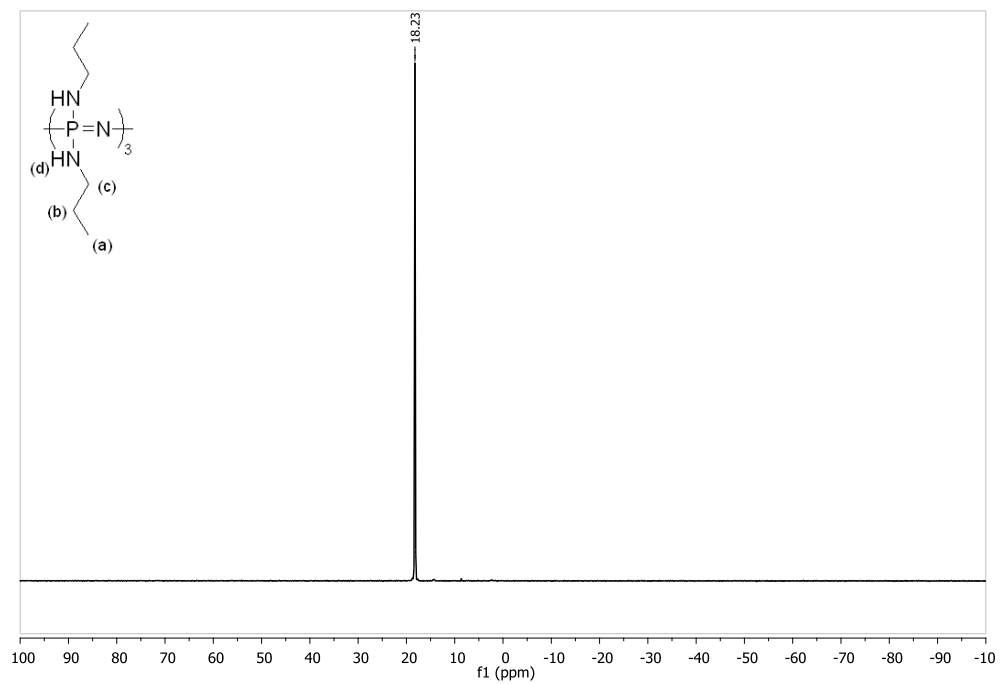


Figure A.6 ^{31}P NMR spectrum synthesized Hexakispropylaminocyclotriphosphazene (HPACTP).

CURRICULUM VITAE

PERSONAL INFORMATION:

Name: Muzaffer Kaan KARAÖZ

Date and Place of Birth: 02.04.1981, ANKARA

Marital Status: Married

Nationality: Turkish

Correspondence Address

Work Address: TÜBİTAK, Eskişehir Yolu 7. Km, Bilim, Sanayi ve Teknoloji Bakanlığı Eski Binası (ODTÜ Karşısı) Çankaya ANKARA

Home Address: Çiğdem Mahallesi, 1550.Cadde, Dünya Bir Vadi Sitesi C7-1. Blok No: 58/7 Çankaya ANKARA

Phone: +90 533 448 97 92 (Mobile)

+90 312 298 94 66 (Work)

e-mail: k.karaoz@metu.edu.tr, kaankaraoz@gmail.com

EDUCATIONAL BACKGROUND:

M.Sc.: METU, Chemical Engineering Department, Ankara, November 2007

B.Sc.: METU, Chemical Engineering Department, Ankara, June 2004

High School: Cumhuriyet Lisesi, June 1999

WORK EXPERIENCE:

September 2007 – Present: Scientific Programs Expert, TÜBİTAK – ANKARA

December 2006 – September 2007: Engineer, ETİ MADEN – General Directorate - ANKARA

December 2004 - December 2006: Engineer, MKE – Ammunition Factory – KIRIKKALE

FOREIGN LANGUAGE:

English – Advanced

French – Intermediate

Spanish – Elementary

PROFESSIONAL MEETINGS:

- Synthesis and Characterization of Hexakis(propylamino)cyclotriphosphazene and Hexaphenoxycyclotriphosphazene and Uses on Polyolefins as Flame Retardants, Muzaffer Kaan Karaöz, Yunus Karataş, İsmail Teoman Tinçer, *46th IUPAC World Polymer Congress (MACRO2016)*, 2016, İstanbul – Türkiye

- Hekzakis(propilamino)siklotrifosfazen ve Hekzafenoksisiklotrifosfazen'in Sentezi, Karakterizasyonu ve Bazı Poliolefinlerde Alev Geciktirici Olarak Kullanımı, Muzaffer Kaan KARAÖZ, Yunus KARATAŞ, İsmail Teoman TİNÇER, *VI. Ulusal Polimer Bilim ve Teknolojisi Kongresi*, 2016, Ankara-Türkiye

- Synthesis and Characterization of Propylamino and Phenoxy Substituted Cyclic Phosphazenes and Their Uses as Flame Retardants in Polyolefins. Muzaffer Kaan Karaöz, Yunus Karataş, İsmail Teoman Tinçer, *2nd International Congress on The World Of Technology And Advanced Materials (WITAM 2016)*, 2016, Kırşehir - Türkiye

PERSONAL INTERESTS:

Aikido, listening to classical music, playing football, hiking, cinema, comics.